5TH EUROPEAN POSTGRADUATE FLUID DYNAMICS CONFERENCE

BOOK OF ABSTRACTS

5th European Postgraduate Fluid Dynamics Conference

9–12 August 2011
Göttingen, Germany

Preface

The 5th European Postgraduate Fluid Dynamics Conference will continue an annual succession of fluid dynamics-themed conferences, organised and attended by doctoral students across Europe. All previous conferences, EPFDC-2007 (Birmingham), EPFDC-2008 (Keele), EPFDC-2009 (Nottingham), EPFDC-2010 (Paris) have shown to be a success and have proved to be an excellent platform for students to both present their research and network with others.
This year the conference, EPFDC 5, will be held in Göttingen, Germany and is jointly hosted by the Institute of Aerodynamics and Flow Technology of the German Aerospace Center and the Max Planck Institute for Dynamics and Self-Organisation.

Following the spirit of preceding years, this conference will provide an open-forum for PhD students from all over Europe giving a short talk or presenting a poster. The sessions will be devoted to the broad scope of topics of fluid- and flow-based research including, but not limited to aerodynamics, geophysical flows, turbulence, hydrodynamic stability, multiphase flow and biofluid dynamics.
The attendees will get the opportunity to share their ideas and their work in an environment of current and future colleagues. Furthermore four accomplished scholars will give plenary talk from these many diverse areas of fluid dynamics.

The Organising Committee of EPFDC 5
Göttingen, 2011

Acknowledgement

The Organizing Committee of the EPFDC 5 wishes to express their gratitude for the generous financial support from the following institutions: The Institute of Aerodynamics and Flow Technology of the German Aerospace Center (DLR), the European Mechanics Society (EUROMECH), the groups of Prof Dr Stephan Herminghaus, Prof Dr Eberhard Bodenschatz and Dr Björn Hof of the Max Planck Institute for Dynamics and Self-Organization (MPI-DS), the International Max Planck Research School for Physics of Biological and Complex Systems (IMPRS) and the Göttingen Graduate School for Neurosciences and Molecular Biosciences (GGNB).

We also thank Prof Bruno Eckhardt and Dr Andreas Schrimpf from the Philipps-Universität Marburg for many fruitful discussions and supportive help in several organising issues. Furthermore, the University of Marburg was responsible for hosting our conference website, what we kindly acknowledge.

Finally, we would like to thank the invited plenary speakers and all the participants for their valuable contributions to making this conference a success.

Contents

Organisation

Organising committee

Kerstin Avila	Max Planck Institute for Dynamics and Selforganization kerstin.avila@mpg.ds.de
Quentin Brosseau	Max Planck Institute for Dynamics and Selforganization quentin.brosseau@mpg.ds.de
Daniel Feldmann	German Aerospace Center Institute of Aerodynamics and Flow Technology daniel.feldmann@dlr.de
Daniel Herde	Max Planck Institute for Dynamics and Selforganization daniel.herde@mpg.ds.de
Susanne Horn	German Aerospace Center Institute of Aerodynamics and Flow Technology susanne.horn@dlr.de
Fabio Di Lorenzo	Max Planck Institute for Dynamics and Selforganization fabio.dilorenzo@ds.mpg.de
Matthew Salewski	Philipps-Universität Marburg salewskm@staff.uni-marburg.de

International committee

Oliver Bain	Nottingham University, United Kingdom
Helene Berthet	Schlumberger-ESPCI PMMH, Paristech, France
Igor Chernyavsky	Nottingham University, United Kingdom
Susanne Claus	Cardiff University, United Kingdom
Vladimir Parezanovic	ENSTA ParisTech, France
Samuel Yoffe	University of Edinburgh, United Kingdom

Conference Program

Monday, 8th August

17:00	–	18:30	Welcome Reception, Registration, Coffee & Snacks

Tuesday, 9th August

8:00	–	8:30	Registration
8:30	–	9:00	Conference Opening
9:00	–	10:00	Plenary talk: Prof Eberhard Bodenschatz
10:00	–	10:20	Coffee break
10:20	–	11:20	Session I: Turbulent flows
11:20	–	11:30	Coffee break
11:30	–	12:30	Session II: Particles and stratification
12:30	–	13:30	Lunch break
13:30	–	14:30	Session III: Buoyancy driven flows
14:30	–	14:40	Coffee break
14:40	–	16:40	Lab Tour (DLR and MPI-DS)
16:40	–	17:00	Poster Session: Preparation
17:00	–	17:30	Poster Session: Short talks
17:30	–		Poster Session: Discussions and BBQ

Wednesday, 10th August

9:00	–	10:00	Plenary talk: Dr Klaus Ehrenfried
10:00	–	10:20	Coffee break
10:20	–	11:20	Session IV: Applied aerodynamics
11:20	–	11:30	Coffee break
11:30	–	12:30	Session V: Environmental applications
12:30	–	13:30	Lunch break
13:30	–	14:30	Session VI: Flow control
14:30	–	14:40	Coffee break
14:40	–	15:40	Session VII: Transition to turbulence
15:40	–	18:30	City Tour

Thursday, 11th August

9:00	–	10:00	Plenary talk: Prof Adélia Sequeira
10:00	–	10:20	Coffee break
10:20	–	11:20	Session VIII: Biofluid dynamics
11:20	–	11:30	Coffee break
11:30	–	12:30	Session IX: Numerical methods
12:30	–	13:30	Lunch break
13:30	–	14:30	Session X: Hydrodynamic stability
14:30	–	14:40	Coffee break
14:40	–	15:40	Session XI: Taylor-Couette flow
15:40	–	18:30	Lab Tour (MPI-DS Fassberg)
18:30	–		Conference dinner at Burgschänke-Plesse

Friday, 12th August

9:00	–	10:00	Plenary talk: Prof Rainer Hollerbach
10:00	–	10:20	Coffee break
10:20	–	11:20	Session XII: Geophysical flows
11:20	–	11:30	Coffee break
11:30	–	12:30	Session XIII: Waves and stability
12:30	–	13:30	Lunch break
13:30	–	14:30	Closing Session

Plenary talks

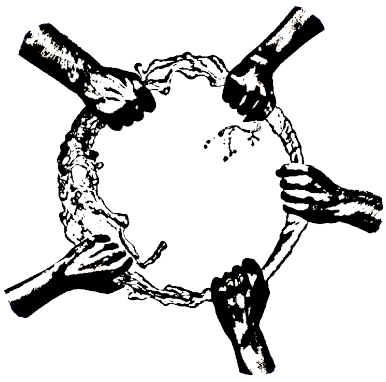

Prof Eberhard Bodenschatz

Max Planck Institute for Dynamics and Self-Organisation
Department of Fluid Dynamics
Pattern Formation and Nanobiocomplexity
Am Fassberg 17
37077 Göttingen, Germany

eberhard.bodenschatz@ds.mpg.de

Eberhard Bodenschatz was born on April 22, 1959 in Rehau. He received his doctorate in theoretical physics from the University of Bayreuth in 1989. In 1991, during his postdoctoral research at the University of California at Santa Barbara, he received a faculty position in experimental physics at Cornell University. From 1992 until 2005, during his tenure at Cornell he was a visiting professor at the University of California at San Diego (1999-2000). In 2003 he became Director and Scientific Member at the Max Planck Institute for Dynamics and Self-Organization. He continues to have close ties to Cornell University, where he is Adjunct Professor of Physics and of Mechanical and Aerospace Engineering (since 2005). Furthermore, he is editor in chief for the New Journal of Physics.

Experiments in turbulence

Tuesday, 9th August, 9:00 - 10:00

Fluid turbulence leads to a dramatic enhancement of transport and mixing and therefore is of great importance in a wide variety of natural and industrial processes from cloud physics to chemical reactors. These effects arise directly from the violent accelerations experienced by fluid particles as they are buffeted by enormous pressure gradients generated in incompressible turbulent flows. Despite the fundamental importance of these issues, only recently with the advance in detector technology (silicon strip, CMOS) it has become possible to measure the 3D particle trajectories in highly turbulent flows. Here we describe the use of a 3D direct imaging particle tracking technique that measures simultaneously the position, velocities, and accelerations of many particles advected by the flow with very high temporal and spatial resolution. We report measurements of the statistical properties of turbulence both in space and in time when measured along the trajectory of particles. Properties reported will include particle acceleration and two particle dispersion. The results are compared with predictions from Richardson (1925), Heisenberg (1948), and Batchelor (1956). In closing we will give an overview of the Göttingen High Pressure Turbulence Facility and of cloud physics experiments on Germany's highest mountain at 2700m.

Dr Klaus Ehrenfried

German Aerospace Center
Institute of Aerodynamics and Flow Technology
Fluid Systems
Bunsenstr. 10
37073 Göttingen, Germany

klaus.ehrenfried@dlr.de

Klaus Ehrenfried studied Physics at the University of Göttingen. He received his doctoral degree in 1991. His doctoral research was done at the Max Planck Institute for Fluid Dynamics in Göttingen where he investigated a fundamental process of the noise generation of helicopters numerically. From 1992 to 1998 he continued his research in the field of helicopter noise at the DLR in Göttingen, where he started to work also experimentally. In 1998 he moved to the Technical University of Berlin. There his main interests were the application of the microphone array technique in wind tunnel experiments and the theoretical description of sound propagation in rotational flows. In 2004 he returned back to the DLR in Göttingen. In 2008 he received his habilitation in aeroacoustics from the Technical University of Berlin. Recently he started to work in the field of aerodynamics and aeroacoustics of high speed trains.

A new test facility for the study of unsteady aerodynamics and aeroacoustics of high speed trains

Wednesday, 10th August, 9:00 - 10:00

The operation of modern high speed trains involves many technical and fundamental problems. Some of these are crucial for the further development of faster and more energy efficient trains. One example is the generation of compression waves during tunnel entry. The waves propagate at speed of sound through the tunnel and are partly reflected at the open end. Some part of the wave energy is emitted as sound wave to the exterior. Both the reflected and the emitted wave can cause problems. The reflected wave hits the incoming train in the tunnel and leads to strong pressure fluctuations at the train. To prevent discomfort or even injury from the passengers the wagons of high speed trains must be pressure sealed, which leads to extra weight of the trains and thereby higher energy consumption. Additionally the emitted waves can cause inconvenience in the neighborhood of tunnel portals. To reduce both effects modern tunnels are constructed with extended portals, which have special openings to reduce the compression waves. Before such constructions are realized extensive numerical and experimental studies have to be performed to proof the efficiency of the design.
Recently a new test facility was build where the generation of the compression waves can be studied using downscaled model trains. An important parameter for the generation process is the Mach number. To be comparable with the full scale world the Mach number in the experiments has to match the value of the real train. This means that the model trains have to run at the same speed as full scale high speed trains. To achieve this the model trains are accelerated by a hydraulic driven catapult. After the acceleration phase the models run on the track at nearly constant speed through a model tunnel. The velocity of the model vehicle is adjusted by the hydraulic pressure. The maximum speed is $100\,\mathrm{m\,s^{-1}}$. The track has a length of about 65 m, and the rail gauge is 57.5 mm. This corresponds to a scaling of 1:25. The facility is designed for model scales between 1:20 and 1:100. The maximum weight of a model is 10 kg. The models are gently decelerated at the end of a track in a long chamber which is filled with small expanded polystyrene spheres.
Beside the topic of tunnel entry and compression waves the new moving model facility allows the investigation of much more phenomena which are difficult to simulate in ordinary wind tunnels. These are for example the effect of unsteady cross wind on the stability of trains or unsteady slip stream effects due to train passage.

Prof Adélia Sequeira

Technical University of Lisbon
Instituto Superior Técnico
Department of Mathematics
Division of Applied Mathematics and Numerical Analysis
Av. Rovisco Pais, 1
1049-001 Lisboa, Portugal

adelia.sequeira@math.ist.utl.pt

Adélia Sequeira is a full Professor at the Mathematics Department of the IST (Instituto Superior Técnico) at the Technical University of Lisbon in Portugal. She earned a Doctoral Degree in Numerical Analysis in 1981, at École Polytechnique in Paris, France, and a second PhD degree in Mathematics in 1985, at the Faculty of Sciences of the University of Lisbon, Portugal. In January 2001 she was awarded the Habilitation degree in Applied Mathematics and Numerical Analysis at IST. She has been the Director of the Research Centre on Mathematics and its Applications (CEMAT/IST) in the period 2001-2007 and vice-Director since 2008. Her research interests are mainly directed at mathematical and numerical analysis in fluid dynamics, with particular emphasis on viscoelastic non-Newtonian fluids as well as on hemodynamic and hemorheological studies.

Absorbing boundary conditions for 3D fluid-structure interaction problems to model blood flow in compliant vessels

Thursday, 9th August, 9:00 - 10:00

Blood flow interacts mechanically with the vessel wall, giving rise to pressure waves propagating in arteries, which deform under the action of blood pressure. In order to capture these phenomena, complex fluid-structure interaction (FSI) problems must be considered, coupling physiologically meaningful models for both the blood and the vessel wall. From the theoretical point of view, this is extremely difficult because of the high non-linearity of the problem and the low regularity of the displacement of the fluid-structure interface. So far, mathematical results have been obtained only in simplified cases. From the numerical point of view, the use of partitioned schemes, which solve iteratively the fluid and the structure sub-problems, supplied with suitable transmission conditions, is difficult to handle in hemodynamic problems, due to the large added mass effect. In this talk we introduce some recent mathematical models of the cardiovascular system, in particular non-Newtonian blood flow models, and comment on their significance to yield realistic and accurate numerical results. Simulations of the mechanical interaction between blood flow and vessel walls will be shown. A 3D FSI model in a compliant vessel is used to describe the pressure wave propagation. The 3D fluid is described through a shear-thinning generalized Newtonian model and the structure by a 3D hyperelastic model. In order to cope with the spurious reflections due to the truncation of the computational domain, several absorbing boundary conditions are analyzed. Firstly, a 1D hyperbolic model that effectively captures the wave propagation nature of blood flow in arteries is coupled with the 3D FSI model. Moreover, absorbing boundary conditions obtained from the 1D model are imposed directly on the outflow sections of the 3D FSI model, and numerical results comparing the different absorbing conditions in an idealized vessel are presented. Results in a realistic carotid bifurcation and in a patient-specific aneurysm are also provided in order to show that the proposed methodology can be applied to physiological geometries.

Prof Rainer Hollerbach

University of Leeds
School of Mathematics
Department of Applied Mathematics
Astrophysical and Geophysical Fluid Dynamics
Woodhouse Lane
Leeds LS2 9JT, United Kingdom

rh@maths.leeds.ac.uk

Rainer Hollerbach grew up in Fairbanks, Alaska, as the son of German emigrants. Following a year at the University of Alaska, he transferred to the University of Chicago, graduating in 1985 with a BA in physics. He did his PhD in geophysics at the University of California San Diego in 1990, studying aspects of the Earth's magnetic field. He spent the next five years in various postdoc positions at the Universities of Newcastle and Exeter in England and Los Alamos National Laboratory in New Mexico, USA. In 1995 he returned to Britain to take up a lectureship in the Department of Mathematics at the University of Glasgow, Scotland. In 2005 he moved to the Department of Applied Mathematics at the University of Leeds, England, where he is currently professor. During his time in Glasgow and Leeds he has also been on sabbatical several times, including a year at Princeton University, a year at Brandenburg Technical University Cottbus (supported by the German Alexander von Humboldt Foundation), a semester at Monash University, Australia, and currently a two year position as visiting professor at the Swiss Federal Institute of Technology Zurich. In 1994 he was awarded a Doornbos Memorial Prize by the Studies of the Earth's Deep Interior Symposium; in 1999 he was awarded a Macelwane Medal by the American Geophysical Union. His research interests continue to revolve around geophysical and astrophysical fluid dynamics, with a particular emphasis on numerical/theoretical modeling of liquid metal experiments.

Theory of liquid metal experiments in rotating cylinders and spheres

Friday, 9th August, 9:00 - 10:00

The Earth's magnetic field is produced by so-called dynamo action in its molten iron outer core. Stars and other astrophysical objects often also have associated magnetic fields, which can significantly influence their structure and evolution. There is therefore considerable interest in performing geophysically and/or astrophysically motivated laboratory experiments involving liquid metals. In this talk I will review four possible such experiments involving liquid metals and externally imposed magnetic fields. Specifically, I will consider cylindrical and spherical geometries, and mechanical and electromagnetic forcing, yielding the four cases

1. Cylindrical Geometry, Mechanical Forcing, e.g. [1, 2, 3].
2. Cylindrical Geometry, Electromagnetic Forcing, e.g. [4].
3. Spherical Geometry, Mechanical Forcing, e.g. [5, 6, 7].
4. Spherical Geometry, Electromagnetic Forcing, e.g. [8]

I will present the relevant theory underlying each configuration, their similarities and differences to one another, and prospects for future experimental developments.

References

[1] Hollerbach, R., Rüdiger, G.: New type of magnetorotational instability in cylindrical Taylor-Couette flow. *Phys. Rev. Lett.* **95**:124501, 2005.
[2] Stefani, F., Gundrum, T., Gerbeth, G., Rüdiger, G., Schultz, M., Szklarski, J., Hollerbach, R.: Experimental evidence for magnetorotational instability in a Taylor-Couette flow under the influence of a helical magnetic field. *Phys. Rev. Lett.* **97**:184502, 2006.

[3] Hollerbach, R., Teeluck, V., Rüdiger, G.: Nonaxisymmetric magnetorotational instabilities in cylindrical Taylor-Couette flow. *Phys. Rev. Lett.* **104**:044502, 2010.
[4] Rüdiger, G., Schultz, M., Shalybkov, D., Hollerbach, R.: Theory of current-driven instability experiments in magnetic Taylor-Couette flows. *Phys. Rev. E* **76**:056309, 2007.
[5] Hollerbach, R., Skinner, S.: Instabilities of magnetically induced shear layers and jets. *Proc. Royal Soc. A* **457**:785, 2001.
[6] Sisan, D. R., Mujica, N., Tillotson, W. A., Huang, Y.-M., Dorland, W., Hassam, A. B., Antonsen, T. M., Lathrop, D. P.: Experimental observation and characterization of the magnetorotational instability. *Phys. Rev. Lett.* **93**:114502, 2004.
[7] Nataf, H.-C., Alboussière, T., Brito, D., Cardin, P., Gagnière, N., Jault, D., Schmitt, D.: Rapidly rotating spherical Couette flow in a dipolar magnetic field: An experimental study of the mean axisymmetric flow. *Phys. Earth Planet. Inter.* **170**:60, 2008.
[8] Hollerbach, R., Wei, X., Jackson, A.: Electromagnetically driven flows in a rapidly rotating spherical shell. *in preparation.*

Session I
Turbulent flows
Tuesday, 9th August, 10:20 – 11:20

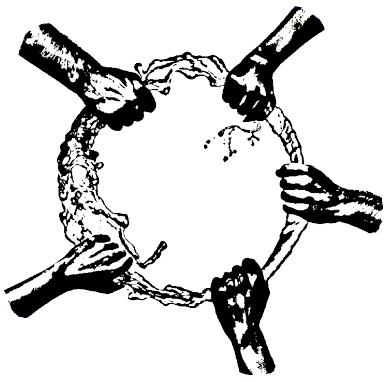

Degrees of Freedom and Energy Spectra for SQG Turbulence

Luke A. K. Blackbourn, Chuong V. Tran and Richard K. Scott
School of Mathematics and Statistics, University of St Andrews, Scotland

Abstract:

The Surface Quasi-Geostrophic (SQG) equation

$$\frac{\partial \theta}{\partial t} + J(\psi, \theta) = \nu \Delta \theta, \tag{1}$$

$$\theta = (-\Delta)^{1/2} \psi \tag{2}$$

is a popular model for geostrophic fluids [1], derived by considering the surface temperature in a rapidly rotating, stratified, uniform potential vorticity field. Here, $\theta(x, y, t)$ is the potential temperature, Δ is the Laplacian, $J(\cdot, \cdot)$ is the Jacobian, defined by $J(f, g) = f_x g_y - f_y g_x$, and ν is the viscosity.

While similar in style to the two-dimensional Navier-Stokes equation, the different relationship between the streamfunction ψ and the active scalar θ renders this system closer to the three-dimensional Navier-Stokes system in some senses [2]. For example, it is generally assumed that in the inviscid limit, the energy dissipation rate remains nonzero, tending to a finite value, unlike the two-dimensional Navier-Stokes system, which has been shown to have vanishing enstrophy dissipation in this limit [3]. Using Kolmogorov theory [4], a $k^{-5/3}$ energy spectrum has been predicted in the energy inertial range, although so far numerical evidence for this is limited and inconclusive.

This talk discusses an analytic alternative, developed in [5], to Kolmogorov theory. The idea is to use local Lyapunov exponents, which can quantify the stability of perturbations to solutions of the SQG equation in phase space. It is shown that the number of degrees of freedom scales like $\Re^{3/2}$, where $\Re$ is the Reynolds number defined in terms of the energy dissipation rate, the viscosity and the domain length scale. By assuming that the number of degrees of freedom is comparable to the number of active Fourier modes, as well as the classical assumption of non-zero energy dissipation in the inviscid limit, it is shown that if the energy spectrum in the energy inertial range has a form $k^{-\alpha}$, then $\alpha = 5/3$ is the only admissible solution, thus confirming the classical result.

Comparing the number of active Fourier modes with the derived number of degrees of freedom also yields the scaling $r = \nu k_\nu^2 \sim \Re^{1/2}$ for the energy dissipation rate r at the energy dissipation wavenumber k_ν. A comparison of this result with the scaling of r for other similar well-known systems, such as the one-dimensional Burgers equation, and the two- and three-dimensional Navier-Stokes equations, highlights the differences in small-scale dynamics between these systems. For example, while the Burgers equation exhibits fully quadratically nonlinear dynamics, leading to finite-time singularities, the two-dimensional Navier-Stokes equation can behave almost linearly, with vorticity gradients growing at most exponentially in time.

Finally, results from a number of direct simulations are presented, which agree with both the classical theory and the results presented here, as well as giving some justification for the assumption of non-zero energy dissipation in the inviscid limit.

References

[1] Pedlosky J., (1987), *Geophysical Fluid Dynamics*, 2nd Edn. Springer.

[2] Constantin P., Majda A., Tabak E., (1994), Formation of strong fronts in 2D quasigeostrophic turbulence, *Nonlinearity, vol. 7, pp. 1495-1533.*

[3] Tran C. V., Dritschel D. G., (2006), Vanishing enstrophy dissipation in two-dimensional Navier- Stokes turbulence in the inviscid limit, *J. Fluid Mech., vol 559, pp. 107-116*

[4] Pierrehumbert R. T., Held I. M., Swanson K. L., (1994) Spectra of local and nonlocal two-dimensional turbulence, *Chaos Solitons Fract., vol. 4, pp. 1111-1116*

[5] Tran C. V., Blackbourn L. A. K., (2009), Number of degrees of freedom of two-dimensional turbulence, *Phys. Rev. E, vol. 79, 056308.*

[6] Tran C. V., Dritschel D. G., (2009), Energy dissipation and resolution of steep gradients in one-dimensional Burgers flows, *Phys. Fluids, vol. 22, 037102.*

[7] Tran C. V.,(2009), Number of degrees of freedom of three-dimensional Navier-Stokes turbulence, *Phys. Fluids, vol. 21, 125103.*

Energy spectrum power-law decay of linearized perturbed shear flows

Stefania Scarsoglio [1], F. De Santi [1], M. Mastinu [1], G. Barletta [1], K. Weaver [2] and D. Tordella [1]

[1] Department of Aeronautics and Space Engineering, Politecnico di Torino, Torino, Italy
[2] Department of Aeronautics and Astronautics, MIT, Cambridge, Massachusetts USA

Abstract:
The -5/3 power-law scaling of the energy spectrum in the inertial range is a well-known notion in the phenomenology of turbulence (in the sense of Kolmogorov 1941), and it is confirmed both in laboratory and numerical simulations (see for instance [1]). We propose to study the state that precedes the onset of instability and transition to turbulence to: (a) understand whether the nonlinear interaction among different scales in fully developed turbulence can affect the energy spectrum, and to (b) quantify the level of generality on the value of the energy decay exponent of the inertial range. In this condition, the system shows all the features (e. g. linearized convective transport, linearized vortical stretching, and molecular diffusion) as those characterizing the turbulent state, except the nonlinear interaction. The perturbative transient dynamics, which is governed by the initial-value problem related to the linearized perturbative Navier-Stokes equations, is very complicated and shows a great variety of different behaviours [2, 3]. We ask whether the linearized perturbative system is able to show a power-law scaling for the energy spectrum in an analogous way to the Kolmogorov argument [4].

We determine the decay exponent of the energy spectrum for arbitrary three-dimensional perturbations acting on three different typical shear flows - i.e. the bluff-body wake, the cross-flow boundary layer and the plane Poiseuille channel flow - for stable and unstable configurations. Then, we evaluate the energy spectrum of the linearized perturbative system - as the wavenumber distribution of the perturbation kinetic energy density in asymptotic condition - and we compare it with the well-known -5/3 Kolmogorov power-law scaling.
In general, we observe about a decade ($k \in [2, 20]$ and $k \in [15, 150]$ for the bluff-body wake and the plane Poiseuille flow, respectively) where longitudinal and oblique perturbations present a power-law decay which is close to -5/3 (violet curves), while purely three-dimensional waves have a decay of about -2 (red curves). For larger wavenumbers ($k > 20$ and $k > 150$ for the bluff-body wake and the plane Poiseuille flow, respectively), all perturbations show a power-law decay very close to -2 (red curves). For longer waves ($k < 1 - 2$ and $k < 10$ for the bluff-body wake and the plane Poiseuille flow, respectively), results do not seem to reveal any characteristic nor universal behavior. The energy spectrum strongly depends, here, on initial and boundary conditions.
This scenario is confirmed by extensive data concerning the bluff-body wake (see (a) and (b) parts of Fig. 1) as well as preliminary results for the plane Poiseuille flow (part (c) of Fig. 1).

So far, we think it possible to formulate the hypotheses that the nonlinear interaction is maybe not the main factor responsible of the specific value of the -5/3 decay exponent in the energy spectrum and the spectral power-law scaling of intermediate waves is a general dynamical property of the Navier-Stokes solutions which encompasses the nonlinear interaction.

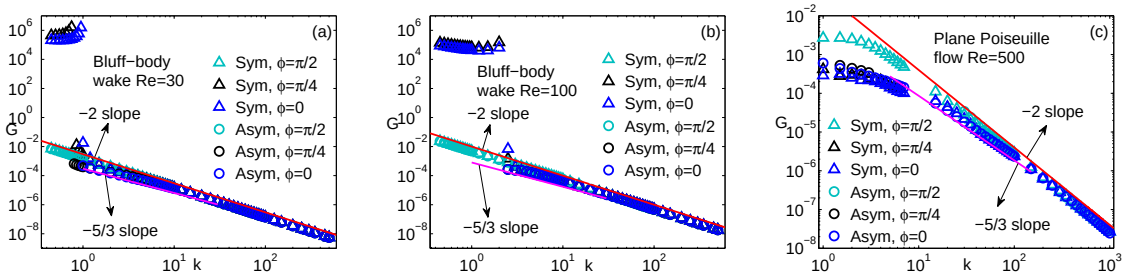

Figure 1: Energy spectrum G of symmetric (triangles) and asymmetric (circles) perturbations (blue: $\phi = 0$, black: $\phi = \pi/4$, light blue: $\phi = \pi/2$). (a)-(b) Bluff-body wake at $Re = 30$ (stable) and $Re = 100$ (unstable), respectively. (c) Plane Poiseuille flow at $R = 500$ (stable). Red and violet curves: -2 and $-5/3$ slopes, respectively.

References

[1] Sreenivasan K. R. and Antonia R. A., (1997), *Annu. Rev. Fluid Mech., vol. 29, pp. 35-72*
[2] Scarsoglio S., Tordella D. and Criminale W. O., (2009), *Stud. Applied Math., vol. 123(2), pp. 153-163*
[3] Criminale W. O., Jackson T. L., Lasseigne D. G. and Joslin R. D., (1997), *J. Fluid Mech., vol. 339, pp. 55-75*
[4] Frisch U., (1995): Cambridge University Press

Exploring turbulence using renormalization methods

S. R. Yoffe†, A. Berera

SUPA, School of Physics and Astronomy, University of Edinburgh, Edinburgh UK
† sam.yoffe@ed.ac.uk

Abstract:
The renormalization group (RG) is a systematic way of exploring the change in a system when viewed at different scales. It can be understood as a coarse-graining procedure, where one removes small lengthscales and studies the behaviour of those which remain. The additional degrees of freedom are integrated out, and their contribution absorbed into the surviving variables. If the system looks the same under this transformation, it is said to be invariant under the renormalization group.

RG methods have been widely used in physics and have enjoyed huge success in many areas, ranging from statistical physics and the study of critical phenomena, to the substantial role they play in particle physics and theories such as quantum electrodynamics (QED) and its strong cousin. They have been used to develop renormalized perturbation theories (RPTs) and have seen uses in defining schemes for numerical work such as large eddy simulation (LES).

Forster, Nelson and Stephen (FNS) [1] used a dynamic RG procedure to study the large-scale, long-time behaviour of randomly stirred hydrodynamics. As small lengthscales are removed, the affect of the lost scales are absorbed into a renormalized viscosity and force. The procedure was extended and repeated by several authors [2, 3, 4, 5, 6], who arrived at contradicting results depending on the method used. It all came down to the validity of a substitution FNS made to evaluate a self-energy integral. Since the FNS approach has found application in many areas such as soft-matter physics and magnetohydrodynamics (for example [7, 8]), this disagreement on the methodology was investigated by us in [9] where it was shown that the substitution is valid, and that all the approaches are in fact compatible and, if treated correctly, all lead to the original result of FNS.

I present an introduction to the renormalization group and its general application, before discussing its applicability to turbulence. An overview of the dynamical procedure used by FNS is given along with validation of their result using the approaches of other authors. Finally, some applications of renormalization methods in turbulence are outlined.

References

[1] Forster D., Nelson D. and Stephen M., (1977), Large-distance and long-time properties of a randomly stirred fluid, *Phys. Rev. A, vol. 16, pp. 732-749*

[2] Yakhot V. and Orszag S. A., (1986), Renormalization group analysis of turbulence. I. Basic theory, *J. Sci. Comp., vol. 1, pp. 3-51*

[3] Ronis D., (1987), Field-theoretic renormalization group and turbulence, *Phys. Rev. A, vol. 36, pp. 3322-3331*

[4] Wang X.-H. and Wu F., (1993), One modification to the Yakhot-Orszag calculation in the renormalization-group theory of turbulence, *Phys. Rev. E, vol. 48, pp. 37-38*

[5] Teodorovich É. V., (1994), On the Yakhot-Orszag theory of turbulence, *Fluid Dynamics, vol. 29, pp. 770-779*

[6] Nandy M. K., (1997), Symmetrization of the self-energy integral in the Yakhot-Orszag renormalization-group calculation, *Phys. Rev. E, vol. 55, pp. 5455-5457*

[7] Medina E., Hwa T., Kardar M. and Zhang Y. C., (1989), Burgers equation with correlated noise: Renormalization-group analysis and applications to directed polymers and interface growth, *Phys. Rev. A, vol. 39, pp. 3053-3075*

[8] Fournier J.-D., Sulem P.-L. and Pouquet A., (1982), Infrared properties of forced magnetohydrodynamic turbulence, *J. Phys. A, vol. 15, pp. 1393*

[9] Berera A. and Yoffe S. R., (2010), Reexamination of the infrared properties of randomly stirred hydrodynamics, *Phys. Rev. E, vol. 82, pp. 066304*

On friction velocity in turbulent channel flow over wind waves

Andrey Zavadsky[1]

[1] School of Mechanical Engineering, Tel-Aviv University

Abstract:
Friction velocity u_* is one of the most important parameters in boundary layer investigations in general, and in particular in studies of water waves' excitation by wind as it is directly related to momentum and energy transfer from air to water. For that reason the friction velocity is routinely used as a scaling factor in nondimensional groups that determine wind-wave field evolution. Accurate determination of u_* is thus of paramount importance. Detailed comparison between two methods to measure u_* in a laboratory wind-wave flume is carried out. The facility consists of a wind tunnel capable of generating wind speed that may exceed 15 m/s atop of a 5 m long wave tank. The description of the experimental facility is given in [1].

The friction velocity is most often determined from the logarithmic fitting of the mean velocity vertical profile $\overline{u(z)}/u_* = (1/\kappa)log(z/z_0)$, where κ is the von Karman constant and z_0 the typical roughness due to wind waves. Alternatively, the values of u_* can be estimated from the vertical distribution of the Reynolds shear stress, $u_* = \lim_{z\to 0}\sqrt{-\overline{u'w'}}$. Note that in the channel flow the total shear stress $\tau = \rho u_*^2 = \mu\partial u/\partial z - \rho\overline{u'w'}$ varies with z due to the pressure gradient p/x. The mean velocity profile $\overline{u(z)}$ is measured by a Pitot tube connected to a sensitive pressure transducer. Hot film anemometry with an X-shaped probe is used to measure the vertical distribution of the Reynolds shear stress. Detailed measurements at different conditions were performed in air and water to accumulate sufficient data for statistical analysis.

The measured mean velocity profiles and the corresponding data on the Reynolds shear stresses are presented in Figure 1 and Figure 2 respectively. In Figure 3(a-b) the comparison of the values of u_* obtained with two methods is shown. It can be clearly seen that the values from the logarithmic profile are consistently higher by about 10-20% than those obtained with thermal anemometry. Other researchers [2] also obtained somewhat higher values of u_* from the logarithmic velocity profiles as compared to the eddy correlation (Reynolds stresses) method and attempted to resolve this inconsistence by suggesting a lower value of . The essential differences between the two methods in relation to wind waves' studies will be discussed. We argue that the values of u_* obtained from Reynolds shear stress are advantageous as they are based on direct measurements, in spite of extrapolation required. The correct estimates of u_* based on the slope of the logarithmic velocity profile, on the other hand, should take into account the wake region.

References

[1] Liberzon D. and Shemer L., (2011), Experimental study of the initial stages of wind waves' spatial evolution, *J. Fluid Mech., in press.*

[2] Tseng, R.-S, Hsu, Y.-H. L. and Jin Wu, (1992), Methods of measuring wind stress over a water surface – discussions of displacement height and von Karman constant, *Boundary-Layer Meteorol, vol. 58, pp. 51–68*

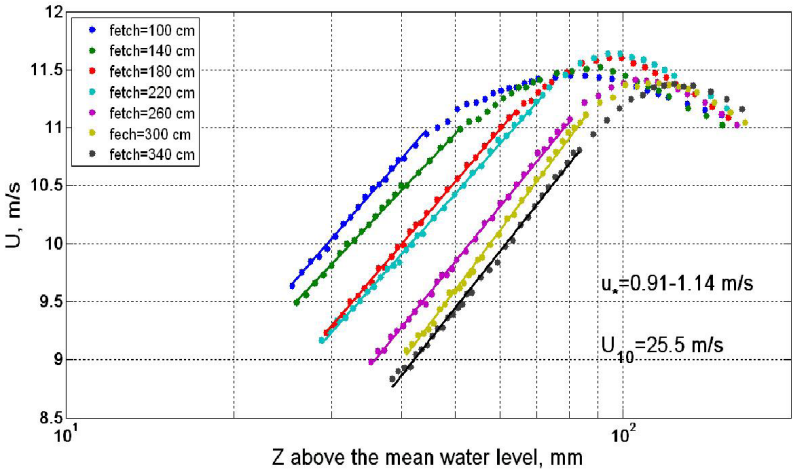

Figure 1: *Vertical distribution of the mean air velocity and the logarithmic fit.*

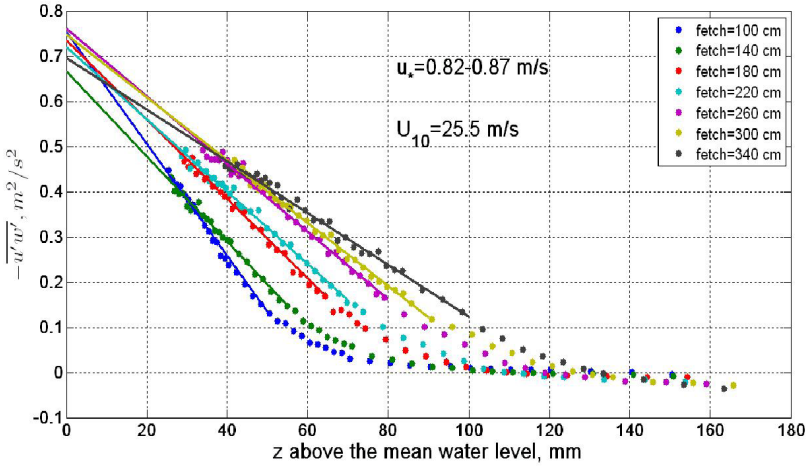

Figure 2: *Vertical distribution of Reynolds stress above the mean water surface.*

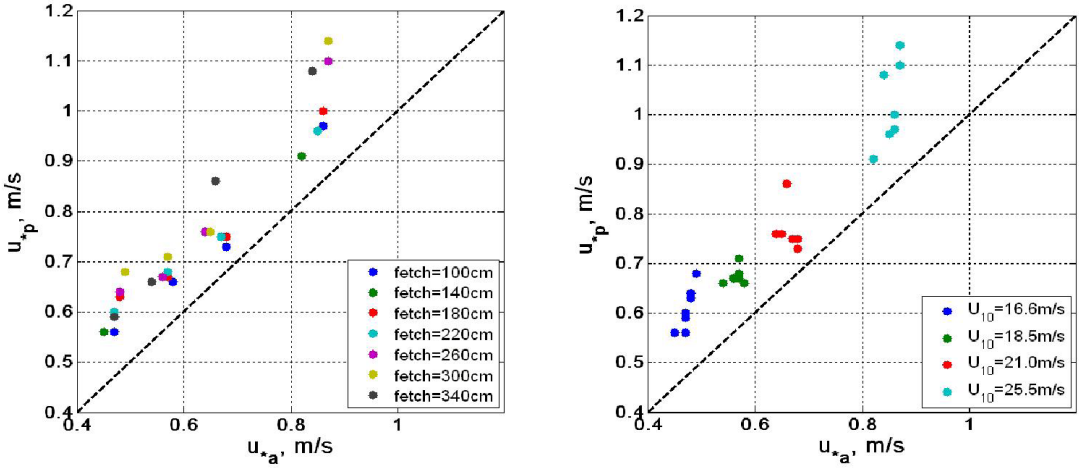

Figure 3: *Friction velocities obtained using the logarithmic fit (u_{*p}) vs. those from the eddy correlation method (u_{*a}): a) fetch dependence; b) as a function of mean wind velocity extrapolated to the height of 10* m.

Session II

Turbulence - Particles and stratification

Tuesday, 10th August, 11:30 – 12:30

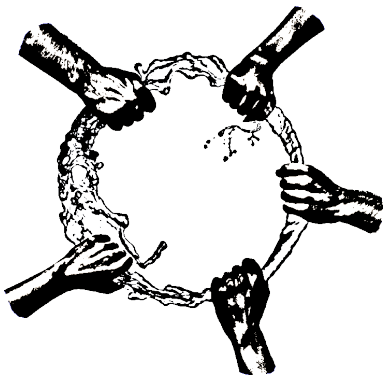

Two-dimensional shearless turbulent mixing: kinetic energy self diffusion, also in the presence of a stable stratification

F. De Santi [1], D. Tordella [1] and J. Riley [2]

[1] Dipartimento di Ingegneria Aeronautica e Spaziale, Politecnico di Torino, Italy
[2] Mechanical Engineering Department, University of Washington, WA

Abstract:
Two-dimensional turbulence is important in many natural and engineering contexts. It presents some special and interesting phenomena that does not occur in three dimensional turbulence. Moreover, it also idealizes geophysical phenomena in the atmosphere, oceans and magnetosphere and provides a starting point for the modeling of these phenomena [1].
In this contest, we would like to present new results concerning the energy turbulent transport in the simplest kind of two dimensional inhomogeneous flow, a turbulent shearless mixing process generated by the interaction of two isotropic turbulent fields with different kinetic energy but the same spectrum shape [2]. The self diffusion of kinetic energy is observed in two cases: with or without a stable density stratification.
In the unstratified case the simulations of mixing with different values of the energy ratio show that, asymptotically in time (in the limit of the observed range), the turbulent diffusion is much larger than the one measured in three dimensions [3, 4, 7]. The analysis of the third and fourth moments of the velocity indicates that the flow is highly intermittent. Moreover, the temporal autocorrelation of the vorticity, at some fixed points, does not depend on the ratio of energy used and on the position.. We can interpret these results as the proof of the existence of a long-range interaction..
In the stratified case the evolution of the flow changes significantly [5, 6]. The energy profile in the mixing region is lower than the minimum value imposed by the initial condition, and therefore we can interpret this as an energy hole. we can interpret this as an energy hole. Finally, the velocity skewness enlightens the generation of an inverse energy flow and intermittent penetration from the low to the high energy field even in the case of mild stratification.

References

[1] Kellay H. and Goldburg W., (2002), Two-dimensional turbulence: a review of some recent experiment, *Rep. Prog. Phys., vol. 65, 845-894*

[2] Veeravalli S. and Warhaft Z. (1989), The shearless turbulence mixing layer, *J. Fluid. Mech., vol.207, 191-229*

[3] Tordella D., Iovieno M. and Bailey P.R., (2008) Sufficient condition for Gaussian departure in turbulence, *Phys.Rev., vol.77*

[4] Tordella, D. and Iovieno, M., (2006), Numerical experiments on the intermediate asymptotic of shear-free turbulent transport and diffusion, ,phJ.Fluid Mech., vol. 549, 429-441

[5] Riley J. and Lelong M.P., (2000), Fluid Motions in the presence of strong stable stratification,*Ann. Rev. Fluid Mech., vol. 32, 617-657*

[6] Riley J. and deBruynKops S.M., (2003), Dynamics of turbulence strongly influenced by buoyancy, *Phys. Fluids, vol. 15, 2047-2059*

[7] Tordella D. and Iovieno M., (2011) Small scale anisotropy in the turbulent shearless mixing. Under revision for *Phys. Rev. Lett.*.

Numerical Study of Particle-Turbulence Interaction in a homogeneous Flow

T. Doychev [1], and M. Uhlmann [1]

[1] Institute for Hydromechanics, KIT, Karlsruhe, Germany

Abstract:
In the present work we have investigated finite size and finite Reynolds number effects of particle laden turbulent homogeneous flow by direct numerical simulation.
The ratio between the particle diameter D and Kolmogorov length scale η is of order $\mathcal{O}(10)$. The terminal particle Reynolds number Re_D based upon the particle diameter, the particle terminal velocity w_∞ and the fluid kinematic viscosity ν is of order of $\mathcal{O}(100)$. The particle terminal velocity w_∞ is defined as the settling velocity of a single particle in an ambient fluid based on the balance between drag and buoyancy using the standard drag formula from [1]. The Stokes number is of order of $\mathcal{O}(10)$. Under these conditions, the point-particle approach loses its validity and in order to describe the flow the interface between the dispersed- and carrier-phase is fully resolved by means of the immersed boundary method [2]. In this work the two-phase flow is dilute, i.e. the volume fraction is set to be below 0.5 %. Therefore dominant effects of inter-particle collisions are avoided.
In order to better understand the effect of the turbulence two types of simulations were performed. In the first, particles are released from rest in an ambient fluid. In the second, particles with the same physical properties are released in a turbulent homogeneous flow field (initially isotropic). Further the effect of the particle Reynolds number was investigated. For this reason two simulations with different particle Reynolds number from the first type were performed. In this study the analysis will focus on three topics: (i) how is the particle settling velocity affected by the presence of turbulence, (ii) what is the spatial structure of the dispersed phase (cluster formation, preferential concentration) and (iii) how is the turbulence flow field affected by the presence of the particles. In this work particular care has been taken to meet the resolution requirements (small scales, box size and time step) of the two-phase flow.

References

[1] Clift R., Grace J.R. and Weber M.E., (1978), *Bubbles, drops and particles*, Academic Press

[2] Uhlmann M., (2005): An immersed boundary method with direct forcing for the simulation of particulate flows, *J. of Comp. Phys., vol 209, pp. 448-476*

3D turbulence modelling extended to thermal stratification

Peter Torma [1]

[1] Department of Hydraulic and Water Resources Engineering, Budapest University of Technology and Economics, Budapest, Hungary

Abstract:
Temperature gradient has an important effect on the flow field by causing buoyancy through density differences and gravitational force. Such stratified flows are common and important in many different domains of fluid mechanics and hydraulic engineering. Buoyancy plays a key role e.g. in case of gravity currents in lakes and reservoirs driven by solar radiation or due to thermal plumes. Buoyancy causes an increase of the turbulence level in unstably stratified situations and a suppression of the turbulence production in stably stratified flow regions, thus stratification effects are included in turbulence models.

The main goal of this study was to upgrade the well-known (low Reynolds number) k-ε two-equation turbulence closure model in the CFD model Panormus so that thermal stratified turbulent flows can be also modelled. Panormus is an open-source community model that solves the Navier-Stokes 3D momentum equations for incompressible fluids using curvilinear non-orthogonal grids with a finite volume method. The standard k-ε model had been originally developed for constant density flows, so within this work it had to be completed with the required buoyancy terms to quantify the thermal gradient's effect in turbulent kinetic energy (TKE) production and dissipation. Two different approaches were built in and analysed: the standard (SGDH) and the general (GGDH) gradient diffusion hypothesis. The latter also considers turbulent velocity fluctuation in the production and dissipation of TKE.

The laboratory experiment used to verify the two different approaches and their model parameters consisted of a water surface heated and cooled at two, horizontally opposite ends of a closed basin generating vertical circulation, which is a simple model of the Great Ocean Conveyor. In this case the observed circulation did not penetrate the layers near the bottom due to the stable stratification. Computed results are compared to these observations. As regards the choice between the buoyancy models and their parameters, formulations are proposed in the literature but they are somewhat controversial. Furthermore most buoyant turbulent models were developed and applied in the area of industrial fire safety engineering and pollutant dispersion. Best agreements were usually obtained with the GGDH approach for buoyant plumes, whereas the SGDH model brought little improvement in velocity and temperature predictions. In our case the SGDH model shows significant improvement against the original model that does not contain buoyancy term in the TKE production and dissipation. With the SGDH the simulated flow pattern and thermal stratification is close to the measured one. In contrast, the GGDH approach gives poor results: a less stable stratification develops and later disappears by mixing processes. It over-predicts the turbulence level. Finally, we found that the flow or temperature field is little sensitive to the new constant added to the k-ε model to account for buoyancy.

Resuspension of particles in turbulent flows using PIV and 3D-PTV

Traugott H [1], Hayse T [2] and Liberzon A [1]

[1] Turbulence Structure Laboratory, School of Mechanical Engineering, Tel Aviv University, Tel Aviv, Israel
[2] Department of Civil and Environmental Engineering, MIT, MA, U.S.A

Abstract

Resuspension of particulate material exposed to a moving fluid is a common occurrence in nature (erosion of soil and river beds) and an important mechanism in a variety of applications such as silicon wafer cleaning, safety measures in nuclear waste and accidental releases, transport of hazards and poisons to the environment. Although there was a significant progress in the field of sediment processes during the past decades, the prediction of the flow conditions at which incipient motion occurs is still one of the most difficult problems in sediment transport. The processes of detachment of a particle from a surface and reentrainment into suspension have not been fully clarified yet. This is partially related to the fact that only few experiments report the precise mode of incipient motion or observed directly the motion of particles at the beginning, during and after the detachment.

Different criteria and models have been proposed to define threshold conditions for the particle incipient motion. Majority assumes particle-turbulence interaction to have a major influence on the phenomena[2, and references therein]. Moreover, entrainment was observed to occur not as completely random process but rather as an intermittent process with groups of particles being suspended. The observations led to models that consider turbulent coherent structures with large vertical velocity components, v, that exceed the particle settling velocity, v_s, to be responsible for the incipient motion. Since in boundary layers velocity components are proportional to the friction velocity, $u_* = \sqrt{\tau_w/\rho}$, the critical conditions for the initiation of suspension (pick up or lift off) are defined in terms of friction velocity, i.e. $u_*/v_s \geq 1$. However, some works reported critical values to be much lower, e.g. $u_*/v_s = 0.25 \div 0.85$. [1, 3].

This study explores the necessary conditions for initial entrainment of particles from smooth and rough beds into zero-mean-shear turbulent flow in an oscillating grid chamber The experiment is not designed to fully mimic the real problem of sediment transport but rather identify key mechanisms, utilizing direct observation and quantification of particle motion at the beginning, during and after lift-off. In the experimental setup, particle image velocimetry (PIV) and three-dimensional particle tracking velocimetry (3D-PTV) are used to determine the properties of turbulent flows and to track the movement of individual particles through the various phases of the resuspension. The combination of the experimental methods allow to correlate in a quantitative manner the flow conditions responsible for rolling, pick-up, detachment and reentrainment of partilces..

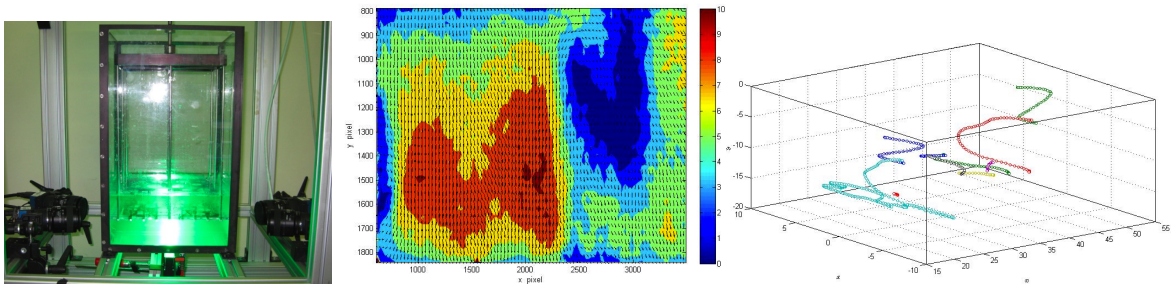

Figure 1: (a) Oscillating grid chamber and 3D-PTV system (b) Velocity field obtained using PIV in oscillating grid chamber. (b) Trajectories of suspended particles.

References

[1] P. Medina, M. A. Sánchez, and J. M. Redondo. Grid stirred turbulence: applications to the initiation of sediment motion and lift-off studies. *Physics and Chemistry of the Earth, Part B: Hydrology, Oceans and Atmosphere*, 26(4):299–304, 2001.

[2] Y. NiNo, F. Lopez, and M. Garcia. Threshold for particle entrainment into suspension. *Sedimentology*, 50(2):247–263, 2003.

[3] J. J. Orlins and J. S. Gulliver. Turbulence quantification and sediment resuspension in an oscillating grid chamber. *Exp. Fluids*, 34(6):662–677, 2003.

Session III
Temperature and buoyancy driven flows
Tuessday, 9th August, 13:30 – 14:30

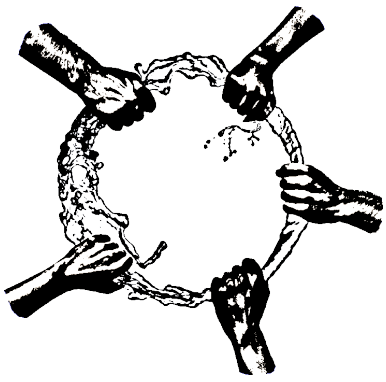

Velocity structures in turbulent Rayleigh-Bénard convection

L. Li [1], R. du Puits [2]

[1,2] Institute of Thermodynamics and Fluid Mechanics, Ilmenau University of Technology, Ilmenau, Germany
E-mail: l.li@tu-ilmenau.de

Abstract:
In our contribution the systematic study of high-resolution local velocity data measured in turbulent Rayleigh-Bénard (RB) convection will be presented. The aim of our study is to compare the measured velocity field inside the boundary layer with data coming from numerical simulation as well as with the theoretical predictions at moderate Rayleigh numbers. In order to reduce the Ra number in the experiment matching the highest one in the simulations ($Ra_{sim} = 3 \times 10^{10}$) we have installed a smaller sample with 2.5m diameter and 2.5m height in our big barrel (see Fig. 1). This will be the first time that a direct comparison between experimental and numerical data becomes possible at high Ra numbers. Our experiments were carried out in a RB convection system-"Barrel of Ilmenau". We investigate the mean velocity profiles close to the cooling plate of the RB system at four different locations. The experiments and the numerical simulation were conducted at the same Ra number $Ra = 3 \times 10^{10}$ and aspect ratios from $\Gamma = 1$ to $\Gamma = 5$, whereas the Prandtl number was fixed at $Pr = 0.7$. A 3D-Laser-Doppler-Anemometer (LDA) was applied in these measurements and the cold-atomized droplets of Di-Ethyl-Hexyl-Sebacat (DEHS) with a size of about $1\mu m$ as tracer particles were injected though an inlet close to the sidewall.

We plot the profiles of the mean horizontal velocity $\sqrt{u^2 + v^2}$ and of the wall-normal velocity component in Fig. 2.Along with the data, we plot the prediction of Prandlt/Blasius for a laminar shear layer over a flat plate. The graph shows that particularly in the outer region of the boundary layer the data deviates from the Prandlt/Blasius model. The mean of the wall-normal component tends to zero over the entire domain of our measurement. In our talk, we also will present profiles of the fluctuations as well as measurements at different positions and at different aspect ratios, which will show some details of how the local heat transport behaves.

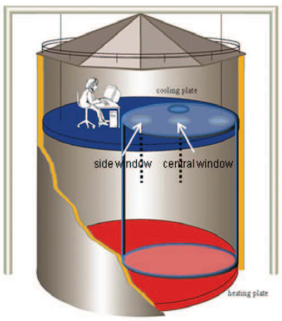

Figure 1: *Sketch of the inset in the "Barrel of Ilmenau" in which the experiment was performed. The lower plate is heated and the upper plate is cooled. The height and the diameter of the small cell are* $2.5m$.

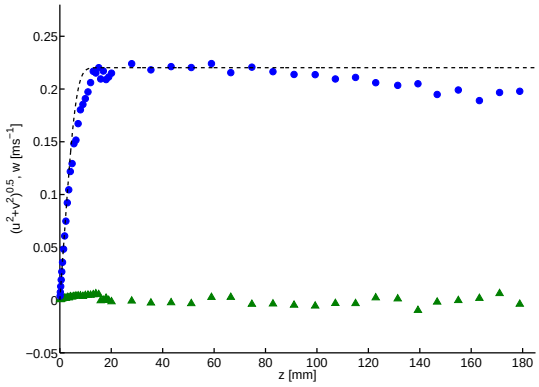

Figure 2: *Profiles of the mean horizontal velocity* $\sqrt{u^2 + v^2}$ *(solid circle) over the plate distance z compared with the Blasius solution (dashed line) as well as the wall-normal velocity component w (solid triangles) at aspect ratio* $\Gamma = 1$, $Ra = 2.88 \times 10^{10}$. *The velocity was measured at the central window.*

Investigation of convection in a rotating cavity

W. Wu [1], R. Pitz-Paal [2]

[1] Solar Research, German Aerospace Center (DLR), Stuttgart, Germany
[2] Solar Research, German Aerospace Center (DLR), Cologne, Germany

Abstract:
Almost one quarter of the world population is still without electricity. Especially in third world regions where no connection to a central power grid, but high insolation levels exist, small-scale concentrating solar power (CSP) systems (100 kW_{el} - 1 MW_{el}) are a promising way for decentralized and sustainable power generation. Therefore, a novel solar particle receiver concept in combination with a small gas turbine system is developed and optimized with regard to high efficiency, high durability and low costs. The inherent feature of storage is an important advantage against wind and photovoltaic technologies, providing dispatchable power.

A key characteristic of the concept is to exploit a receiver rotation in order to adjust the receiver outlet temperature to different load conditions. Within the scope of identifying the thermal receiver efficiency numerical and experimental investigations regarding convection losses of a rotating cavity are conducted.

Natural convection in rotating frames is a complex transport phenomenon. In order to determine the actual fluid motion centrifugal and Coriolis forces need to be taken under consideration along with buoyancy, momentum and viscous effects. The respective importance of buoyancy and rotation can be related by the dimensionless Rossby number Ro which is formed as [1]

$$Ro = \frac{\sqrt{g\beta\Delta T/L}}{2\Omega}, \tag{1}$$

with the gravitational acceleration g, the thermal expansion coefficient β, the temperature difference ΔT, a characteristic length scale L and the angular rotation speed Ω.

Preliminary CFD simulations of a horizontal cylindrical receiver with homogeneously heated side and back walls and a vertical cavity opening have been carried out indicating reduced convection losses due to rotation. As no rotation is induced ($Ro \to \infty$) a convective flow pattern well-known from literature ([2], [3]) can be observed: Cold ambient air enters the cavity at the lower half of the aperture and is then heated up at the lower hot wall. When encountering the back wall the air flows upwards, turns back along the upper wall and exits the cavity as a hot plume. While the fluid motion emerges mainly near the wall boundaries the cavity middle exhibits a relatively stagnant and stratified core. However, as the rotation rate increases with $Ro < 1$ the stratified temperature fields are tilted due to the combination of the vertical gravitational accelaration and the mainly horizontal Coriolis force. Since the Coriolis force dominates, the hot buoyancy flow is driven cavity inwards again and enhanced flow mixing occurs inducing a more uniform temperature distribution in space. In consequence of this, the temperature gradient between the hot air inside the cavity and the cold ambient air decreases leading to less energy and mass transfer across the aperture boundaries and therefore reduced heat losses. The presented results are in good qualitative agreement with numerical simulations done by Yang et al. [4] for a closed horizontal cylinder.

An experimental set-up with a model receiver in laboratory scale is built up in order to validate the numerical findings. The receiver walls are heated uniformly using heating wires whereas the convective heat losses can be measured by determining the difference between the electrical input power and the energy thermally emitted.

References

[1] Julien K., Legg S., McWilliams J. and Werne J., (1997), Rapidly rotating turbulent Rayleigh-Bernard convection, *J. Fluid Mech., vol. 322, pp. 243-273*

[2] Clausing A.M., (1981), An analysis of convective losses from cavity solar central receivers, *Solar Energy, vol. 27, pp. 295-300*

[3] Taumoefolau T., Paitoonsurikarn S., Hughes G. and Lovegrove K., (2004), Experimental investigation of natural convection heat loss from a model solar concentrator cavity receiver, *Journal of Solar Energy Engineering, vol. 126, pp. 801-807*

[4] Yang H.Q., Yang K.T. and Lloyd J.R., (1988), Rotational effects on natural convection in a horizontal cylinder, *AIChE Journal, vol. 34*

Buoyancy driven, multi-phase flow simulations with the Smoothed Particle Hydrodynamics

Kamil Szewc [1]

[1] Institute of Fluid-flow Machinery, Polish Academy of Sciences, ul. Fiszera 14, Gdańsk, Poland

Abstract:
The Smoothed Particle Hydrodynamics (SPH) is a fully lagrangian, particle-based technique for fluid-flow computations. This approach was independently proposed by Gingold & Monaghan [1] and Lucy [2] to simulate some astrophysical phenomena. The main idea behind the SPH approach is to introduce the kernel interpolants for flow quantities so that the fluid dynamics is represented by particle evolution equations. The main advantage over eulerian techniques is no requirement of the grid. Therefore, it is natural approach to simulate multi-phase or free-surface flows. Buoyancy driven, multi-phase flows are very common in many scientific and technological issues such nuclear reactor systems, foundry systems and many geophysical and astrophysical processes. Since in the SPH technique there is no necessity to track and locate the interfaces, this technique is one of the most relevant ways to simulate such flows. The SPH verification of the treatment of the natural convection phenomena has been done with the square wall-heated cavity flow. Obtained solutions have been compared with the benchmark data computed by de Vahl Devis using the second-order central difference scheme [3]. To simulate the multi-phase flows with large density differences, the Hu and Adams SPH variant has been used [4]. The validations of the surface tension SPH treatments has been performed with standard numerical tests: the square-droplet deformation, the Rayleigh-Taylor instability and the air bubble raising in a water (cf. Fig. 1).

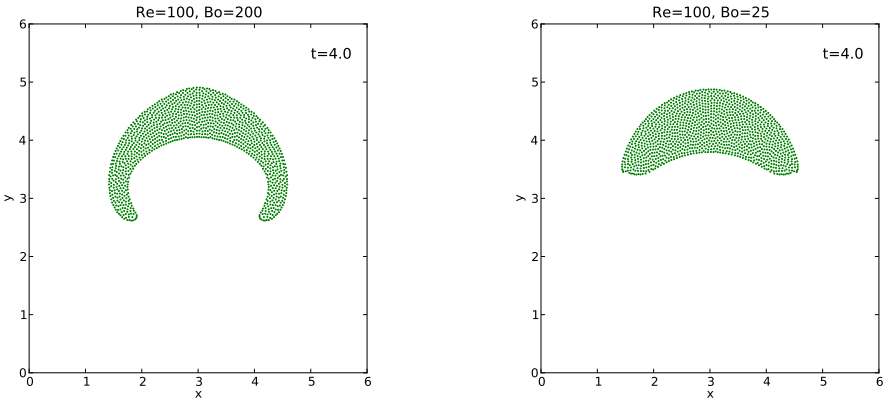

Figure 1: *The air bubble (initially circular) raising in a water. Data obtained with the medium Reynolds number ($Re = 100$) at $t = 4$. Left: $Bo = 200$ - low surface tension. Right: $Bo = 25$ - high surface tension.*

References

[1] Gingold R.A., Monaghan J.J., (1977), Smoothed Particle Hydrodynamics: Theory and Application to Non-spherical stars, *Mon. Not. R. Astron. Soc., vol.* ***181****, pp. 375-389*

[2] Lucy L.B., (1977), A numerical approach to the testing of the fission hypothesis, *Astron. J., vol.* ***82****, pp. 1013-1024*

[3] de Vahl Davis G., (1983), Natural convection of air in a square cavity, a bench mark numerical solution, *Int. J. Numer. Meth. Fluids, vol.* ***3****, pp. 249-264*

[4] Hu X.Y., Adams N.A., (2006), A multi-phase SPH method for macroscopic and mesoscopic flows, *J. Comput. Phys., vol.* ***213****, pp. 844-861*

The rise heights of fountains

H. C. Burridge and G. R. Hunt

Department of Civil and Environmental Engineering, Imperial College London, London, SW7 2AZ, UK.

Our study focuses on the rise heights of Boussinesq turbulent fountains of saline-aqueous solutions from an axisymmetric source. These fountains have been the subject of study by numerous researchers beginning with Turner [1] and their rise heights can be primarily described by a dependence on the Froude number at the fountain's source, $Fr_0 = w_0/\sqrt{r_0 g_0'}$, where w_0 is the vertical velocity at the source, g_0' the reduced gravity and r_0 the radius of the source (at $z = 0$). Through studying a diverse range ($0.4 \leq Fr_0 \leq 45$) of fountains, the results from our experiments add new insights into the nature and physics of fountains, in addition to confirming the results of previous studies.

Key to our results are two previously unreported features of turbulent fountain dynamics. Firstly, we observe that for a limited range of source conditions ($1.0 \leq Fr_0 \leq 1.7$) the initial rise height is *less* than the steady rise height. This is contrary to accepted fountain behaviour where the flow rises to an initial height, z_i, before a returning counterflow develops around the rising core of fluid. The momentum exchanged between the rising core and the downflowing counterflow lessens the fountain's rise height and turbulent fountains are then observed to fluctuate in height about a mean quasi-steady height, z_{ss}. Secondly, for fountains of $Fr_0 \geq 5.5$ the initial vortex, which forms at the fountain's front, separates from the main body of the fountain reaching heights, z_v, far in excess of the fountain's maximum height. Both of these features affect the rise height ratio, $\lambda = z_i/z_{ss}$, which Turner [1] reported as constant, $\lambda = 1.43$, for forced fountains. Examining the rise height ratio from our experiments leads us to propose a new classification of fountains into five classes (rather than the existing three) as shown in table 1.

We conclude that, except for highly forced fountains, it is not appropriate to assume a constant rise ratio.

Fountain class	Fr_0 **range**	λ **(low & high** Fr_0**)**	λ **trend for increasing** Fr_0	**Rise heights**
Very weak	0.4 - 1.0	1.1 & 1.0	Approximately constant	$z_{ss}/r_0 = 0.81 Fr_0^{2/3}$ $z_i \geq z_{ss}$
Weak	1.0 - 1.7	1.0 & 0.5	Strongly decreasing	$z_{ss}/r_0 = 0.86 Fr_0^2$ $z_i \leq z_{ss}$
Intermediate	1.7 - 2.8	1.4 & 1.3	Decreasing (to $\lambda \approx 1.0$) then increasing	$z_{ss}/r_0 = 0.86 Fr_0^2$ $z_i > z_{ss}$
Forced	2.8 - 5.5	1.0 & 1.45	Weakly increasing	$z_{ss}/r_0 = 2.46 Fr_0$ $z_i \geq z_{ss}$, $z_v > z_i$
Highly forced	≥ 5.5	1.45 & 1.45	Constant	$z_{ss}/r_0 = 2.46 Fr_0$ $z_i > z_{ss}$, $z_v > z_i$

Table 1: Summary of rise heights and rise height ratio trends for the five fountain classes.

References

[1] Turner J. S. (1966), Jets and plumes with negative or reversing buoyancy, *J. Fluid Mech., 26, 779-792*

Poster session
Tuesday, 9th August, 17:00 – 18:30

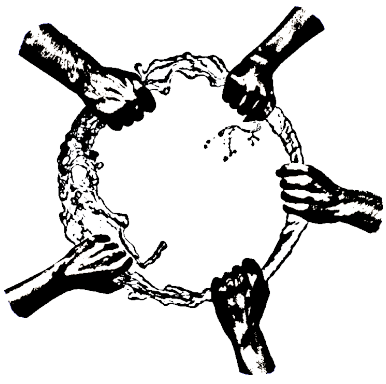

Microfluidic Drops as Tunable Bio-Environments

Christian Dammann [1], Bernd Nöding [1] and Sarah Köster [1]

[1] Institute for X-Ray Physics / Courant Research Centre Nano-Spectroscopy and X-Ray Imaging, Georg-August-Universität Göttingen, Germany

Abstract:
The structure and function of biological systems is determined by their bio-environment. Therefore, a drop-based microfluidic device is tailored to probe context-sensitivity of biological systems. In this device a series of monodisperse aqueous drops is created[1] and used as picoliter bio-compartments (fig. 1). The drops are subsequently manipulated by changing flow rates only and no steering by means of electrical fields is therefore necessary. This manipulation process starts with the change of drop composition from drop to drop. Thus, the biological system is encapsulated in drops with tunable chemical content. The drops are densified and a statistical fraction of the plentifully produced drops is collected. These drops are then stored in the device for long-time observations by means of constrictions in the microfluidic channel.[2] Our fluid manipulation method is designed to enable the reconstruction of the content composition of each individual drop. Possible applications of this tool are manifold. The device proves to be suitable for *in vitro* studies on cytoskeletal proteins. We focus on the assembly and network formation of vimentin intermediate filaments. The assembly of vimentin depends on the ionic strength of monovalent ions. By contrast divalent ions act as effective cross-linkers of vimentin networks.[3, 4] We are able to directly image the networks of the fluorescently tagged protein and show that divalent ions induce compaction of these networks. Our device demonstrates the well-defined conditions of low Reynolds number flow which can be used as a tool for studies in a broad range of research fields.

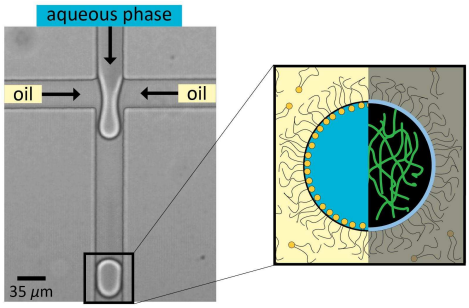

Figure 1: *We use the aqueous phase of a microemulsion as isolated containers for the encapsulation of bio-systems.*

References

[1] S. L. Anna, N. Bontoux and H. A. Stone (2003), Formation of Dispersions Using "Flow Focusing" in Microchannels, *Appl. Phys. Lett., 82, 364*

[2] C. H. J. Schmitz, A. C. Rowat, S. Köster and D. A. Weitz, (2009), Dropspots: A Picoliter Array in a Microfluidic Device, *Lab Chip, 9, 44-49*

[3] S. Köster, Y.-C. Lin, H. Herrmann and D. A. Weitz, (2010): Nanomechanics of Vimentin Intermediate Filament Networks, *Soft Matter, 6, 1910-1914*

[4] Y.-C. Lin, N. Y. Yao, C. P. Broedersz, H. Herrmann, F. C. MacKintosh and D. A. Weitz, (2010): Origins of Elasticity in Intermediate Filament Networks, *Phys. Rev. Lett., 104, 058101*

A study of PVC in high swirl number sudden expansion flow in cylindrical vortex chamber

D. Dekterev[1]

[1] Institute of Thermophysics SB RAS, Novosibirsk, Russian Federation

Abstract:
High swirl number flows are typical for many technical applications such as separators, scrubbers, hydroelectric turbines [1], and etc. The precessing vortex core (PVC) is the most interesting unsteady phenomenon that occurs in such flows [2, 3]; it is the one that is studied in this paper. The possibility of predicting the precession frequency allows avoiding undesired operation modes of some devices. Comprehensive knowledge of the PVC characteristics enables full control over this type of flow. Our laboratory has established a hydrodynamic set-up with a tangential vortex chamber. The chamber design allows easy modification of a swirl number and a sudden expansion ratio in a short period of time. The chamber is made of Plexiglas that allows obtaining flow visualization data by standard methods and using advanced optical techniques such as PIV. The paper provides visualization of various types of flows, frequency characteristics for various flow rates and swirl numbers, as well as PIV data of the velocity fields in certain regimes. The experimental results are compared with the calculated data (Figure 1, 2).

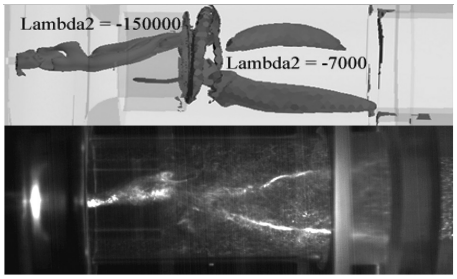

Figure 1: *Typical flow pattern*

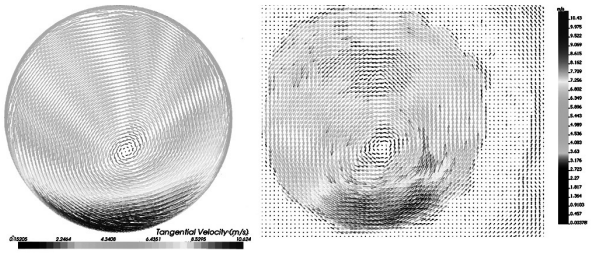

Figure 2: *Numerical and PIV fields of tangential velocity of PVC*

The author is grateful for financial support of the work by the Russian Foundation for Basic Research and the Ministry of Education and Science of the Russian Federation within the frames of Federal Target Program "Scientific and Educational Cadres of Innovative Russia" for 2009-2013 years.

References:

[1] Gupta A.K., Lilley D.G., Syred N., (1984): *Swirl Flows, Abacus Press*, Tunbridge Wells, UK

[2] Alekseenko S.V., Kuibin P.A. and Okulov V.L., (2007): *Theory of Concentrated Vortices*, An Introduction, Springer.

[3] Syred N., (2006), A review of oscillation mechanisms and the role of the precessing vortex core (PVC) in swirl combustion systems, *Prog. Energy Combust. Sc., vol. 32 (2), pp. 93–161.*

On the penetration height of turbulent fountains in uniform calm ambient

P. Dimitriadis [1] and P. Papanicolaou[1]

[1] School of Civil Engineering, National technical University of Athens (NTUA), Athens, Greece

Abstract:
Two-dimensional (2D) spatio-temporal temperature records are obtained on the plane of symmetry o round vertical negatively buoyant jets using LIF (laser induced fluorescent) technique and a calibrated imaging process. A jet of salt water solution is injected upwards in a tank filled with homogeneou fresh water. Following the works of [1] and [2], the penetration depth at steady state is considered taking into account the intermittent behavior of the flow, as shown in Figure 1, at maximum distance reached for small Richardson numbers initially (jet-like behavior). Different penetration heights are more accurately determined based on the way one may define it through the analysis on the 2D concentration and flow intermittency around the steady state terminal rise height (time-averaged maximum height, absolute maximum height, time-averaged concentration and intermitten concentration). The penetration depth is expected to reach the value of $z/l_m = 2$, where l_m is the characteristic length scale [3] and z the distance from the nozzle. The distributions of the normalized mean excess temperature and turbulence intensity are also investigated and compared to those of the positively buoyant jets.

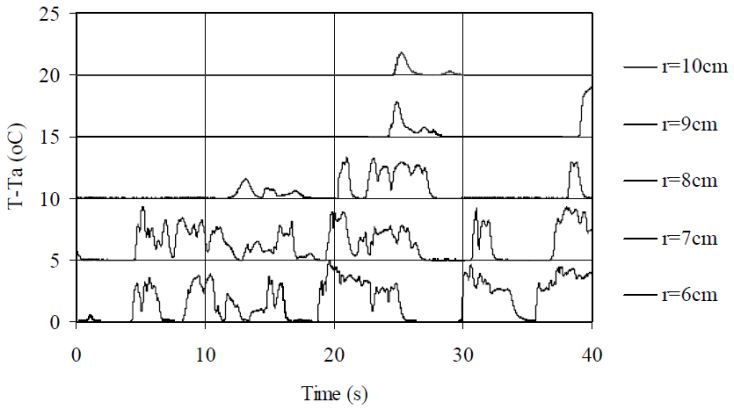

Figure 2. Simultaneous temperature records of five thermistors at z/l_M=2 and at different distances r from jet axis.

Figure 1: *Intermittent behavior of the fountain around the steady state terminal height [2].*

References

[1] Papanicolaou, P.N., and Kokkalis, T.J., (2008), Vertical buoyancy preserving and non preserving fountains in a homogeneous calm ambient, *Int. J. Heat Mass Trans. 51, pp. 4109–4120*

[2] Spetsiotis D.N., and Papanicolaou, P.N, (2008), Measurements in a hot, negatively buoyant jet, discharged in homogeneous calm ambient, *e-Proceedings of the Protection and Restoration of the Environment IX, 29 June 3 July 2008*, Kefalonia, Greece, Paper 202, pp. 8.

[3] Fischer H.B., E.J. List, R.C.Y. Koh, J. Imberger, and N.H. Brooks, (1979), Mixing in inland and coastal waters, *Academic Press.*

Enhanced transfer phenomena by artificially generated vorticity in turbulent flows

Akram Ghanem[1], Charbel Habchi[1,2], Thierry Lemenand[1], Dominique Della Valle[1,3], Hassan Peerhossaini[1]

[1] Thermofluids, Complex Flows and Energy Research Group, Laboratoire de Thermocintique, CNRS UMR 6607, Nantes University, Nantes, France
[2] Ecole des Mines de Douai, Douai, France
[3] ONIRIS – Nantes, Nantes, France

Abstract:
Vortex generators are being increasingly incorporated in modern multifunctional heat exchanger / reactors due to their proven influence on heat and mass transfer enhancement. Longitudinal and transverse pressure-driven vortices and shear instability driven flow structures generated by flow separation behind the turbulence promoters play a crucial role in convective transport phenomena. The High Efficiency Vortex (HEV), an innovative static mixer and a low-energy consumption heat exchanger designed to exploit these vortices, is a circular tube equipped with several rows of four diametrically-opposite trapezoidal vortex generators each. The tabs are fixed at a 30° inclination angle with respect to the wall [1] (figure 1a).
The pressure difference generated on the trapezoidal tab initiates a streamwise swirling motion in the form of two longitudinal counter-rotating vortex pairs (CVP). Moreover, owing to the Kelvin-Helmholtz instability, the shear layer generated at the tab edges serves as a production site of turbulence kinetic energy (TKE). This shear layer becomes unstable further downstream from the tabs giving rise to periodic hairpin vortices [2], as shown in figure 1b.
The vortices described above constitute the main mechanisms of heat and mass transfer enhancement: the development of highly turbulent shear layers, the reduction of the laminar sublayer thickness near the wall, and the swirl movement of the streamwise vortex (figure 2) that enhances convective transfer [3]. The metallic tabs also provide a supplementary contact area with the fluid boosting the conductive heat flux.
Computations of global mixing efficiency based on turbulence kinetic energy dissipation rate prove the ability of the HEV static mixer to enhance mixing by 40 times above and over that in a plain turbulent tube flow reactor [4]. Numerical results have demonstrated that the convective heat transfer, characterized by Nusselt number, is enhanced in the HEV static mixer by 500 % with respect to empty-tube heat exchangers; while inducing a moderate increase in friction factor and pressure losses as seen in figure 3 [3].
The purpose of this work is to show experimentally the effects of hydrodynamics on the transfer processes accompanying such flows in an attempt to compare with the results of the numerical studies available in the literature. Another aim is to validate the high efficiency of the HEV static mixer found numerically in the previous work.

References

[1] Chemineer, Kenics, (1998), Static Mixing Technology, *Chemineer Inc., Bulletin 800*

[2] FD. Dong and H. Meng, (2004), Flow past a trapezoidal tab, *Journal of Fluid Mechanics, vol. 510, pp. 219–242*

[3] Hakim Mohand Kaci, Charbel Habchi, Thierry Lemenand, Dominique Della Valle and Hassan Peerhossaini, (2010), Flow structure and heat transfer induced by embedded vorticity, *International Journal of Heat and Mass Transfer, vol. 53, pp. 3575–3584*

[4] Hakim Mohand Kaci, Thierry Lemenand, Dominique Della Valle, Hassan Peerhossaini, (2009), Effects of embedded streamwise vorticity on turbulent mixing, *Chemical Engineering and Processing, vol. 48, pp. 1457–1474*

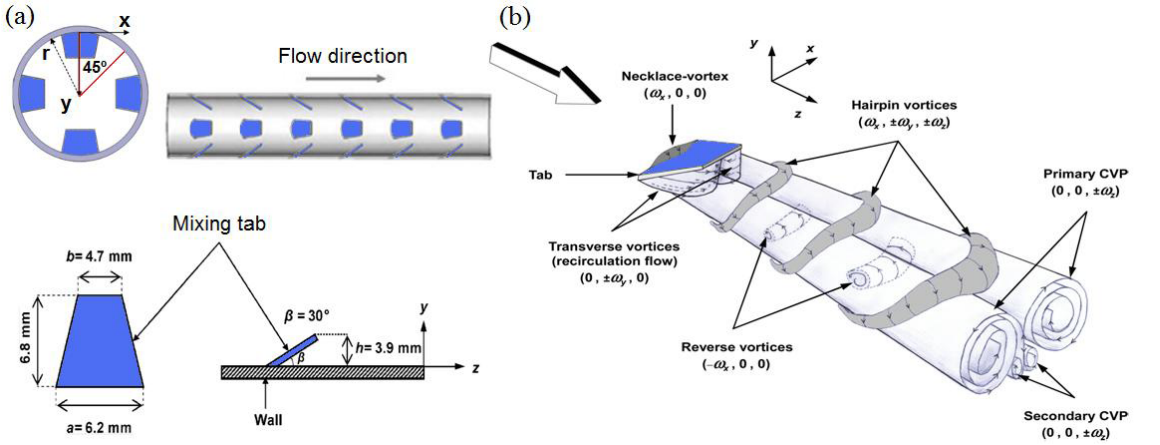

Figure 1: *(a) HEV static mixer geometry and (b) flow structure produced by a trapezoidal vortex generator*

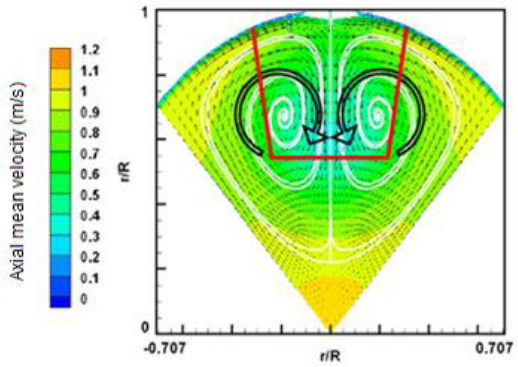

Figure 2: *Velocity field downstream a trapezoidal tab for* $Re = 15000$

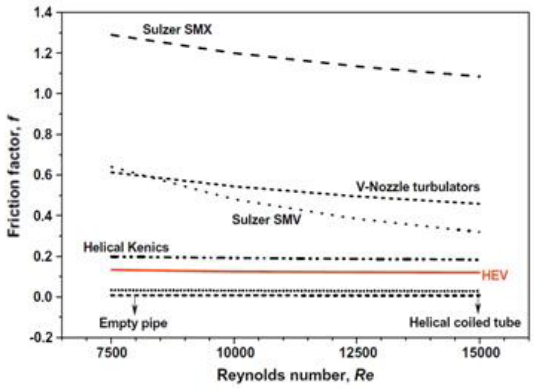

Figure 3: *Friction factor for different heat exchangers*

Simulation of Low Mach Number Flows

Natalie Happenhofer [1] Hannes Grimm-Strele [1] Othmar Koch [1] Friedrich Kupka [1] Herbert Muthsam [1] Florian Zaussinger [2]

[1] Faculty of Mathematics, University of Vienna, Vienna , Austria
[2] Department Aerodynamics and Fluid Mechanics , Brandenburg University of Technology Cottbus, Cottbus, Germany

Abstract:

Many astrophysical phenomena of interest occur in the low Mach number regime, where the characteristic fluid velocity is small compared to the speed of sound. As the Mach number approaches zero, compressible flow solvers suffer servere deficiencies since, for explicit schemes, the timestep must satisfy the Courant-Friedrichs-Lewy conditions where numerical stability considerations lead to very small timesteps due to the prevailing acoustic wave speeds. On the other hand, implicit methods suffer from stiffness since the eigenvalues of the system often vary by orders of magnitude; consider quite generally the difficulties of implementing an implicit solver in multidimensions, keeping efficient parallelization in mind.

In stellar physics, the problem of tackling low Mach number flows has predominantly been adressed by using the Boussinesq or the anelastic approximation which, however, are valid under physical conditions only which by no means can be expected to always be met. Therefore, we extended the semi-implicit method numerical method designed by Kwatra et al. to solve the compressible Euler equations [1] to the Navier-Stokes equations. This method uses the pressure evolution equation to derive a generalized Poisson equation predicting the pressure at the next time step. This implicit treatment of the pressure term leads to an alleviation of the stringent CFL-condition imposed by the sound speed.

We coupled this scheme to an implicit-explicit Runge-Kutta scheme which treats the diffusive terms implicitly [2]. Therefore, the only time step restrictions emerge from the fluid velocity and the viscous term and, compared to a standard explicit method, our solver proves to be highly efficient.

We have performed simulations of convection and double-diffusive convection in stars. The phenomenon of double-diffusive convection has recently gained importance since it plays an important role in stellar evolution theory and due to the fast developments in the supercomputing area, simulations with the necessary grid resolution are now feasible.

We compare our results to those of F. Zaussinger, who assumed the fluid to be incompressible [3].

References

[1] Nipun Kwatra, Jonathan Su, Jon T. Gretarsson, Ronald Fedkiw, (2009), A method for avoiding the acoustic time step restriction in compressible flow, *Journal of Computational Physics, vol. 228, pp. 4146-4161*

[2] Friedrich Kupka, Othmar Koch, Natalie Happenhofer, (2011), Total–Variation–Diminishing Implicit–Explicit Runge–Kutta Methods for the Simulation of Semiconvection in Astrophysics *Journal of Computational Physics, in preparation*

[3] Florian Zaussinger, (2010) *Numerical simulation of double-diffusive convection.* PhD thesis, University of Vienna

Turbulent channel flow with dispersed phase - physics and numerics

Maria Knorps [1]

[1] Institute of Fluid-Flow Machinery, Polish Academy of Sciences, Gdańsk, Poland

Abstract:
The problem of modeling two-phase turbulence has been encountered in many physical and technical issues. Dispersed phase dynamics in turbulent flow is one of the cases describing e.g. aerosols, first stages of cloud formation, dynamics of fuel in combustion chamber etc. There exist several ways of modeling such flows. In present approach, referred as Eulerian - Lagrangian approach, fluid flow is governed by Navier-Stokes set of equations (NSE), and dispersed phase is represented by Lagrangian particles with set of equations:

$$\frac{d\mathbf{x}}{dt} = \mathbf{v}, \tag{1}$$

$$\frac{d\mathbf{v}}{dt} = \frac{\mathbf{u}_{f@p} - \mathbf{v}}{\tau_p}(1 + 0.15Re_p^{0.687}), \tag{2}$$

where $\mathbf{x}$ and $\mathbf{v}$ are position and velocity of the particle, $\mathbf{u}_{f@p}$ is fluid velocity at particle position, τ_p is particle momentum relaxation time.
Large Eddy Simulation (LES) is performed for fluid , because of its lower requirements for computation power than Direct Numerical Simulation (DNS). On the other hand small scales of fluid motion are not well resolved. It is observed, that small eddies have a significant impact on particle motion, especially for particles with small inertia.
In the presentation statistics of particle motion in turbulent channel flow and comparison between LES and DNS case will be shown. Origins of differences in results will be explained and few approaches to deal with this problem sketched.

References

[1] Pozorski J., Łuniewski M., (2008), Analysis of SGS particle dispersion model in LES of channel flow. *Quality and Reliability of Large-Eddy Simulations, pp 331-342*, Springer

[2] Marchioli C., Soldati A., Kuerten J.G.M., Arcen B., Taniére A., Goldensoph G., Squires K.D., Cargnelutti M.F., Portela L., (2008), Statistics of particle dispersion in DNS of wall-bounded turbulence., *Int. J. Multiphase Flow, vol.34, pp. 879-893*

[3] Bersellu L.C., Iliescu T., Layton W.J., (2006): *Mathematics of Large Eddy Simulation of Turbulent Flows*, Springer

[4] Pozorski J., Apte S.V., (2008), Filtered particle tracking in isotropic turbulence and stochastic modeling of subgrid-scale dispersion., *Int. J. Multiphase Flow, vol.35, pp. 118-128*

Multi sized nanoparticle effect on convective heat transfer in turbulent flows

Dinesh Kumar [1]

[1] Engineering Mechanics Unit, Jawaharlal Nehru Centre for Advanced Scientific Research, Bangalore, India

Abstract:
Numerical computation is being carried out for the fluid heat transfer with nanoparticles involves usually single sized particle. However, the present extension involves convective heat transfer enhancement for nanofluids with multi sized nanoparticles. Comparison between the cases when single sized and multi sized nanoparticle dispersion is considered for various volume weighted particle diameter in the turbulent flow conditions. The objective is to investigate the effects of multi sized nanoparticle volume fraction on the flow and heat transfer characteristics in the conditions closer to the experiments. As nanopowder used for experiments contains multi sized particles distribution. The Al_2O_3 nanoparticles ($50 - 150$ nm) were used with 0.5% volume concentration. The effect of Brownian force, thermophoresis force and van der Waals force has been taken into account. The results indicate that when multi sized particle dispersion is considered the enhancement in convective heat transfer is relatively suppressed in compare to single sized nanoparticle. A possible explanation for this interesting result is expected as the aggregation of nanoparticles and heat transport between particles and fluid. This finding confirms that effect and behavior of multi sized particle dispersion on heat transfer mechanism of nanofluid in turbulent flow is different from heat transfer in still flow conditions. The results obtained for multi sized heat transfer characteristics reveal interesting behavior of convective heat transfer that warrant further study on the effects of the multi sized nanoparticle, especially in the turbulent flow conditions.

Large scale motion and local heat flux in turbulent Rayleigh-Bénard convection of SF_6 in cylindrical containers

S. Wagner [1], O. Shishkina [1] and C. Wagner [1]

[1] German Aerospace Center (DLR), Institute of Aerodynamics and Flow Technology, Göttingen, Germany

Abstract:
Highly resolved direct numerical simulations (DNS) of turbulent Rayleigh-Bénard convection (RBC) in a cylindrical domain with aspect-ratio $\Gamma = 1$ have been performed for a Prandtl number $Pr = 0.786$. This corresponds to SF_6 at a pressure of 1 bar and about 20° C. Rayleigh numbers considered in the simulations cover five decades ($Ra = 10^4 - 10^9$). The governing equations in Oberbeck-Boussinesq approximation are solved using a fourth order finite volume code in cylindrical coordinates [1]. Thereby the spatial resolution is due to [2] but with an increased number of nodes in the boundary-layer.

In the talk the spatial distribution of the heat flux and its correlation with the large scale motion will be discussed. The Nusselt number distribution in vertical direction is analysed by the means of convergence of time-averaging. This means that long-time-averaged fields have been calculated (> 500 free-fall time units). The calculated Nusselt numbers are in good agreement with experiments [3] (as shown in figure 1) and are within the Grossmann-Lohse theory [4].

The second part of the presentation is devoted to the time-averaged local heat fluxes and large scale motion. It is shown how the plane of the large scale circulation (LSC) can be determined from the time-averaged fields. Then the distribution of the local heat flux in this plane and its correlation to the velocity field are analysed (compare figure 2).This allows to locate the regions of large heat flux in the considered plane and assign to them large scale flow structures. Finally the azimuthal LSC motion will be discussed.

References

[1] Shishkina, O., Wagner, C., (2005), A fourth order accurate finite volume scheme for numerical simulations of turbulent Rayleigh-Bénard convection in cylindrical containers, *C. R. Mecanique, vol. 333, pp. 17–28*

[2] Shishkina, O. Stevens, R. J. A. M., Grossmann, S., Lohse, D., (2010), Boundary layer structure in turbulent thermal convection and its consequences for the required numerical resolution, *New Journal of Physics, vol. 120:75022*

[3] Burnishev, Y., Segre, E., Steinberg, V., (2010), Strong symmetrical non-Oberbeck-Boussinesq turbulent convection and the role of compressibility, *Physics of Fluids, vol. 22:035108*

[4] Ahlers, G., Grossmann, S., Lohse, D., (2009), Heat transfer and large scale dynamics in turbulent Rayleigh-Bénard convection, *Reviews of Modern Physics, vol. 81, pp. 503–537*

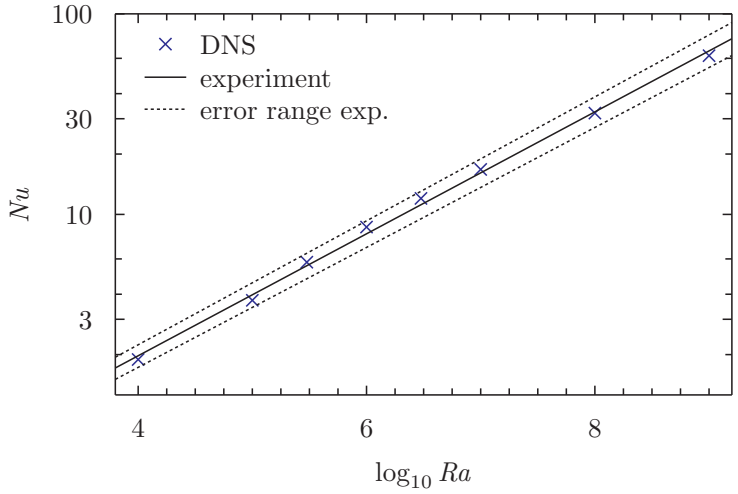

Figure 1: Nusselt number $Nu(Ra, Pr = 0.768)$ from DNS in comparison with experiments [3] ($Nu(Ra, Pr = 0.8) = 0.12 \pm 0.01 \cdot Ra^{0.304 \pm 0.005}$ measured for $Ra \in [4 \cdot 10^8, 4 \cdot 10^{11}]$).

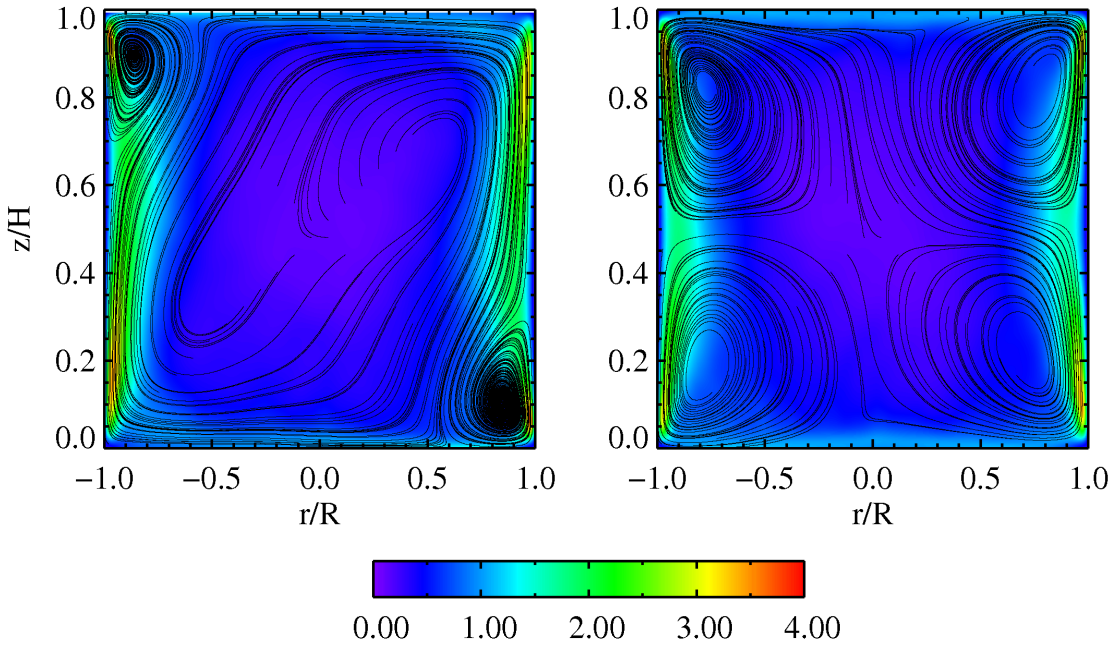

Figure 2: Local dimensionless heat flux in units of the Nusselt number (color) and streamlines of the velocity field in one $r-z-$plane (temporal averaged fields) for $Ra = 10^7$. left: looking straight on the LSC, right: orthogonal to the LSC

Physical Modelling of impinging jets to aid nuclear sludge bed re-suspension

C. Lakhanpal [1], M. Fairweather[1], S. Biggs[1] and J. Peakall[2]

[1] School of Process, Environmental & Materials Engineering, University of Leeds
[2] School of Earth and Environment, University of Leeds

Abstract:
Legacy nuclear wastes exist in a large number of ponds, silos and tanks across various sites throughout the world. In the United Kingdom and specifically Sellafield, these are mostly the result of fuel reprocessing for both Magnox and AGR nuclear power generation programmes that began in the late 1950s.

Spent fuel is stored in cooling ponds prior to being reprocessed. However, the metal casing of Magnox fuel (an alloy of magnesium) is susceptible to corrosion if the physical conditions of the pond are not strictly controlled and this has resulted in magnesium hydroxide sludge being formed at the base of cooling ponds. Effective methods of re-suspending this sludge are therefore a key component to the efficient decommissioning of legacy plant. Additionally, after the fuel is reprocessed, the fission products that are separated from the reusable uranium and plutonium are stored as highly active liquor in large, cooled tanks. Particulate matter within the liquor has a tendency to settle out of suspension and without an effective means to re-suspend them; they can form radioactive and thermal hot-spots on the base of the tank. Formation of hot-spots may then lead to accelerated corrosion processes of the tank base. To hinder settling processes from taking place the tanks are equipped with an array of jet ballasts which are periodically fired to produce impinging jets of liquid onto the base of the tank to encourage full re-suspension of solid particles.

This project aims to address the challenge and issues relating to sludge re-suspension using impinging jets; the full characteristics of which using appropriate simulants have not been studied before. The applications of this project have been linked to have direct relevance in Aerospace, Chemical and Mining industries. Progress would be reported further to presentation from EPFDC 2010; Investigation into the *turbulent radial wall jet* formed as a result of single phase jet impingement on a flat plate using experimental facilities developed at *Sorby Fluid Dynamics Laboratory at University of Leeds* would also be presented.

References

[1] Dennis, F. *et al.*, (2007), Dounreay hot particles: the story so far, *J. of Radiol. Prot. 27 (3A), A3–A11*

[2] Fairweather, M. and Hargrave, G.K., (2002), Experimental investigation of an axisymmetric, impinging turbulent jet. 1. Velocity field, *Experiments in Fluids, vol. 33,pp. 464–471*

[3] Fairweather, M. and Hargrave, G.K., (2002), Experimental investigation of an axisymmetric, impinging turbulent jet. 2. Scalar field, *Experiments in Fluids, vol. 33, pp. 539–544*

[4] Hargrave, G.K. *et al.*, (2006), The 3D velocity field of an impacting turbulent jet, *Journal of Physics, vol. 45, pp. 162–172*

[5] Poelma, C. and Ooms G., (2006), Particle-turbulence interaction in a homogeneous, isotropic turbulent suspension, *Appl. Mech. Rev., vol. 59 (1-6), pp. 78–90*

[6] Poreh, M. and Bandyopadhyay, P., (1975), Mean and turbulence characteristics of three-dimensional wall jets, *Journal of Fluid Mechanics, vol. 71, pp. 541–562*

Pipe flow of shear-thinning fluid.

Lopez Carranza, S. [1], Jenny, M. [1] and Nouar, C. [1]

[1] Laboratoire d'Énergétique et de Mécanique Théorique et Appliquée (UMR 7563 CNRS) , INPL, Nancy, France

Abstract:
Comparatively to the newtonian case, very few studies have been devoted to the transition to turbulence in a pipe for non-newtonian fluids, despite the importance of this problem in the design and the control in several industrial processes such as in oil-well cementing, extrusion of molten polymers, paper coating, *etc.* These flows are mainly characterized by, on one hand, a stratification of the viscosity between the wall and the pipe axis and on the other hand, a nonlinear variation of the viscosity with the shear rate [1]. Pipe flow of purely viscous shear-thinning fluid is studied using a pseudospectral Petrov-Galerkin code inspired by Meseguer et al[2]. The rheological behaviour of the fluid is assumed to be described by the Carreau-Yasuda's model: $\mu = [1 + (\lambda\dot{\gamma})^a]^{(n-1)/a}$, where $0 < n < 1$ is the shear-thinning index, λ is a dimensionless constant time of the fluid and $\dot{\gamma}$ is the second invariant of the strain rate tensor. The time discretization uses a semi-implicit fourth-order scheme. The nonlinear viscous and convective terms are calculated in the physical space and integrated via the Adams-Bashforth explicit formula, while the linear terms are calculated via an implicit scheme. Firstly, a linear stability analysis is conducted, concluding that the flow is linearly stable for all Re and rheological parameters studied. Secondly, the optimal perturbation, i.e. the perturbation which leads to the maximum linear amplification, is injected into the fully non linear code. Numerical results show that the nonlinear dependency $\mu(\dot{\gamma})$ leads to: (i) reduction of viscous dissipation, which is related to two new terms in the Reynolds-Orr equation and (ii) the formation of a broad spectrum of azimuthal modes which affects significantly the mechanisms of transition to turbulence.

References

[1] A. Esmael, C. Nouar, Transitional flow of a yield stress fluid in a pipe: Evidence of a Robust coherent structure, Physical review E, 2008.

[2] 'A. Meseguer, F Mellibosky, On a solenoidal Fourier-Chebyshev spectral method for stability analysis of the Hagen-Poiseuille flow, Applied Numerical Mathematics **57**, 920-938, 2007.

Local stability analysis of swirling shear flows

Dhiren Mistry [1], Ubaid Ali Qadri [1] and Matthew Juniper [1]

[1] Department of Engineering, University of Cambridge, Cambridge, United Kingdom

Abstract:
We report on the stability analysis of the steady axisymmetric solutions obtained by Vyazmina *et al* [1] for vortex breakdown in incompressible flows at $Re = 200$. A local linear stability analysis is implemented to determine the absolute/convective characteristics of the flow [2]. We apply the WKBJ approximation (*i.e.* we assume a locally parallel base flow) and superpose small perturbations of the form $\hat{\mathbf{u}}(r)\exp(\mathrm{i}(kx + m\theta - \omega t))$, where k is the local complex wavenumber and ω is the local complex angular frequency. The absolute frequency, ω_0, is calculated at each axial location. This distribution of ω_0 is interpolated with a Padé polynomial and then continued analytically into the complex x-plane. The linear global frequency, ω_g, and the wavemaker position are then estimated from the position of the relevant saddle point of ω_0 in the complex x-plane and compared with the global analysis.

We use a swirl parameter of 1.0 ($Sw = 1.0$) as our reference case. The local analysis predicts two regions of absolute instability that correspond to the recirculation bubble (i) and the wake (ii). The results are in good agreement with the DNS results of Gallaire *et al* [3]. By comparing ω_g with that from the global analysis, we determine that the wake region of absolute instability is the wavemaker region.

The flow becomes linearly globally unstable at $Sw = 0.915$. The distribution of $\omega_{0,i}$ for this flow indicates that the wake region is not absolutely unstable, figure 1(a). However, the direct mode growth in the wake region is significantly greater than that in the bubble region. A comparison of ω_g from the local and global analysis confirms that the wake is the wavemaker region for this flow. This illustrates a case in which a flow becomes more globally unstable through the coupling of two regions of instability.

The flow becomes linearly globally unstable for azimuthal wavenumber $m = 2$ at $Sw = 1.161$. The wake region for this flow is absolutely unstable, figure 1(a). We find that perturbations for this flow only grow in the wake region; no growth is observed in the recirculation bubble. The $m = 2$ instability modes do not exhibit the coupled global dynamics as described for the $m = 1$ case. Rather, it is only the wake region of the flow that is responsible for the global mode characteristics. For this reason, a necessary requirement for global instability for the $m = 2$ case is a sufficiently large region of absolute instability.

We finally compare $\omega_{g,i}$ of the linear global modes as calculated by the local analysis and the global analysis, figure 1(b). For quickly evolving flows, such as those in this study, the local analysis does not capture the more complex instability characteristics shown in the global analysis. Nonetheless, the local analysis provides insight not easily attainable through global analyses.

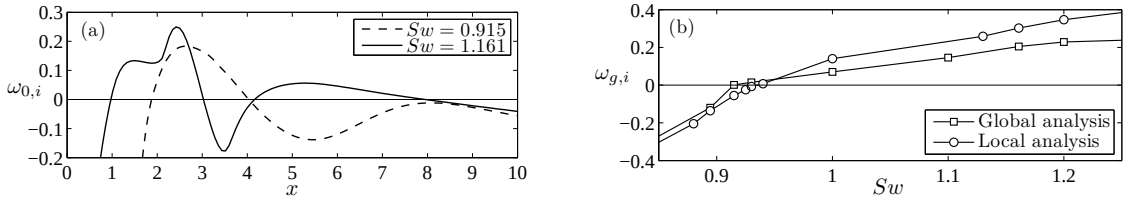

Figure 1: (a) Distribution of the local absolute growth rate, $\omega_{0,i}$, for $Sw = 0.915$ (dashed line) with $m = 1$ and for $Sw = 1.161$ (solid line) with $m = 2$. Both cases are marginally globally unstable. (b) The linear global mode growth rates of the local analysis (circles) and global analysis (squares) are compared for an azimuthal wavenumber of $m = 1$.

References

[1] Vyazmina, E., Nichols, J.W., Chomaz, J-M. and Schmid, P., (2009), The bifurcation structure of viscous steady axisymmetric vortex breakdown with open lateral boundaries, *Phys. Fluids, vol. 22, no. 74107.*

[2] Huerre, P. and Monkewitz, P., (1990), Local and global instabilities in spatially developing flows, *Annu. Rev. Fluid Mech., vol. 22, pp. 473-537.*

[3] Gallaire, F., Ruith, M., Meiburg, E., Chomax, J-M. and Huerre, P., (2006), Spiral vortex breakdown as a global mode, *J. Fluid Mech., vol. 549, pp. 71-80.*

Level set simulation of incompressible two-phase flows

Andrey Ovsyannikov [1], Mikhael Gorokhovski [1]

[1] Laboratory of Fluid Mechanics and Acoustics, Ecole Centrale de Lyon, Ecully, France

Abstract:

For the last two decades level set methods have become very popular and have been used in a large variety of applications such as compressible and incompressible two phase flow, flame propagation, computer vision and image processing, kinetic crystal growth and many others. Originally the level set method was devised by S. Osher and J. A. Sethian [1] as a simple and versatile method for computing and analyzing the motion of an interface in two or three dimensions and it was capable of computing geometric properties of highly complicated boundaries without explicitly tracking the interface.
The main idea of this approach is to track the interface by a scalar ϕ (the level set function) and the interface is represented by the zero contour of this function. Scalar ϕ is defined to be equal to zero at the location of the phase interface, and $\phi > 0$ in fluid one and $\phi < 0$ in fluid two. The evolution of ϕ is given by

$$\frac{\partial \phi}{\partial t} + \mathbf{u} \cdot \nabla \phi = 0 \tag{1}$$

For numerical reasons, one would like ϕ to be a smooth function; thus one of the most popular definitions is that of a signed distance function, i.e., $|\nabla \phi| = 1$. The level set method allows to easy dermine geometrical characteriscs such as normal vector and interface curvature, generalizes well to three dimensions and may be appleid for problems with very complex interface topology. But level set technique is not free from shortcomings. The major drawbacks of the standard level-set method are

1. that it does not inherently preserve the volume inside interface,
2. converging curvature evaluation is difficult.

In context of simulation of two-phase incompressible flows [2] these disadvantages are crucial and lead to inaccurate results. The first leads to mass conserving errors and the second - to the errors in evaluation of surface tension force.
In our simulations we use recently proposed methods [3, 4] which considerably improve the accuracy of the standard level set method. The perfomance of this approach is assessed through both classical level set transport tests and simple two-phase flow examples including topology changes. The Navier–Stokes equations are solved on cartesian grid with a high-order projection method which implements 5th-order WENO finite difference scheme for approximation of convective terms. Also we compare our results with the results of classical level set method. Finally the new approach is applied to simulate the deformation and breakup of an isolated drop in immiscible liquid phase undergoing shear flow. The results of computations are in good agreement with theoretical and experimental results.

References

[1] Osher S., Sethian J., (1988), Fronts propagating with curvature-dependent speed: algorithms based on Hamilton-Jacobi formulations, *J.Comput.Phys., vol. 79, pp. 12-49.*

[2] Sussman M., Smereka P., Osher S., (1994), A level set method for computing solutions to incompressible two-phase flow, *J.Comput.Phys., vol. 114, pp. 146-159.*

[3] Nourgaliev R., Wiri S., Dinh T. and Theofanous T., (2005), On improving mass conservation of level set method by reducing spatial discretization errors, *Int.J.Multiph Flow, vol. 31 (12), pp. 1329-1336.*

[4] Hartmann D., Meinke M., Schroder W., (2010), The constrained reinitialization equation for level set methods, *J.Comput.Phys., vol. 229, pp. 1514-1535.*

Motion of Inertial Particles in a Cellular Flow Field

Jens C. Pfeifer [1] and Bruno Eckhardt [1]

[1] Fachbereich Physik, Philipps-Universität Marburg, Germany

Abstract:
The motion of small particles in a fluid under the influence of gravity is of great interest for understanding processes in nature as well as for technological application. In a still fluid, movement is determined by drag forces as well as inertial effects. The problem becomes interesting for nonuniform flows when interaction between the flow and the particle becomes important and leads to more complicated motion. For a low concentration of spherical particles and a low Reynolds number, the motion follows from the Maxey-Riley equations[1] and their simplification. A simple yet interesting example of a non-uniform and steady flow is given by an infinitely extended periodic cellular 2-dimensional flow field of counter-rotating vortices. This system has been studied for several years and special aspects have been considered (e.g. [2],[3]).

We complement these studies by providing a comprehensive survey of possible motions for all parameters. Following [2], we consider the reduced equation

$$\dot{\vec{x}} = \vec{v}, \qquad \dot{\vec{v}} = -AW\hat{e}_y + A(\vec{u} - \vec{v}) + R(\vec{u} + \frac{1}{2}\vec{v})\nabla\vec{u}$$

with a velocity field $\vec{u} = (\sin(x)\cos(y), -\cos(x)\sin(y))$. The parameters are gravity W, the inertia of the particle A and the mass ratio R. The latter one covers air bubbles in water ($R = 2$), aerosols ($R = 0$) and neutrally buoyant particles ($R = 2/3$). We identify the main patterns of motion and their bifurcations, using AUTO[4] for their determination and continuation.

In the bubble limit, particles are attracted by fixed points in the center of each cell. For most parameter values, this leads to only two possibilities: either the particles are trapped inside a cell or, with sufficient gravity, propagate along a central snaking orbit. Other patterns turn out to be unstable.

For particles slightly heavier than the surrounding fluid, stable suspending orbits are found as well as propagating ones. This is notable because centrifugal forces tend to push the particles outwards, away from the center.

In the aerosol limit, the central fixed points are repelling as well. This leads to a rich variety of different patterns, almost all of them being connected by heteroclinic bifurcations. Notable patterns include particles moving against gravitational force and particles being suspended. Moreover, in some regions of parameter space, only unstable periodic orbits of uncommon periodicity are found, suggesting chaotic motion, see fig. 1.

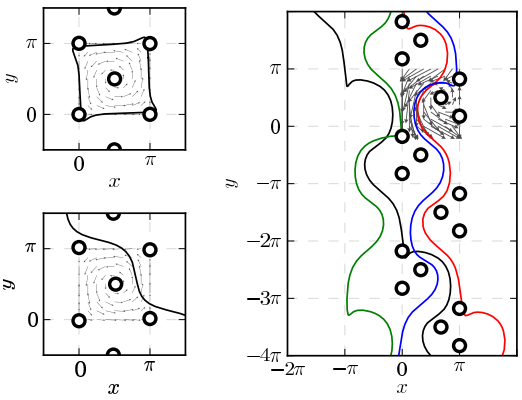

Figure 1: *Examples of periodic trajectories in the aerosol limit ($R = 0$), gravity downwards. Trapped motion (upper left), upward pointing stairs (lower left) and a chaotic downward track (right, all unstable).*
Circles: unstable fixed points. Arrows: Effective velocity field, $\dot{\vec{v}}|_{\vec{v}=0}$

References

[1] Maxey M. R. and Riley J. J., (1983): Equation of motion for a small rigid sphere in a nonuniform flow, *Physics of Fluids, 26(4): 883-889*

[2] Maxey M. R., (1987): The motion of small spherical particles in a cellular flow field, *Physics of Fluids, 30(7): 1915-1928*

[3] Rubin J., Jones C. K. R. T., and Maxey M. R., (1995): Settling and asymptotic motion of aerosol particles in a cellular flow field, *Journal of Nonlinear Science, 5: 337-358*

[4] Doedel E. J. and Oldeman B. E., (2009): AUTO-07P, *http://cmvl.cs.concordia.ca/auto/*

Detailed numerical simulation of turbulent compressible flows

W. Rozema [1]

[1] Computational Mechanics and Numerical Mathematics, University of Groningen, Groningen, The Netherlands

Abstract:
One of the goals of this research is to improve the existing computational methods for direct numerical simulation of turbulent compressible flows. Currently, in most numerical methods the convective terms of the Navier-Stokes equation unphysically generate or destroy energy. Also, often numerical methods deliberately dissipate too much energy, in order to guarantee the smoothness of numerical solutions. By unphysically changing the energy of numerical solutions, such numerical methods interfere with the turbulent energy cascade. We believe that this is unattractive, because the energy cascade is the important mechanism that drives turbulence.

For incompressible flows, accurate simulation methods exist that do not unphysically generate or destroy energy [1]. The philosophy underlying these methods is that the important physical properties of the incompressible Navier-Stokes equations should be preserved numerically. It turns out, that for such methods the numerical energy norm decreases all the time, making the methods intrinsically stable.

We are interested in whether the convenient properties of such methods for incompressible flows can be generalized to simulation methods for compressible flows. We try to sort out what physical properties are important for compressible flows, and how these properties can be preserved numerically. Unfortunately, it seems that proving stability of compressible flow simulations is impossible, because the numerical energy norm is not appropriate.

References

[1] Verstappen R.W.C.P. and Veldman A.E.P., (2003), Symmetry-preserving discretization of turbulent flow, *Journal of Computational Physics, vol. 187, pp. 343-368.*

Lifetime studies of localized turbulence in pipe flow of dilute polymer solutions

Devranjan Samanta [1], C. Wagner [2] and B. Hof [3]

[1] MPIDS, Goettingen, Germany
[2] Saarbrucken University, Saarbrucken, Germany
[3] MPIDS, Goettingen, Germany

Abstract:
At low Reynolds number, turbulence occurs in the form of localized spots which have a finite lifetime and the probability of decay is exponentially distributed, characteristic of a memoryless process [1, 2, 3, 4]. In this present study we extend the lifetime studies to dilute polymer solutions in pipe flow in the drag reduction regime [5]. Experiments have been carried out in a 900 D pipe of 4 mm diameter using different concentrations of polyacrylamide (PAAM) in water. Probability of the puff decay increases with the increase of polymer concentration in the pipe flow 1. As shown by our lifetime studies 1, with increasing polymer concentration turbulence is only encountered at larger Reynolds number. This agrees with previous observations of transition delay. Our lifetime measurements allow us to quantify this process and to determine its dependence on the Weissenberg effect.

References

[1] Hof B., Westerweel J., Schneider T. and Eckhardt B., (2006), Finite lifetime of turbulence in shear flows, *Science, 2006,443, 59-62*

[2] Avila M., Willis A. P. and Hof B., (2006): On the transient nature of localized pipe flow turbulence*Journal of fluid mechanics 2010, 646, 127-136*

[3] Hof B., Lozar A., Kuik D. J. and Westerweel J., (2008): Repellor or attractor? Selecting the dynamical model for the onset of turbulence, *Phys. Rev. Lett. 2008101 (21) 214501*

[4] Kuik D. J., Polema C. and Westerweel J., (2010): Quantitative measurement of the lifetime of localized turbulence in pipe flow, *Journal of fluid mechanics 2010, 645 , 529-539*

[5] Toms B. A., (1948): Some observations on the flow of linear polymer solutions through straight tubes at large Reynolds number, *Proc. 1st Intl. Congr. Rheol.*, N. Holland, Amsterdam 2:135-41

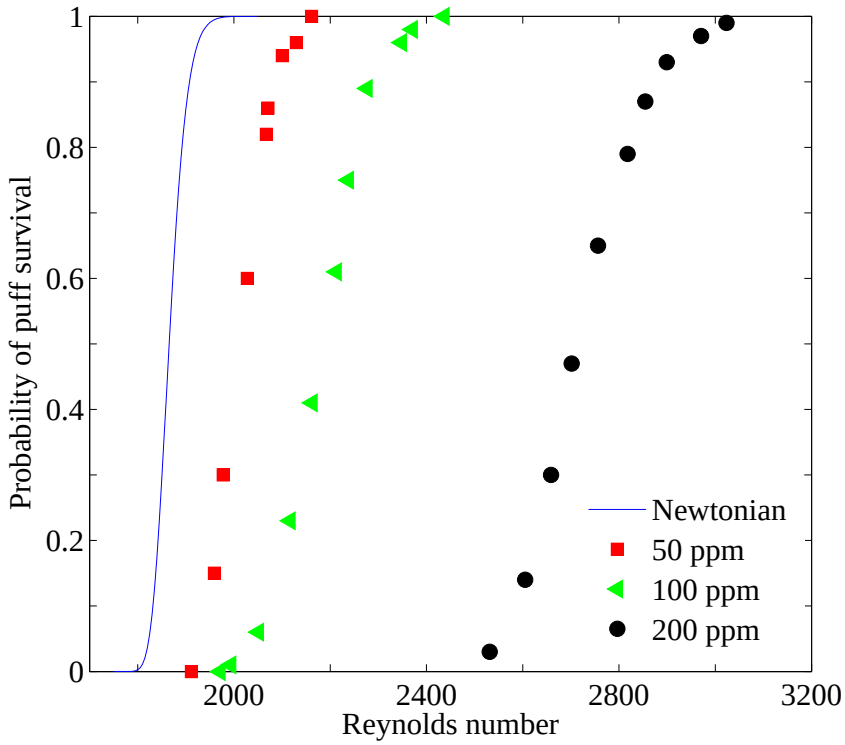

Figure 1: *Influence of polymer concentration on probability of puff survivals*

Trapped Modes of the Helmholtz equation

Cristina Sargent[1]

[1] Imperial College, London, United Kingdom

Abstract:
Physically, trapped modes are oscillations of finite energy in a domain which is unbounded in at least one direction. These oscillations occur locally to some structure and decay to zero at large distances away from it. Mathematically the existence of a trapped mode at a discrete frequency or wavenumber is equivalent to the existence of an eigenfunction corresponding to a point eigenvalue of the appropriate operator, plus boundary conditions. Trapped modes are important as they have been found to exist in a wide range of physical situations. We consider a number of different theoretical problems concerning trapped modes in the vicinity of obstacles and approach each problem from an acoustical viewpoint. The problem is initially investigated for simple, two-dimensional cases and the existence of trapped modes is established using the boundary element method. The procedure is then extended to progressively more complex geometries and the relationships between geometric parameters and the existence of trapped mode are considered.

1.1 Investigation method

We consider the propagation of acoustic waves in two dimensions, described by the linear wave equation. If the motion is assumed to be time-harmonic, the potential, say U, may be expanded in the form: $U(\mathbf{x},t) = \phi(\mathbf{x})e^{-i\omega t}$ where ϕ is the reduced velocity potential, and the linear wave equation reduces to the Helmholtz equation:

$$(\nabla^2 + k^2)\phi = 0, \quad k^2 = \frac{\omega^2}{c^2} \tag{1}$$

subject to appropriate boundary conditions. In this context c is the speed of sound in still air. If a non-trivial potential ϕ can be found which satisfies equation above and the boundary conditions (including a condition requiring exponential decay at infinity), then the value k^2 corresponding to the potential ϕ, is an eigenvalue of the problem.

Using concepts of potential theory we derive an integral representation of the problem. Using the boundary element method (BEM), we write the unknown potential as a summation of integrals over the discretised domain boundary. For a division of N boundary elements S_j, the potential ϕ can be written in the form:

$$c(\mathbf{x}')\phi(\mathbf{x}') = \sum_{j=1}^{N} \left\{ \int_{S_j} \left[\phi(\mathbf{x}) \frac{\partial G(\mathbf{x},\mathbf{x}')}{\partial n} - G(\mathbf{x},\mathbf{x}') \frac{\partial \phi(\mathbf{x})}{\partial n} \right] ds(\mathbf{x}) \right\}, \quad \mathbf{x} \in S_j \tag{2}$$

Thus we can approximate any boundary using simple geometrical forms. The equation above holds for each nodal point $j = 1, \ldots, N$ and and once the boundary conditions are applied we have a system of N equations with N unknowns, which are either ϕ or its normal derivative:

$$M\mathbf{X} = 0 \tag{3}$$

where the matrix $M = M(k)$ is obtained by computing the integrals in equation 2, along the boundary elements, and $\mathbf{X}$ is a vector storing the unknowns.

In order to find trapped modes, i.e. non-unique, non-trivial solutions to our problem, we identify those values of k for which the determinant of the matrix $M(k)$ is zero and the solution has exponential decay away from the trapping structure.

To validate the method, we studied test problems and we have been able to replicate known results which were obtained using different methods. The method can be applied with increasing degrees of accuracy in order to identify and eliminate spurious eigenvalues. We are now investigating geometries for which we do not have comparable results. More complex geometries are investigated in order to establish existence/non-existence of trapped modes and the correlation with various geometrical parameters.

Combined Particle Image Thermography (PIT) and Velocimetry (PIV) in Mixed Convective Air Flows

D. Schmeling [1], J. Bosbach [1] and C. Wagner [1]

[1] Institute of Aerodynamics and Flow Technology, German Aerospace Center (DLR), Göttingen, Germany

Abstract:

Simultaneous measurements of instantaneous velocity and temperature fields provide a mighty tool to study the dynamics of thermal plumes and their influence on the local and global heat transfer in thermal and mixed convection. An established technique to conduct such measurements in liquids is the combination of Particle Image Thermography (PIT) and Particle Image Velocimetry (PIV) with thermochromic liquid crystals (TLCs) as tracer particles [1]. The intention of our work is to adapt this promising measurement technique to air flows with continuous fluid exchange. Such flows are found not only in many technical applications, like e.g. indoor climatisation, but also in more fundamental thermal convection problems of air with a Prandtl number of $Pr \approx 0.7$. The feasibility of this measurement technique for pure thermal convection has already been demonstrated in a cubical Rayleigh-Bénard cell with air as working fluid [2].

The general requirements which must be fulfilled to apply TLCs as tracer particles in air flows for combined PIT and PIV are the following: First, in order to conduct PIT, they have to provide a temperature depending reflection of different wavelengths with a short temperature response time. Second, for accurate PIV the tracer particles must posses good following behaviour, a high light scattering efficiency is required and a long lifetime. For systems with continuous fluid exchange, the tracer particles need to be continuously produced at a high rate. Further it has to be considered, that the colour play of the TLCs, which is exploited in the PIT measurement technique to locally detect the fluid temperatures, not only depends on the temperature but furthermore on, e.g. the angle between the incident illumination and line of view, the background light as well as the size and the age of the droplets. Consequently, a spatially resolved calibration is needed for high precision measurements, and the used particles have to be generated with a narrow size distribution. While all of the above discussed issues are addressed in our ongoing study, the present paper focuses on recent progress on particle generation, characterisation and illumination as well as image processing.

The investigated convection cell has a quadratic cross section of 500 mm × 500 mm and an aspect ratio between length and height of $\Gamma_{xz} = 5$ (see Figure 1a). During feasibility testing the heatable bottom of the cell as well as its ceiling were kept at room temperature and an additional heat source was used for the formation of a spatially fixed area of rising warm air. Furthermore, the particles were sprayed directly into the convection cell with an airbrush system in these first tests. For illumination of the particles a specially developed white light sheet based on LEDs was used. The particle images are recorded with a double shutter colour CCD camera, so that temperatures and velocities could be calculated from the local hue values and the local particle image displacements between subsequent recordings, respectively.

Particle images with different colours were recorded for different mean cell temperatures. Based on these images first points of a hue - temperature calibration curve were determined (see Figure 1b). A feasibility test of combined PIT and PIV was conducted with the additional heat source (see Figure 1a) for the formation of a spatially fixed area of rising warm air. The resulting hue (temperature) and pixel displacement (velocity) fields are shown in Figures 2a and 2b, respectively. Thereby, R20C6W TLCs (©Hallcrest) were used and the presented hue values were obtained using a filter technique based on the saturation value of the HLS colour space. This filtering is necesscary to identify those particles which are neither background nor small particles scattering white light. The local temperatures at the sensor positions are: $T_1 \approx 22.0$°C and $T_2 \approx 20.5$°C. As a result, the areas with warm air (high hue values) are in good correlation with those of upward oriented velocity.

Concluding we can say, that the usage of the tiny TLC particles as tracer particles for PIV as well as their usage as small thermometers in air flows is possible. Additionally we found that the colour active range of the tiny TLC particles (≈ 1.3 K) is way smaller than their nominal range (6 K). An estimation of the limits in the spatial and temporal resolution of this combined measurement technique is an open task. Clarifying measurements with a point wise calibration and investigations of the relaxation time of the crystals will be conducted in the near future.

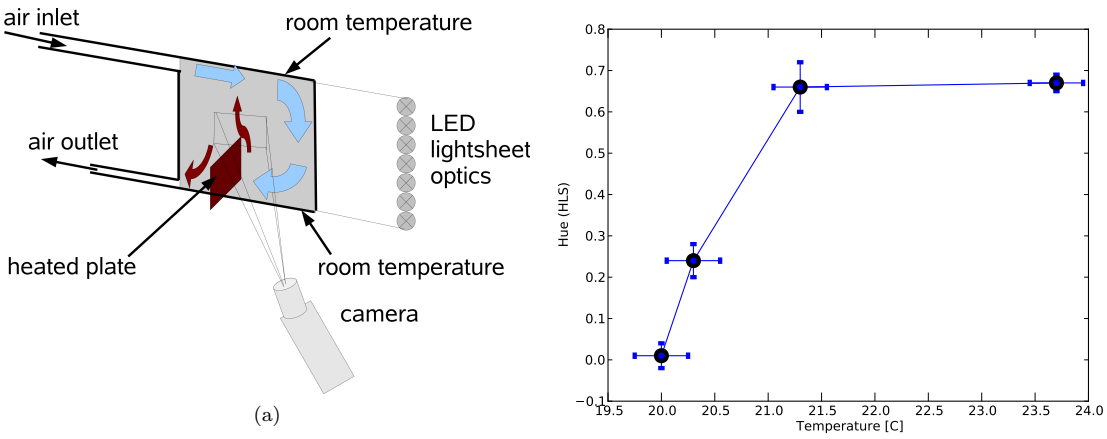

(a) (b)

Figure 1: (a) Sketch of the experimental setup used for first test of combined PIT and PIV, (b) hue - temperature calibration based on four different mean cell temperatures.

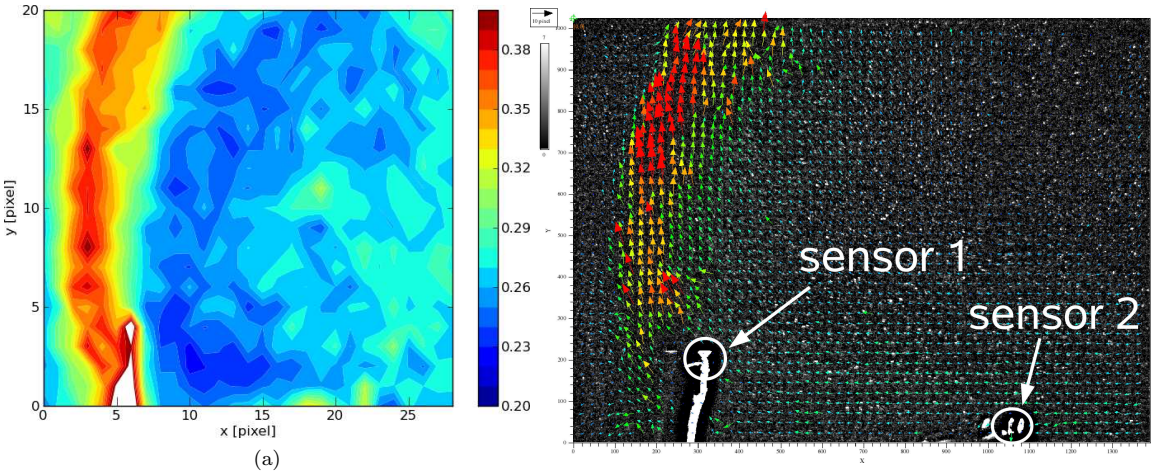

(a) (b)

Figure 2: Instantaneous hue (temperature) and pixel displacement (velocity) fields. (a) Hue values after filtering, (b) to b/w converted image with pixel displacement vectors calculated by means of PIV.

References

[1] Dabiri D., (2009): Digital particle image thermography / velocimetry: a review, , *Exp. Fluids, vol. 46, pp. 191-241.*

[2] Schmeling D., Czapp M., Bosbach J., Wagner C., (2010): Development of Combined Particle Image Velocimetry and Particle Image Thermography for Air Flows, *International Heat Transfer Conference (IHTC14)*, Washington, DC, USA

Application of laser techniques for study of flow structure in a model draft tube

S.G. Skrypkin[1,2] and I.V. Litvinov[1,2]

[1] Department of Heat Power Engineering, Institute of Thermophysics SB RAS, Novosibirsk, Russia
[2] Physics Department of the Novosibirsk State University, Novosibirsk, Russia

Abstract:
Draft tube is an important part of the hydropower station and used to connect exit of the hydroturbine and lower pond. Main problems at operation of the draft tubes are related to enhancement of efficiency and stability of the flow [1]. For optimization of the draft tube design detailed studies are needed. The current work has been done using specially build closed hydrodynamic loop. The test section was designed based on model geometry of TURBINE-99 [2] (Fig.1). The test section was made using plexiglas and provided optical access to all parts of the studied flow. During the experiments flow visualization using 3 Wt laser sheet and high speed camera has been performed. Besides advanced nonintrusive techniques such as stereo-PIV and two-component LDA systems have been applied. The measurement results will be presented in our presentation.

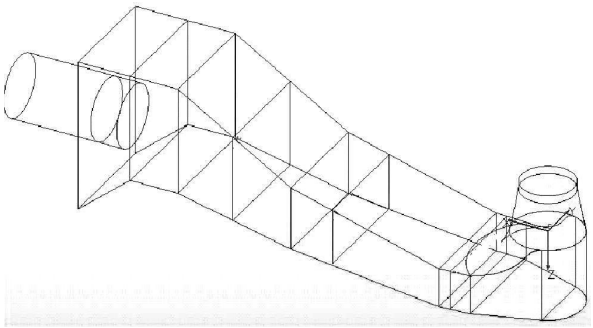

Figure 1: *Test section*

The authors are pleased to acknowledge financial support of the work by the Russian Foundation for Basic Research and the Ministry of Education and Science of the Russian Federation within frames of Federal Target Program "Scientific and Educational Cadres of Innovative Russia" for 2009-2013 years.

References

[1] Gubin M.F., (1970), Draft tubes of hydropower stations, *Moscow. Energia270 p.*

[2] Cervantes M. J., Engström T. F., Gustavsson L. H., (2005), *Proceedings of the third IAHR/ERCOFTAC Workshop on draft tube flows. Turbine-99 III*, Lulea University of Technology

Numerical and experimental modeling vortex formation in a vortex hydrodynamic chamber

Alexey Vinokurov[1,2] and Dmitry Dekterev[1]

[1] Department of Heat Power Engineering, Institute of Thermophysics SB RAS, Novosibirsk, Russia
[2] Physics Department of the Novosibirsk State University, Novosibirsk, Russia

Abstract:
Vortical flows are widely used in many fields of technology, so actuality of their study does not give rise to doubts. Scrubbers and cyclone separators are used in industry for gas scrubbing and deaeration of fuels. Flame stability in burners is reached through using vortical flows. Unsteady phenomena behind a hydroturbine's rotor also are researched a lot. The purpose of this work is investigation of unsteady phenomena in fluid flows, particularly precessing vortex core, which is generated when the vortical flow outflows from the cylindrical nozzle. Numerical simulation of the problem with real parameters was carried out with using CFD program STAR-CCM+. For simulation of steady problem k-ϵ-model of turbulence was used. For calculation of unsteady problem implicit time scheme, Detached Eddy Simulation method and Spalart-Almaras Detached Eddy model of turbulence were used. Visualization of the vortex structures was carried out using λ_2 criterion. Experimental studies were carried out also and results of numerical and experimental modeling agree to each other. Simulation of unsteady problem shows the existence of secondary central vortex, which also was observed at the experiment.

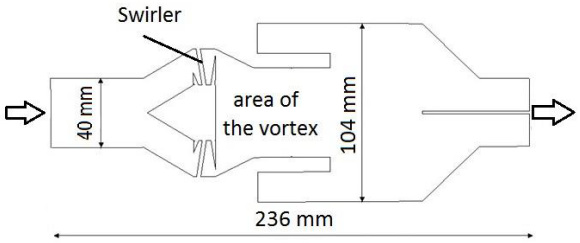

Figure 1: *Scheme of plant*

The authors are pleased to acknowledge financial support of the work by the Russian Foundation for Basic Research and the Ministry of Education and Science of the Russian Federation within frames of Federal Target Program "Scientific and Educational Cadres of Innovative Russia" for 2009-2013 years.

References

[1] S.V. Alekseenko, P.A. Kuibin and V.L. Okulov, (2007), *Theory of Concentrated Vortices. An Introduction*, Springer

[2] C.E. Cala, E.C. Fernandes, M.V. Heitor and S.I. Shtork, (2006), Coherent structures in unsteady swirling jet flow, *Exp. Fluids, vol. 40, pp. 267–276*

Thermal and chemical interactions between solid fuel particles and flowing gas

Izabela Wardach-Święcicka [1], Dariusz Kardaś [1], Jacek Pozorski [1]

[1] The Szewalski Institute of Fluid Flow Machinery Polish Academy of Sciences, Gdańsk, Poland

Abstract:
Two-phase flow with dispersed particles in a gas stream is important in power engineering [1], moreover, it is interesting from research reasons. Interactions between ,,cold" solid phase and ,,hot" gas phase may lead to shape, mass and volume changes of the particles. Those parameters have an impact on the aerodynamic properties determining for example the residence time of particles in combustion chamber. This last one is a main parameter which influences on whole combustion process efficiency. Mass exchange between solid particle and surrounding gases results in the additional mass, momentum and energy source in flow, moreover violent volume changes of the particle may significant modify its trajectory. The modeling of turbulence in that case becomes an important issue. The different methods of turbulence modeling give different results [2]. The values of particles concentrations or velocity field of continuous phase become significant information. Described problem is a real practical phenomenon. Dispersed phase flow with changing mass and density solid phase, it is for example pulverized coal combustion in a real industry boiler. In this case, in the first stage of process called pyrolysis, such phenomena as vaporization and devolatilization (mass changes), and swelling or shirking of grains (volume changes), take place, [3]. These processes happen due to heat transfer from hot flue gases to a fuel particle. As it was mentioned before, analysis of the thermal processing of various solid fuels has an important practical meaning. Solid fuel like coal or biomass may have different physical and chemical properties depending on its origin, what may have an essential effect on the combustion process. As a result, efficiency of energy conversion may decrease and thus operating of the heat and power plants becomes more difficult. Numerical modeling is practically the only way of broadening knowledge about thermal processing of solid particles. It gives detailed information about temperature and velocity field in the particles vicinity.

The aim of this work is to investigate the solid particles – gas interactions. For this purpose numerical modeling was carried out by means of a commercial code for simulations of two-phase dispersed flows with in-house models accounting for mass and density change of solid phase. In the studied case the particles are treated as a spherical moving grains carried by a swirling stream of hot gases. In contrast to numerical simulations results given by others authors and referred to heated channel flows [4], [5], the particles are treated as an open system where in result of heat transfer with the surrounding hot gases, the mass transfer (the volatiles are released) and density change (the particles are swelling and shrinking) take place. Presented analysis is a continuation of the work concerning the motion of single solid particle in a heating chanel [6]. The mass and density changes were determined in the wide range of the temperature (Figure 1 and Figure 2) according to the experimental data received from Institute for Chemical Processing of Coal in Zabrze, [7]. In the simulations two types of particles were taken into account: the particles with a density, calculated from the standard law determined by commercial code, and the particles with user-defined density. The results of these simulations were presented and compared. To determine the kinetic constants for rate of pyrolysis the in-house one-dimensional model was used. The mathematical model is based on the mass, momentum and energy equations for porous spherical solid particle heated by hot gas stream.

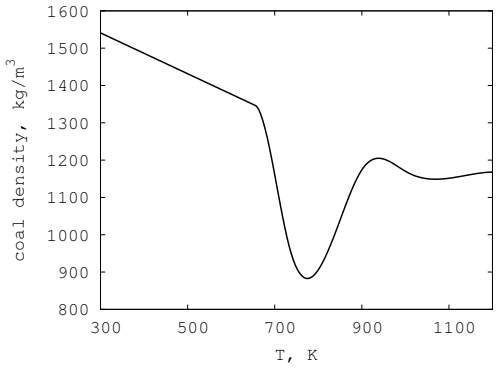

Figure 1: *Apparent density of coal particle in the function of temperature, [7].*

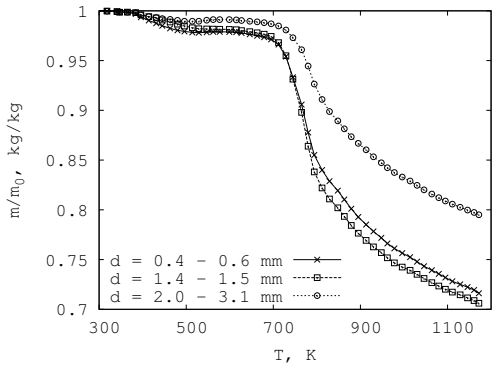

Figure 2: *Mass of the particle measured during pyrolysis process, thermogravimetric data, [7].*

References

[1] Moin P., Apte S.V., (2006), LES of multiphase reacting flows in complex combustors, *AIAA Journal, vol. 44, pp. 698-708.*

[2] Apte S.V., Mahesh K., Moin P., Oefelein J.C., (2003), Large-eddy simulation of swirling particle-laden flows in a coaxial-jet combustor, *International Journal of Multiphase Flow, vol. 29, pp. 1311-1331.*

[3] Tomeczek J., (1992), *Coal combustion. The academic scripts, in Polish.*, Silesian University of Technology.

[4] Pozorski J., Łuniewski M., (2011), Analysis of SGS effects on dispersed particles in LES of heated channel flow. Quality and Reliability of Large-Eddy Simulations II, *ERCOFTAC Series, vol. 16(1), pp. 171-180.*

[5] Jaszczur M., (2010), A numerical analysis of the fully developed non-isothermal particle laden turbulent channel flow, *Proceedings of The 19th Polish National Fluid Dynamics Conference*, Poznań, on CD.

[6] Wardach-Święcicka I., Kardaś D., (2010), Modeling of single solid particle combustion in a free stream flue gases, *Proceedings of The 19th Polish National Fluid Dynamics Conference*, Poznań, on CD.

[7] Ściążko M., (2005), *Modeling of pressure generation from the thermally plastified packed bed coal grains, Technical Report, in Polish*, Institure for Chemical Proccesing of Coal, Zabrze, 2005.

The edge of chaos in plane Poiseuille flow

Stefan Zammert and Bruno Eckhardt [1]

[1] Fachbereich Physik, Philipps-Universität Marburg, Germany

Abstract:
Plane Poiseuille flow has the well known feature that its laminar flow becomes linearly unstable at $Re = 5772.22$ [1]. But even for Reynolds numbers where the laminar flow is stable it is possible to obtain sustaining turbulence in experiments as well as in numerical simulations for appropriate initial conditions. The boundary separating initial conditions which become turbulent from those becoming laminar is called *edge of chaos*[2]. The dynamics on the boundary was already investigated in other shear flows like pipe or plane Couette flow[3, 4]. We used the technique of edge-tracking [2, 3] to investigate the edge of chaos for plane Poiseuille flow in small computational domains with spanwise and streamwise extends of 2π. For direct numerical simulations we use the *channelflow*-code developed by John Gibson [5].

In our simulations we identified a simple travelling wave to be a local attractor in this boundary. A visualization of this travelling wave is shown in figure 1. This wave is fully three dimensional and has a strong lowspeed streak. A stability analysis of this states shows that it has a stable manifold of codimension one for Reynolds numbers bigger than 510 up to Reynolds number which are above the critical one from the laminar flow. An attractor in the edge of chaos, as the found travelling wave, is called a *edge state* [3].

At the critical Reynolds number where the laminar profile undergoes a subcritical pitchfork bifurcation a travelling wave is created that can be continued to Reynolds numbers below 4700 in our computational domain. This travelling wave is different from the above edge state. If the Reynolds number is decreased the travelling wave rapidly undergoes an impressive amount of bifurcations which create further travelling waves and periodic orbits. Some of these objects seem to influence on the dynamics in the laminar-turbulent boundary, at least for some range in Reynolds numbers. We will show how particular states are connected to the laminar-turbulent boundary and discuss possible structures of the state space depending on the Reynolds number.

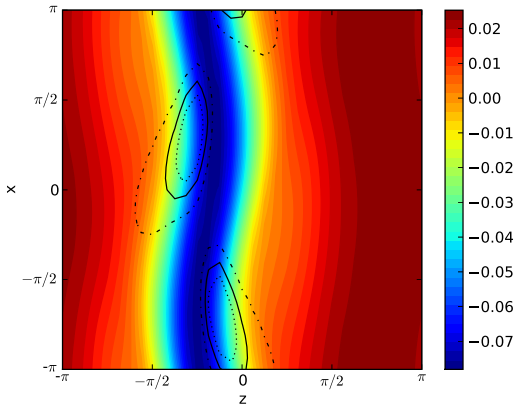

Figure 1: *Color plot of the streamwise velocities in the midplane for the travelling wave which is a edge state at Re=1400. Additionally, isocontours for the Q vortex criterion at 0.0002 (dash dotted), 0.0005 (solid) and 0.0007 (dotted) are shown.*

References

[1] Orszag S. (1971), Accurate solution of the Orr-Sommerfeld stability equation, *Journal of Fluid Mechanics, vol. 50, p. 689-703*

[2] Skufca J. D., Yorke, J. A. and Eckhardt B. (2006), Edge of Chaos in a Parallel Shear Flow, *Phys. Rev. Lett., vol. 96, p. 174101*

[3] Schneider T. M., Gibson, J. F., Lagha M., De Lillo F. and Eckhardt B. (2008), Laminar-turbulent boundary in plane Couette flow, *Phys. Rev. E, vol. 78, p. 037301*

[4] Schneider T. M., Eckhardt B. and Yorke J. (2007), Turbulence Transition and the Edge of Chaos in Pipe Flow, *Phys. Rev. Lett., vol. 99, p. 034502*

[5] Gibson J. F., *www.channelflow.org*

Session IV
Applied aerodynamics
Wednesday, 10th August, 10:20 – 11:20

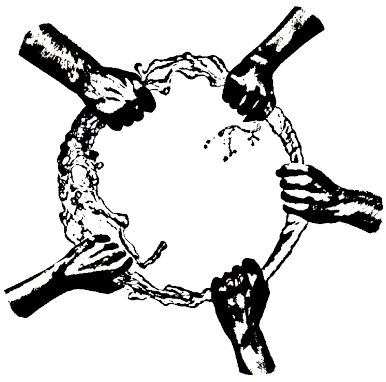

Flow over a wind turbine: simulation and validation

I. Herraez [1], H. Plischka [1], B. Stoevesandt [2] and J.Peinke [1]

[1] Forwind, Center for Wind Energy Research, Oldenburg, Germany
[2] Fraunhofer IWES, Institute for Wind Energy and Energy System Technology, Oldenburg, Germany

Abstract:
This work is part of the IEA Wind Task 29 MEXNEXT, which aims at achieving a better understanding of the flow over wind turbines [1], [2]. This is done by means of numerical simulations and the measurements of the MEXICO-project [3]. 20 research institutes from 11 different countries participate in this project, each of them focusing on different simulation models and/or aerodynamic effects.

The simulation of the wind turbine aerodynamics is a challenging task involving a great uncertainty due to its complexity and the lack of validated models. However, it is of great importance for optimizing the performance of those machines and reducing their costs.

The most promising technique for simulating the wind turbine aerodynamics is the CFD method. The high computational cost of CFD simulations makes necessary to divide the computational domain in several parts and run the simulations in parallel. With commercial CFD programmes, one licence has to be paid for every processor running the simulation. This limitation makes the simulation process very expensive, both in terms of time and money. Open source CFD software is very attractive in this sense, since it allows the use of any number of processors during the simulations with no economic cost at all. Therefore, a comparatively extremely inexpensive and fast simulation is therewith possible (assuming enough computer capacity). Furthermore this kind of codes allow the user to modify and extend freely the program (this is of obvious interest for research purposes).

For these reasons, the open source software OpenFOAM is used within this work. The scope is not only to investigate the aerodynamics of wind turbines but also to assess the capability and possible constraints of this open source CFD code.

RANS simulations are performed for axi-symmetric flow with constant wind speed and non-varying operating conditions. URANS simulations are carried out for transient analyses, like e.g. yaw misalignment.

The turbine of the MEXICO-project, which is simulated within this work, has 3 blades and a rotor diameter of 4.5 m. The measurements were performed at the Large Scale Low Speed Facility of the German-Dutch DNW wind tunnel. The open section of the wind tunnel is 9.5 x 9.5 m^2. Different wind speeds, rotational speeds, pitch angles, and flow directions were measured. The available data include pressure distributions and load measurements along several stations of the blades as well as flow field measurements taken by means of Particle Image Velocimetry (PIV) [3]. The quality and quantity of the measurements is high enough for assuring a good basis for the validation of computational models.

After validating the numerical results, discrepancies between measurements and simulations are analysed in detail and improvement proposals for the models are done.

References

[1] T. Lutz (2011): Near Wake studies of the Mexico Rotor , *EWEA Annual Event*

[2] J.G. Schepers, K. Boorsma, C. Kim, T. Cho (2011): Results from Mexnext: Analysis of detailed aerodynamic measurements on a 4.5 m diameter rotor placed in the large German Dutch Wind Tunnel DNW, *EWEA Annual Event*

[3] J. G. Schepers and H. Snel, (2007): Model Experiments in Controlled Conditions, Final report, *CN-E-07-042, Energy Research Center of the Netherlands, ECN*

Cross-wind investigation for a simplified high-speed train model using Large Eddy Simulation (LES)

Stefanie Schiffer [1] and Claus Wagner [1]

[1] Institute of Aerodynamics and Flow Technology, German Aerospace Center, Göttingen, Germany

Abstract:
The flow around a simplified model of a leading car of a high-speed train was investigated using Large Eddy Simulation (LES). Since the front of a train is subjected to the largest forces [1], the focus of this study was laid on the aerodynamic forces acting at the train nose when examining cross-wind stability of the model. Regarding the high computational costs of LES, as a first test case a Reynolds number of 2.8×10^5, based on the free stream velocity and the scaled standard train width, has been considered (Figures 1a-b and 2a-b). Further simulations have been performed for various angles of attack to examine cross-wind effects. For subgrid-scale modeling the Smagorinsky model [2] in combination with van Driest damping were used. The simulations have been carried out with a second order central differencing method on an unstructured grid with more than 1.3×10^6 cells.

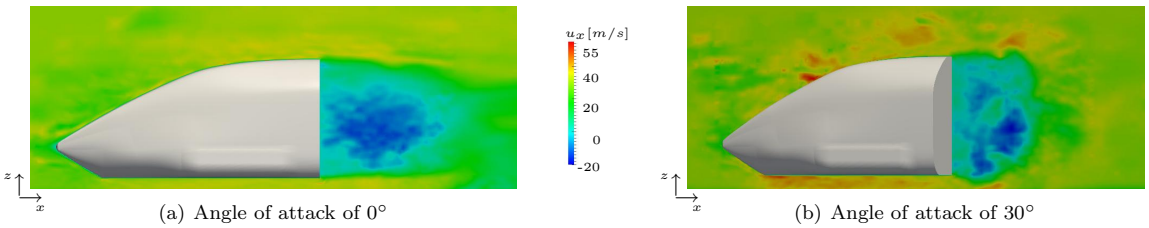

(a) Angle of attack of 0° (b) Angle of attack of 30°

Figure 1: Instantaneous velocity field around the simplified train model in streamwise direction

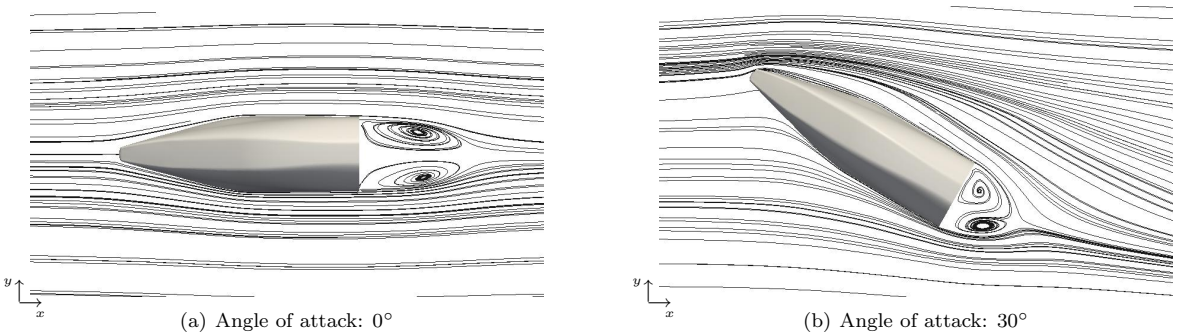

(a) Angle of attack: 0° (b) Angle of attack: 30°

Figure 2: Time averaged streamlines projected onto a plane for different angles of attack of the flow around the simplified train model

References

[1] Gawthorpe, R. G., (1978), Aerodynamics of Trains in the Open Air, *IMechE Railway Engineer International*

[2] Smagorinsky, J., (1963), General Circulation Experiments with the Primitive Equations, *Mon. Weath. Rev., vol. 91, pp. 99-164*

Experimental studies on the "Phantom Yaw Effect" at maneuvering slender bodies

Oliver Wysocki and Erich Schuelein

Department of High Speed Configurations, German Aerospace Centre, Goettingen, Germany

Abstract:

Asymmetric vortices can occur unexpectedly on slender bodies at high angles of attack. These vortices separating from the nose or/and shoulder region induce a side force and also a corresponding yawing moment often referred to as "phantom yaw".

In the last decades, there have been many experimental and also numerical studies on this phenomenon. The aim was to understand this effect and to find the influencing parameters. There have also been investigations on using the asymmetric vortices for control purposes in addition to the fins. Despite this, another target of research has been the suppression of the vortex inducing side forces and yawing moments in order to increase the stability of e.g. a missile in a maneuver.

Most of the wind tunnel tests have been done without model motion at several but fixed angles of attack. Since slender bodies as missiles achieve these high angles of attack via very rapid pitching maneuvers, the model motion is supposed to have some impact on the test results. One reason for the lack of dynamic test data at high Reynolds numbers are high inertial and aerodynamical forces acting on the test model and it's support. They result in contradicting design issues. On the one hand, the support needs to be stiff to withstand all forces and moments and on the other hand, the aerodynamic behaviour of the model shall not be changed by the support.

Nonetheless, a maneuver simulator has been built at the DLR Goettingen. By means of this device, wind tunnel tests in a transonic wind tunnel at high Mach and Reynolds numbers, pitching rates of up to $\omega = 700^{\circ}/s$ and pitching maneuvers from $\alpha = 0 \ldots 45^{\circ}$ have been done.

We compared the "phantom yaw"' emergence at a clean configuration with the ones at a configuration housing a pair of symmetric longitudinal slot nozzles which were fed by natural ventilation. The results showed a yawing moment for the clean configuration at angles of attack higher than $\alpha = 38^{\circ}$. They also showed that the jet flow through the slot nozzles successfully suppressed the yawing moment by causing a fixed separation. Differences between static and dynamic tests could be seen as well.

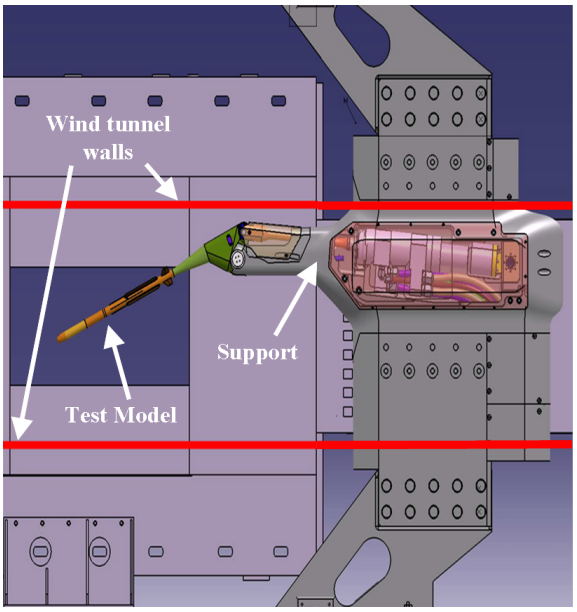

Figure 1: *The Maneuver Simulator in the TWG*

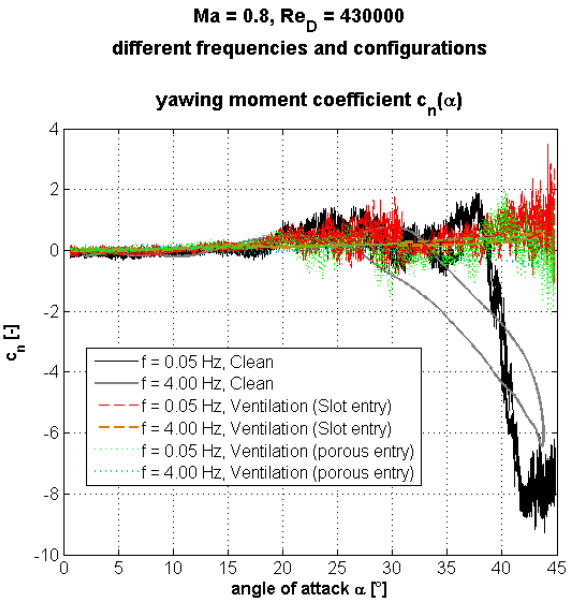

Figure 2: *Test results from TWG experiments*

Improved Mathematical Model for Hydroelastic Vibrations of Partially Filled Shell

Iryna Kononenko [1] and Uliana Ogorodnyk [2]

[1] Department of Mathematics and Mechanics, Kharkov National University/ Kharkov, Ukraine
[2] Department of Dynamics and Strength of Machines Division, Institute for Mechanical Engineering Problems/ Kharkov, Ukraine

Abstract:
A problem of durability for a tank containing a liquid is considered. This problem is reduced to a three-dimensional problem of fluid-elastic harmonic vibrations for partially filled shells of revolution [1]. The shell with complex geometry is considered (characterized by a system of cylindrical, conical and spherical surfaces), see figure 1.

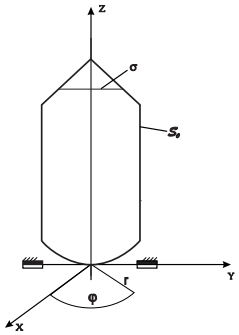

Figure 1: *Example of the considered shells*

Corresponding mathematical model is developed. Advantage of the model that it can handle analytically behavior of the pressure in the vicinity of the nodes reducing initial 3D problem to 1D integral equation.

Numerical solution of the derived hypersingular integral equation is built using special quadrature formulas of the interpolative type with the nodes which are zeros of the second kind Chebychev polynomials for a hypersingular integral and integral with a smooth kernel [2], [3]. Used computational technique has a quick convergence and requires neglectable amount of CPU time.

Simulation codes are developed to determine dynamic pressure to the shell and free liquid surfaces. FEM/ANSYS packages are used to compare and validate results in the case of the unit shells (conical, cylindrical, spherical).

References

[1] DiBenedetto E., (2010): *Classical Mechanics: Theory and Mathematical Modeling*, Birkhauser

[2] Lifanov I.K., Poltavskii L. N., Vainikko G., (2004): *Hypersingular integral equations and their applications*, Chapman and Hall

[3] Gandel Yu.V., Kononenko A.S., (2006), Justification of the Numerical Solution of a Hypersingular Integral Equation, *Differential Equations, vol. 42, nom. 9, pp. 1326 - 1333*

Session V
Environmental and engineering applications
Wednesday, 10th August, 11:30 – 12:30

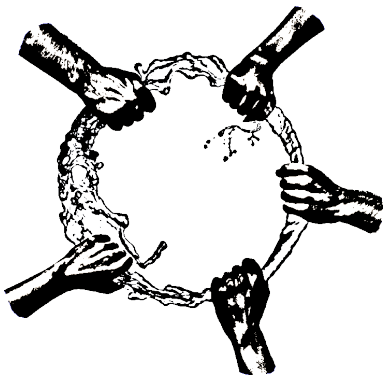

The excitation of internal waves by a submerged turbulent round jet

E. Ezhova, D. Sergeev, A. Kandaurov, and Yu. Troitskaya

Department of Nonlinear Geophysical Processes, Institute of Applied Physics RAS, Nizhny Novgorod, Russia

Abstract:
Sewage disposal by coastal cities to the ocean is an example of man's impact on offshore zone. It produces sensible stress on coastal water areas including effects on hydrodynamics of coastal zone and coastal ecosystems. The series of major international oceanographic experiments near the sewage disposal system described in [1] showed that there existed anomalous peaks in the spectra of the optical images of the surface region close to the collector. A typical outfall construction consists of a submarine pipeline with a diffuser at a far offshore end. Fresh water is discharged into ambient salt water producing buoyant plumes. A hypothesis put forward in this work is that the anomalies are the manifestations of the internal waves generated by the plumes oscillating in the pycnocline region.
We investigated hydrodynamic processes near submerged wastewater outfalls basing on the laboratory scale modeling [2]. The experiments were carried out in Large Thermally Stratified Tank of IAP RAS (LTST) with overall sizes: 20m*4m*2m where the thermocline-like stratification was created. The experiments showed that the internal waves were generated intensively during the discharge process. The structure and surface manifestations of these waves were explored and it was shown that they might be manifested at the surface [2, 3]. In order to investigate the mechanism of the internal waves excitation a new series of experiments in LTST was performed. The water with density of the lower stratification layer was discharged vertically upwards from the round nozzle (d=6 mm) at rates from 110 to 210 cm/s. The rates and the distance from the nozzle to the thermocline were chosen to provide the axial jet velocity and the jet radius near the thermocline equal to those in the experiments with buoyant jets. The temperature oscillations were measured during the experiment by means of the string of 13 thermistors, placed vertically 50 cm far from the source. In order to investigate the behaviour of the jet in the thermocline region we performed underwater survey. The spectra of the jet oscillations were compared to the spectra of the internal waves, showing good correspondence.
The type of an unstable mode generating the internal waves was determined basing on the underwater survey data. It turned out that the axisymmetric mode prevailed at the generation frequency. However, this mode has to be stable for the mean velocity profiles of the jet obtained from the experiment in the context of the linear hydrodynamic stability theory for the parallel flows. In order to explain the excitation of the axisymmetric mode, the stability analysis of the nonparallel jet with self-similar velocity profiles (which is a model of a jet close and in the lower part of the thermocline) was performed using the approximation suggested in [4, 5]. It was shown that the mode becomes unstable under experimental conditions. The estimated frequency of the most unstable disturbances is in good agreement with the internal waves' frequency.

References

[1] Keeler R., Bondur V. and Gibson C., (2005), Optical satellite imagery detection of internal wave effects from a submerged turbulent outfall in the stratified ocean, *Geophys. Res. Lett., vol. 32, L12610, doi:10.1029/2005GL022390.*

[2] Bondur V., Grebenyuk Yu., Ezhova E., Kazakov V., Sergeev D., Soustova I. and Troitskaya Yu., (2010), Surface manifestations of internal waves investigated by a subsurface buoyant jet. Part 2. Internal wave field, *Izvestiya, Atmospheric and Oceanic Physics, vol. 46, no.3, pp. 347-359.*

[3] Bondur V., Grebenyuk Yu., Ezhova E., Kazakov V., Sergeev D., Soustova I. and Troitskaya Yu., (2010), Surface manifestations of internal waves investigated by a subsurface buoyant jet. Part 3. Surface manifestations of internal waves, *Izvestiya, Atmospheric and Oceanic Physics, vol. 46, no.4, pp. 482-491.*

[4] McAlpine A. and Drazin P.G., (1998), On the spatio-temporal development of small perturbations of Jeffery-Hamel flows , *Fluid Dyn. Research, vol. 22, pp. 123-138.*

[5] Shtern V. and Hussain F., (2003), Effect of deceleration on jet instability, *Journal of Fluid Mechanics, vol. 480, pp. 283-309.*

A new hydro-morphodynamic solver for the shallow waters

M. Postacchini [1] and M. Brocchini [1]

[1] Department of ISAC, Università Politecnica delle Marche, Ancona, Italy

Abstract:
A hydro-morphodynamic numerical model is illustrated as a novel contribution to the investigation and prediction of nearshore flows and seabed changes forced by waves and currents. The model includes a robust hydrodynamic solver [1] for the integration of the Nonlinear Shallow Water Equations (NSWE) by using a WAF approach, that well reproduces the dynamics of both inner surf zone and swash zone flows [2]. Further, a flexible solver for the resolution of the Exner equation has been used to evaluate the morphological evolution of the seabed, by means of closure laws based on both bed-load and suspended-load transport. Coupling of NSWE and Exner equations and updating of the solution is made by means of a sequential splitting scheme [3].

The model has been validated in great detail by reproducing both analytical and numerical solutions, available in the literature. The capability to reproduce the bed-load transport has been evaluated by using three different closures to simulate the motion of a submerged dune induced by a current [4] and dam-break events [5], [6] (see also figure 1). The suspended-load transport rate has been evaluated by reproducing swash-type events. The results, obtained using two different closure laws, have been compared with the analytical solution of Pritchard and Hogg [7]. Other comparative tests have been performed to validate the total transport. In this case, bed-load and suspended-load laws have been used to reproduce some experimental tests (see figure 2) that have been carried out in the wave flume hosted in the Hydraulic Laboratory of the Università Politecnica delle Marche (Ancona, Italy).

In summary, all the validation tests suggest a good behavior of the model at reproducing both erosive and accretive events and confirming that it behaves similarly to a fully-coupled hydro-morphodynamic model.

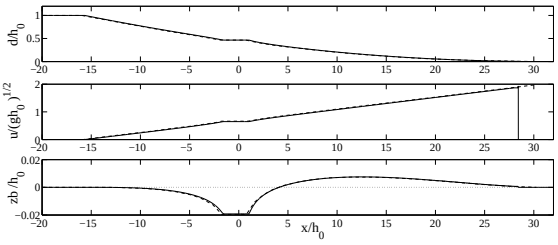

Figure 1: *Comparison between exact Riemann solutions of [5] (dashed lines) and numerical results (solid lines); from top to bottom: dimensionless depth, velocity and seabed evolution*

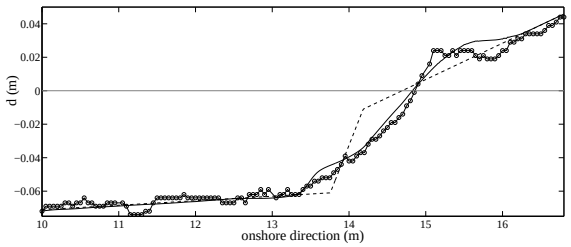

Figure 2: *Seabed evolution of a laboratory beach: comparison of the final results of the solver (solid line) and experimental data (circles) with respect to the initial seabed (dashed line)*

References

[1] Brocchini, M., Bernetti, R., Mancinelli, A. and Albertini, G., (2001), An efficient solver for nearshore flows based on the WAF method, *Coast. Engng., vol. 43, pp. 105-129*

[2] Brocchini, M. and Dodd, N., (2008), Nonlinear shallow water equations modeling for coastal engineering, *WW-A.S.C.E., vol. 134 (2), pp. 104-120*

[3] Postacchini, M., Brocchini, M., Landon, M. and Mancinelli, A., (2011), A multi-purpose, intra-wave, shallow water hydro-morphodynamic solver, *Coast. Engng., under peer review*

[4] Hudson, J., Damgaard, J., Chesher, T. and Cooper, A., (2005), Numerical approaches for 1D morphodynamic modelling, *Coast. Engng., vol. 52, pp. 691-707*

[5] Briganti, R., Dodd, N., Kelly, D.M. and Pokrajac, D., (2011), An efficient and flexible solver for the simulation of the morphodynamics of fast evolving flows on coarse sediment beaches, *Int. J. Numer. Meth. Fluids, in print*

[6] Kelly, D.M. and Dodd, N., (2009), Floating grid characteristics method for unsteady flow over a mobile bed, *Comput. Fluids, vol. 38, pp. 899-909*

[7] Pritchard, D. and Hogg, A.J., (2005), On the transport of suspended sediment by a swash event on a plane beach, *Coast. Engng., vol. 52, pp. 1-23*

Finite element/boundary element coupling for airbag deployment

T.M. van Opstal [1], E.H. van Brummelen [1]

[1] Mechanical Engineering, Eindhoven, University of Technology, Eindhoven, the Netherlands

Abstract:
In a small percentage of airbag deployments, out-of-position impact occurs, usually resulting in severe injuries. To understand and improve the inflation process, a precise understanding of the airbag dynamics is required. This can be provided by accurate numerical simulations. These simulations are however a complicated endeavor, mainly on account of the large displacements and length-scale disparities inherently involved. On the one hand, a realistic stowed airbag constitutes a labyrinth of intricate folds. On the other, the final configuration is a relatively simple bulb. To date, the complex behavior on the small scales have been overly simplified (e.g. [1]) rendering the results inappropriate for analysis of out-of-position situations.
The approach proposed here is to identify subdomains of the fluidic domain eligible to resolution of the small scales. The boundary element method is deemed suitable for the discretization of these subregions for a number of reasons:

- the large displacements do not entail mesh skewing,
- the solution is calculated exclusively where it is required: at the coupling interface,
- the structure mesh can be inhereted by the fluid.

On the down side, the involved integrals contain singularities, and the resulting matrix system (though smaller) is full.
To assess this approach, a potential model [3] is adopted for the fluid and the wave equation [2] for the membrane. The latter is discretized with the classical finite element method. Due to the full matrix structure, the penalty of adding the necessary constraints of volume conservation and closing the pure Neumann system, is limited. Due to the typically low mass of the membrane, the added-mass effect [4] dictates the use of a strongly coupled time-integration scheme. A final feature of the proposed methodology is the treatment of contact through a potential force. Performance is demonstrated with numerical examples such as the inflation of a pancake-shaped enclosure [5].

References

[1] Marklund, P.-O. and Nilsson, L., (2002), Simulation of airbag inflation processes using a coupled fluid structure approach, *Computational Mechanics*, vol. 29, no. 4-5, pp. 289–297.

[2] Yong, D., (2006), Strings, Chains and Ropes, *SIAM*, vol. 48, no. 4, pp. 771-781.

[3] S. Liapis, (1996), An adaptive boundary element method for the solution of potential flow problems, *Engineering Analysis with Boundary Elements*, vol. 18, pp. 29–37.

[4] Brummelen, van, E. H., (2009), Added Mass Effects of Compressible and Incompressible Flows in Fluid-Structure Interaction, *Journal of Applied Mechanics*, vol. 76, no. 2.

[5] P.H. Saksono, W.G. Dettmer and D.Perić, (2007), An adaptive remeshing strategy for flows with moving boundaries and fluid–structure interaction, *International Journal for Numerical Methods in Engineering*, vol. 71, pp. 1009–1050.

Numerical Simulation of Free-Surface Flow in a Single-Screw Extruder

M. Lübke [1] and O. Wünsch [1]

[1] Department of Mechanical Engineering, Fluid Dynamcis, University of Kassel, Kassel, Germany

Abstract:
In polymer processing industry, extruders are used to perform functions such as melting, conveying and devolatization. In the process of devolatization the detection of the free-surface is important due to the fact that the degassing performance depends on the interfacial area. This study concerns numerical simulation of free-surface flows of highly viscous Newtonian liquids in a single-screw extruder. The numerical treatment of a partially filled single-screw extruder is a challenging task due to the small gaps between the screw and the surrounding barrel and the large differences in density and viscosity between the two phases, e.g. polymer melt and air. Furthermore, the rotation of the screw leads to a continuous renewing of the free-surface. For this purpose an Euler-Euler two-phase Volume of Fluid Method (VOF) within the open source framework OpenFOAM is used and modified. The main focus lies on the investigation of the numerical diffusion introduced by the advection of the interface and the air entrainment into the liquid phase in order to control the effects over a long period of time.
First a simplified two-dimensional model of a single-screw extruder consisting of a rotating cylindrical barrel and a fixed internal plate is considered, see Figure 1. Different flow phenomena, including the forming of an interface cusp, can be observed. The resulting flow and the shape of the phase interface are compared against the experiments by [1]. Good agreement is obtained between the numerical and experimental results. Finally the free-surface flow in a partially filled single-screw extruder with dynamic mesh motion is presented (Figure 2).

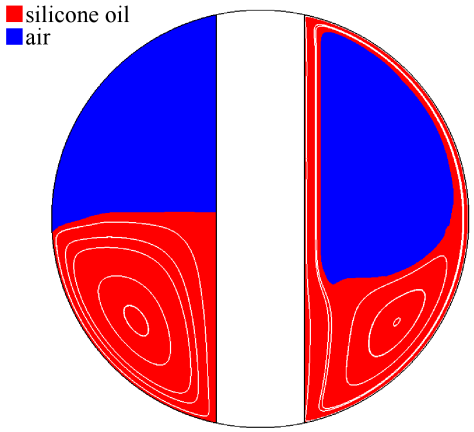

Figure 1: *Predicted free-surface and streamlines in the simplified partially field single-screw extruder model*

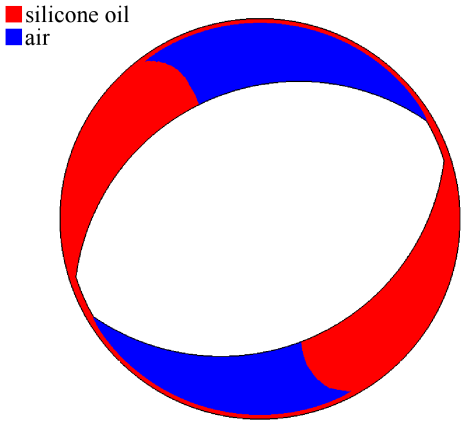

Figure 2: *Free-surface of a highly viscous liquid (silicone oil) in a partially field single-screw extruder*

References

[1] Böhme G., Pokriefke G. and Müller A., (2006), Viscous flow phenomena in a partially filled rotor-stator system, *Arch App Mech, vol. 75, pp. 619-634*

Session VI
Flow control
Wednesday, 10th August, 13:30 – 14:30

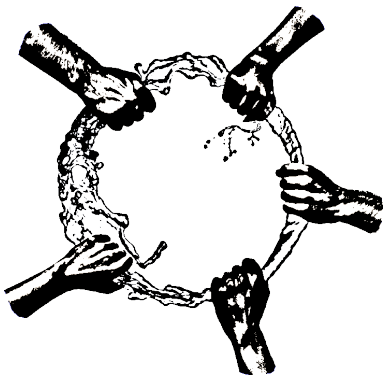

Stability and control of the flow in a plane channel with a sudden expansion

Andrea Fani [1], Simone Camarri [1] and Maria Vittoria Salvetti [1]

[1] Department of Aerospace Engineering, University of Pisa, Italy
E-mail: andrea.fani@for.unipi.it

Abstract:
In the present work we investigate the stability properties of the flow in a 2D-plane channel with a symmetric sudden expansion, which is a possible schematization of a plane diffuser. The laminar flow in 2D diffusers may produce either symmetric or nonsymmetric steady solutions, depending on the value of the Reynolds number as compared with some critical value (see for example [1] and Figure 1). Both the intriguing physics of these flows and their importance in engineering applications have attracted considerable previous attention. Indeed, the diffuser is an important component in many flow devices, such as piping systems and turbomachines. Large effort is often dedicated to optimize the pressure recovery in the diffuser.
The stability properties of the flow are studied in the context of linear theory by looking for the leading global mode, defined as the global mode of largest growth rate. We obtained the growth rate as a function of the Reynolds number and it allowed us to calculate the critical Reynolds number, at which the growth rate is zero.The characteristics of both direct and adjoint unstable modes are described and discussed. These results are in good agreement with literature (see for example [1]).
From this information it is possible to characterize the sensitivity of the considered instabilities to perturbations. Similar analyses have been carried out for example for the flow past a circular cylinder in [2], where the regions of the flow most sensitive to momentum forcing and mass injection are identified, or in [3], where the sensitivity to base-flow modification due to a steady force is discussed.
In this work, perturbations are considered that may be produced by a realistic control strategy. The sensitivity analysis of the flow instability with respect to the considered perturbations are used to provide qualitative hints and quantitative information for the control of the detected instabilities, through a sensitivity map.
We applied the previous theoretical analysis to investigate the effect of a small control device, chosen as a small cylinder of diameter d^* located at the position (x_0, y_0). The cylinder diameter and position were chosen so as to stabilize the symmetric flow configuration, on the basis of the previous analysis. The actual effectiveness of the control strategy was assessed through numerical simulation of the flow in the symmetric channel with the control cylinder. The results are in agreement with the theoretical predictions, as shown in Figure 2.

References

[1] T. Rusak Z. Hawa, "The dynamics of a laminar flow in a symmetric channel with a sudden expansion," *Journal of Fluid Mechanics*, **436**, 283-320 (2001).

[2] F. Giannetti, P. Luchini, "Structural sensitivity of the first instability of the cylinder wake," *Journal of Fluid Mechanics*, **581**, 167-197 (2007).

[3] O. Marquet, D. Sipp, L.Jacquin, "Sensitivity analysis and passive control of cylinder flow," *Journal of Fluid Mechanics*, **615**, 221-252 (2008).

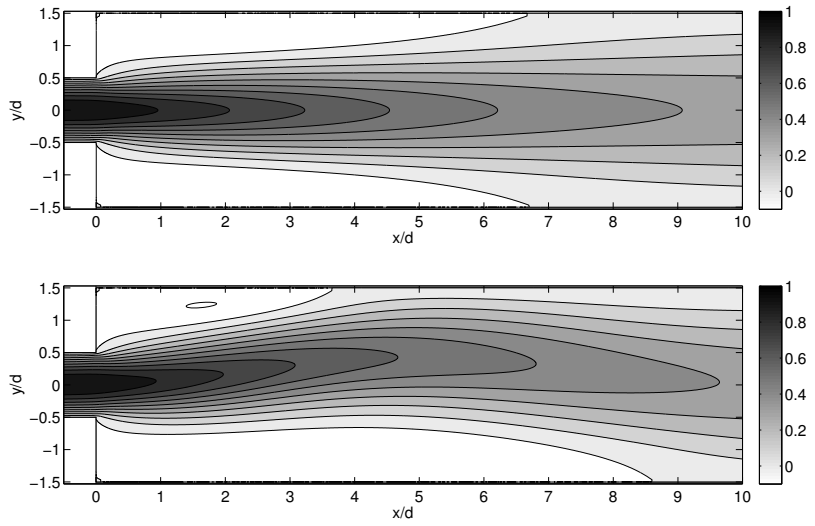

Figure 1: *Re=100. Symmetric unstable solution and asymmetric stable solution, streamwise velocity.*

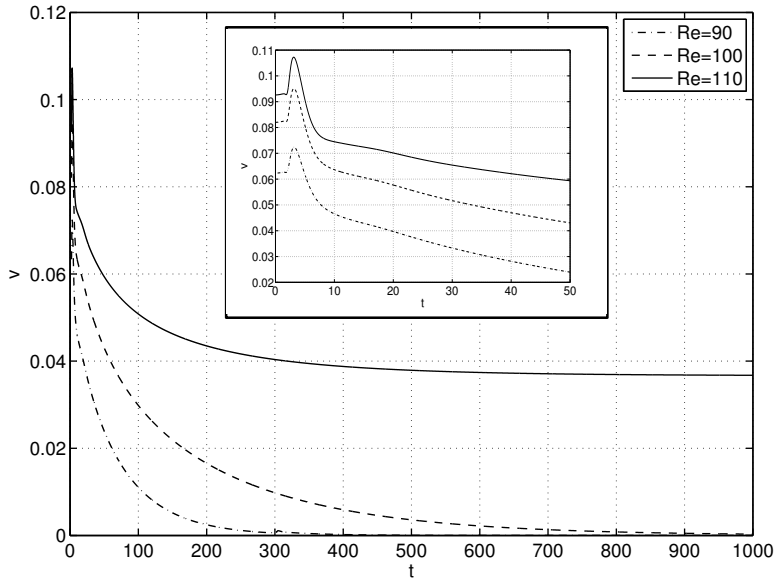

Figure 2: *Time trace of the transverse velocity component at a given point along the channel centerline (v=0 symmetric solution). The effect of the control cylinder is a decrease of the growth rate. For Re=90 and Re=100 the asymmetric instability was damped. For Re=110 the stabilizing effect of the cylinder is not enough to suppress the instability, but the flow is less asymmetric than the initial one.*

Experiments on the drag of superhydrophobic surfaces & interface visualisation

B. R. K. Gruncell [1], I. M. Campbell[2], N. Shirtcliffe[3], N. D. Sandham, & [1], G. McHale[3]

[1] AFM Group, University of Southampton, UK
[2] Wolfson Unit MTIA,University of Southampton, UK
[3] Physics, Nottingham Trent University, UK

Abstract:
Previous experiments have shown that an air layer can reduce the drag on a submerged surface by more than 80% when a sufficient amount of air is blown onto the surface [1]. Recently, experiments have also shown that an air layer (plastron) can be retained by a superhydrophobic surface when it is immersed in water and that such surfaces can also produce a drag reduction of up to 50% in certain circumstances [2]. The interface between the air and water provides a lower shear stress than the interface between water and solid and hence reduces the viscous drag.

In this contribution the existence of a plastron on samples is firstly confirmed experimentally using confocal microscopy. Reflected light is used to determine the position of the air-water interface in relation to the solid substrate. Figure 1 shows that the interface is curved between the roughness elements, with some roughness elements protruding above the air-water interface. The plastron is stable over an immersion period of at least 24 hours but disappears when ethanol is added to the water.

Secondly, this work aims to explore the effect of superhydrophobic surfaces on a flat plate in the laminar, transitional and turbulent regimes. A range of superhydrophobic surfaces have been tested in a towing tank to determine the effect on viscous drag. A flat plate measuring 0.40m × 0.25m has recessed areas allowing for the surface properties to be changed whilst maintaining the experimental setup. Refinements to the experimental setup have produced a repeatability of 1-2%, with turbulators used to trip the flow. A wide range of superhydrophobic surfaces have been tested, from copper nano-flowers to sand grains with a superhydrophobic coating. Samples were tested in a Reynolds number range of $1.6\times10^5 < Re < 1.5\times10^6$. All samples were initially compared to a blank perspex sheet and were found to produce an increase in drag. This increase in drag is attributed to the surface roughness leading to an earlier transition and the effect of roughness on the log-law. The effect of the plastron was explored by returning the surface to a Wenzel (wetted) state by applying ethanol. The plastron was found to have no effect on drag or transition location for all samples tested.

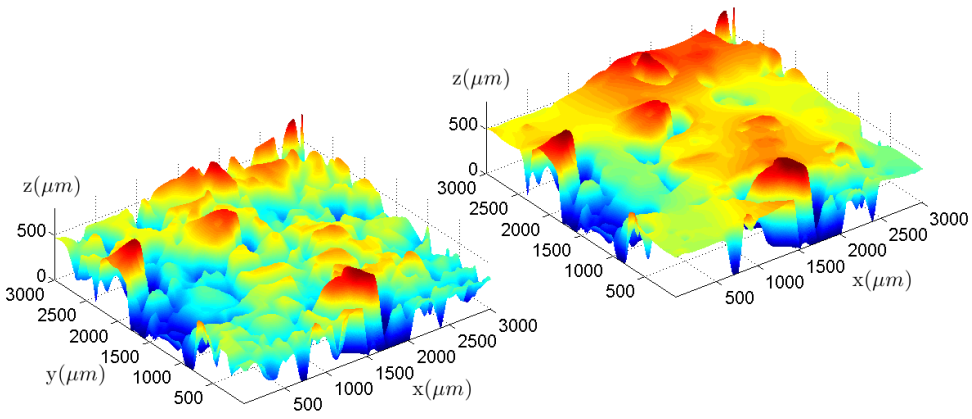

Figure 1: *Surface plots of a) solid substrate and b) air-water interface over a superhydrophobic surface*

References

[1] Elbing B. R., *et. al*, (2008), *Journal of Fluid Mechanics, vol. 612, pp. 201-236*

[2] Henoch C., *et al.* (2006): *Proc. 3rd AIAA Flow Control Conference*, AIAA 2006-3192

Adjoint-based control of turbulent jets

D. Marinc [1], H. Foysi [2]

[1] Aerodynamic Institut Aachen, RWTH Aachen University, Aachen, Germany
[2] Aerodynamic Institut Aachen, RWTH Aachen University, Aachen, Germany

Abstract:
The noise reduction of systems containing turbulent flows is an active research area. There are successful examples of noise control with the predictions of simplified models or educated guessing (trial and error) and sources responsible for sound generation could be identified [3]. Nevertheless it is still a long way to the complete understanding of the mechanisms for sound generation and the best control strategies are still unclear.

Thus, optimal flow control, based on adjoint methods have become popular, lately [4]. The so called adjoint-equations arise from a calculus of variation and enable one to calculate the gradient of a given cost-functional with respect to some control in a reasonable amount of computational time, even under the presence of implicit constraints. These gradient information can be used in an iterative gradient-based optimization algorithm, to obtain the optimal control.

In this work we focus on the noise-reduction of 2D- and 3D-turbulent-plane-jets with a Mach-number $Ma = 0.9$ at a moderate high Reynoldsnumber of $Re = 2000$, based on the inlet velocity, density, viscosity and jet-diameter. The cost-functional, we aim to minimize, is chosen as an integral over the square of the pressure-fluctuations in the near-farfield. As control serves a small volume at the two shearlayers of the jet near the inflow, where heating/cooling can be applied. The code works on a cartesian grid using a 6th-order optimized DRP (dispersion-relation-preserving) central difference scheme [1] for spatial and a 4th-order LD-DRK (low dissipation low dispersion Runge-Kutta) scheme [2] for temporal discretization.

Successful control calculations of 2D- and 3D-plane-jets will be presented, with a noise reduction over several decibel. Furthermore, problems arising from the first-optimize-then-discretize approach will be discussed. In this approach the adjoint equations of the continuous system are discretized (instead of calculating the adjoint of the discretized system) and it has the advantage that for the implementation of the adjoint-equations the same numeric schemes can be used as for the normal flow solver. However, it is well known that, because of numerical inaccuracies and inconsistencies e.g. in the boundary treatment, gradients calculated with the first-optimize-then-discretize approach lack accuracy, especially over long time intervals.

We will give quantitative estimates of these inaccuracies, by comparing the obtained gradient with results from finite differencing (see fig. 1). The inaccuracies limit the length of the control interval. As, e.g. to obtain well converged statistics, long control intervals are often required, we will show an example for receding-horizon optimization [5], where one splits the long interval into shorter subintervals (see fig. 2).

References

[1] Johansson, S., (2004), High Order Finite Difference Operators with the Summation by Parts Property Based on DRP Schemes. *Technical Report, 2004-035*

[2] Hu, F.Q., Hussaini, M.Y., Manthey, J.L., (1995), Low-Dissipation and Low-Dispersion Runge-Kutta Schemes for Computational Acoustics. *J. of Comp. Phys., vol. 124, pp. 177-191*

[3] Ewert, R., Schröder, W., (2003), Acoustic perturbation equations based on flow decomposition via source filtering. *J. of Comp. Phys., vol. 188, pp. 365-398*

[4] Wei, M., Freund, J.B., (2005), A noise-controlled free shear flow. *J. of Fluid Mech., vol. 546, pp. 123-152*

[5] Collis, S.S. and Chang, Y. and Kellog, S. and Prabhu, R.D, (2000), Large eddy simulation and turbulence control. *AIAA, 2000-2564*

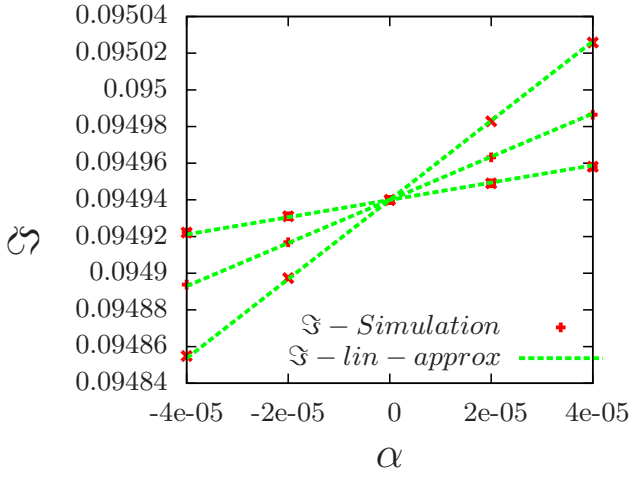

Figure 1: *Shown is the cost-functional for different, randomly chosen, control directions for a simple anti-sound example, where sound emerging from a periodic perturbation is canceled by a control via superposition. The line shows estimates from a first-order taylor series expansion. The crosses are values obtained by solving the Navier-Stokes-equations. As the example shown here is numerically non-challenging the agreement is very good.*

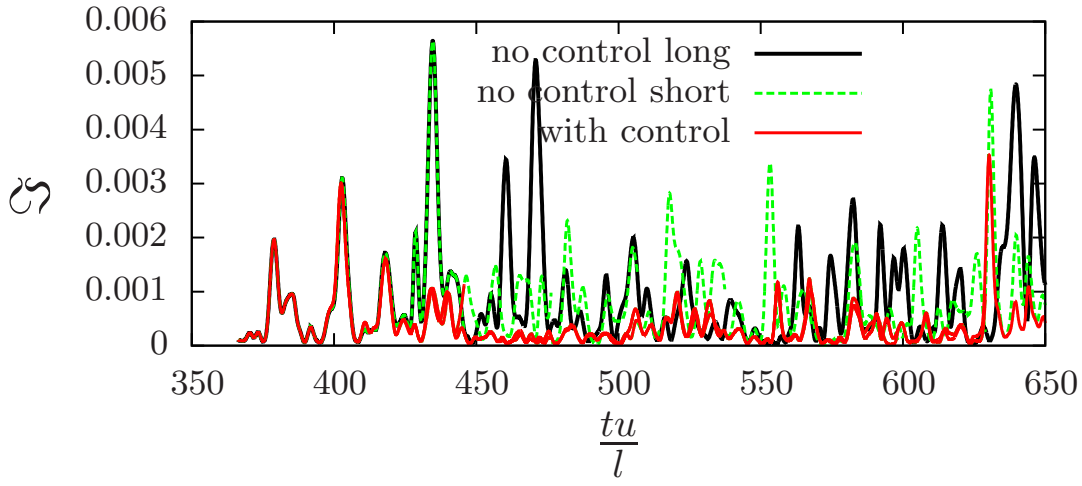

Figure 2: *Cost-functional over time for a long control calculation of a 2D-jet, accomplished with a receding horizon. Shown are the controlled case, the uncontrolled case and the uncontrolled case for every subinterval of the receding horizon calculation.*

Passive control of boundary layer separation in a two-dimensional symmetrical diffuser

A. Mariotti [1], A.N. Grozescu [1], G. Buresti [1] and M.V. Salvetti [1]

[1] Dip. Ingegneria Aerospaziale, Università di Pisa, Pisa, Italy

Abstract:
The object of the present work is the control of boundary-layer separation in a two-dimensional symmetrical diffuser at low Reynolds numbers, through a passive method. The pressure recovery given by a diffuser increases with the expansion rate of the diffuser section, but boundary-layer separation may occur when this rate becomes too large and this leads to a significant deterioration of the diffuser efficiency. The final goal is thus to increase the pressure recovery inside the diffuser by reducing or, if possible, by avoiding the flow separation. The passive control method consists in modifying the geometry of the diffuser walls using appropriately-shaped cavities. The use of cavities is inspired by the idea of trapped vortices (see e.g.[1]). The vortices forming inside these cavities introduce energy into the boundary layer, thus delaying separation. In most of the applications in the literature, which concern external aerodynamics problems, these cavities are significantly larger than the boundary-layer thickness. The difficulty of this approach is to obtain a stable vortex inside the cavity. In the case of the diffuser an additional difficulty arises from the fact that the cavities modify the expansion rate and this in turn affects the boundary-layer separation. Thus, to obtain an efficient control, a compromise must be found between the strength of the trapped vortex and the modification of the diverging wall geometry due to the cavity introduction.
In the present work we focus on the laminar flow inside a 2D plane diffuser having an expansion rate of 2 and a diffusion angle of 7 degrees. The Reynolds number, based on the inlet axial velocity and the half of the inlet section of the diffuser, h, is Re=500. An optimization procedure is developed to identify the best cavity geometry, which can maximize the pressure recovery in the diffuser and minimize the boundary layer separation extent. The cavities used as flow control device have in front a semi-elliptical shape and end with a spline shape tangent to the diffuser diverging walls (see figure 1).Preliminary simulations of the diffuser configuration without cavities have been first carried out by using three different codes, viz. AERO, OpenFOAM and Fluent. AERO is a in-house developed numerical code based on a mixed finite-volume/finite-element discretization on unstructured grids (see e.g.[2]), OpenFOAM is one of the most widely used open-source packages for CFD applications, while Fluent is one of the most diffused commercial codes. Grid sensitivity studies have been performed and the three codes have given consistent results. This configuration is characterized by a large asymmetric zone of separated flow (see figure 2) and gives an adimensionalized pressure recovery of 0.39-0.40 depending on the height of the inlet boundary layer, which was varied from 0 to 0.20h. The optimization of the cavity shape is carried out through the Multi-Objective Genetic Algorithm MOGA-II. The optimization parameters are the distance from the inlet of the location on the wall at which the cavity starts, its total length and the length of the two axes of the semi-ellipse. The objective functional is the pressure recovery coefficient. The optimization is carried out for different inlet boundary-layer thicknesses. For all the considered inlet boundary-layer thicknesses, the most important parameter is the axis of the semi-ellipse normal to the wall, because it determines the width of the trapped vortex region. The increase of the cavity width produces an improvement of the diffuser pressure recovery as long as the flow reattaches immediately downstream of the vortex contained in the cavity (see figure 1). The optimum cavity normal axis is found to be in about a half of the boundary-layer thickness at the beginning of the diffuser diverging part. As for the other parameters, all the optimal cavities start at the beginning of the divergent part of the diffuser and have a total length of more than the 80% of the diffuser, which correspond to a reduced diverging-wall angle. The introduction of the optimal cavity leads to an increase in pressure recovery of more than 13% (see figure 4) and to a strong reduction of the separation extent (compare figure 3 to figure 2). Gains remain significant also for small changes of the cavity shape parameters. Thus, the robustness of this result permits to use the same flow control device in a range of different operating conditions.

References

[1] S.I.Chernyshenko, B. Galletti, A. Iollo and L. Zannetti, (2003), Trapped vorticies and a favourable pressure gradient, *J. Fluid Mech., vol. 482, pp. 235-255*

[2] S. Camarri, M. V. Salvetti, B. Koobus and A. Dervieux, (2004), A low-diffusion MUSCL scheme for LES on unstructured grids, *Comp. Fluids, vol. 33, pp. 1101-1129*

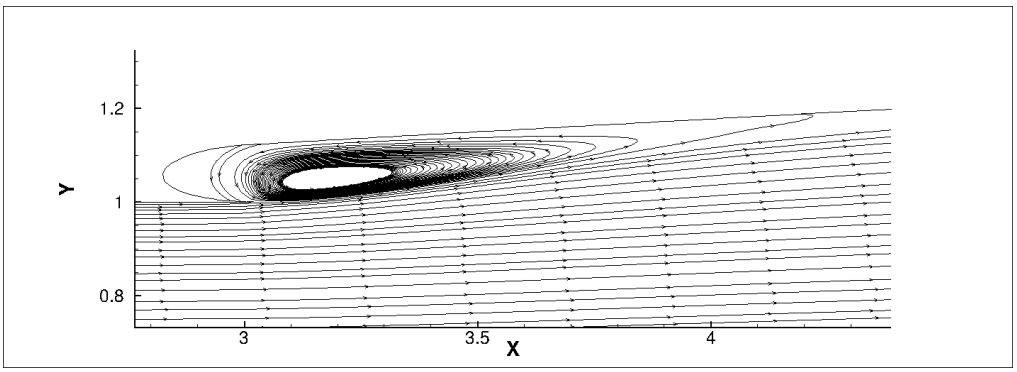

Figure 1: *Geometry of the cavity region and streamlines for the optimized configuration*

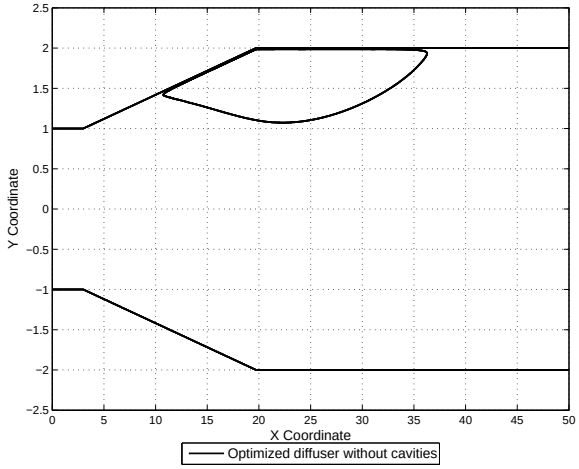

Figure 2: *Flow separation extent in the optimized diffuser without cavities*

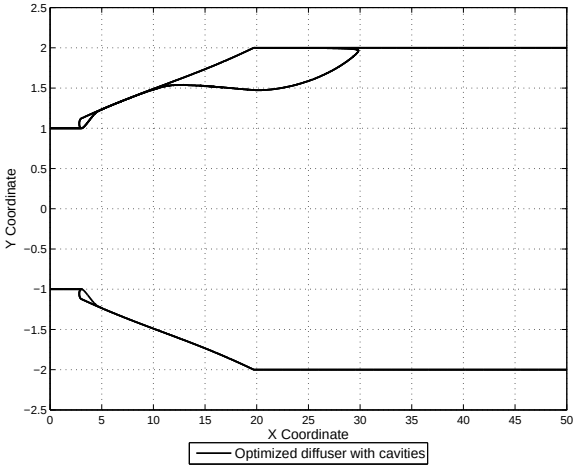

Figure 3: *Flow separation extent in the optimized diffuser with cavities*

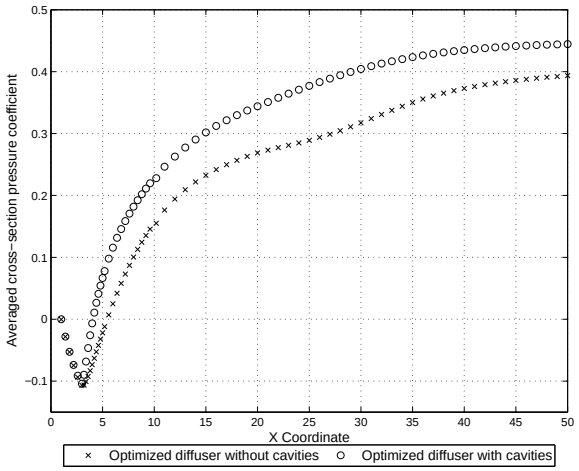

Figure 4: *Averaged cross-section pressure coefficient*

Session XIII
Transition to turbulence
Wednesday, 10th August, 14:40 – 15:40

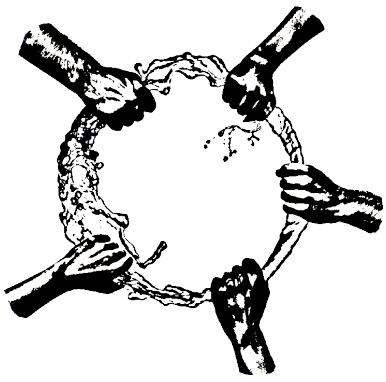

Numerical study and modelling of laminar-turbulent oblique bands in plane Couette flow

Joran Rolland [1]

[1] LadHyX, École polytechnique, Palaiseau, France

Abstract:

Plane Couette flow, like other shear flows (for instance, Taylor–Couette flow with counter rotation cylinders) has a discontinuous transition to turbulence. One of the most striking feature of this transition is the formation of coherent modulation of turbulence. Prigent *et al.* [1] studied experimentally this phenomenon in Taylor–Couette and plane Couette flow, and showed in the case of Taylor-Couette flow that it could be understood as a pattern formation problem. Barkley and Tuckerman (see [2] for a comprehensive review) showed that this phenomenon in plane Couette flow could be reproduced in Direct Numerical Simulations. They proposed an order parameter abd showed that the relationship between angle wavelength and Reynolds number could be extacted from the force balance in the so called laminar region.

We present a numerical study of the pattern formation in plane Couette flow taking into accound both "macroscopic" and "microscopic" aspects of the phenomenon.

Using an order parameter similar to that of Barkley and Tuckerman [3], we show that similarly to Taylor–Couette flow [1], the pattern formation can be thoroughly described by a Landau equation with an additive noise. All the features seen numerically in small periodical domains [2, 3] are described by this model. The few parameters that it contains can be extracted and compare well to the experimental case of Taylor–Couette flow (see [1] and references therein)

We show that allowing the bands to have the two orientations leads to the observation of orientation and wavelength fluctuation in small domains [4] and defects in large ones [1, 4]. We propose a definition for the residency time of the system in one orientation and wavelength, and study its behaviour with Reynolds number. We show that it can be understood as a jump process, following an Arhenius-type law for the residency time. This behaviour is included in the Landau–Langevin model that we introduced.

Finally, we present some hydrodynamical processes of this particular organisation of turbulence. We show that similarly to Poiseuille pipe flow, a Kelvin Helmholtz instability can be seen mainly in the intermediate region between the so called laminar and turbulent areas. We show the onset of the instability and the spanwise advection in DNS visualisations [6]. We extract of the coherent background flow from DNS data, and use it to build a model for local and global stability analysis. The relation between this instability and the bands is discussed [5, 6]

References

[1] Prigent A., Grégoire G., Chaté H., Dauchot O., van Saarloos W. (2002), Large-scale finite-wavelength Modulation within Turbulent Shear Flows, *Phys. Rev. Let., vol. 89, 014501*

[2] Tuckerman L., Barkley D. (2011), Patterns and dynamics in transitional plane Couette flow , *Phys. Fluids, vol. 23, 041301*

[3] Rolland J., Manneville P., (2011), GinzburgLandau description of laminar-turbulent oblique band formation in transitional plane Couette flow, *Eur. Phys. J. B, vol. 80, pp. 529–544*

[4] Rolland J., Manneville P., (2011), Pattern fluctuations in transitional plane Couette flow, *J. Stat. Phys., vol. 142, pp. 577–591*

[5] Shimizu M., Kida S. (2009), A driving mechanism of a turbulent puff in pipe flow, *Fluid. Dyn. Res., vol. 41, 045501*

[6] Rolland J., In preparation

Statistics of turbulent transitional flow structures in a pipe flow at low Reynolds number

J. Krauss, Ö. Ertunç, Ch. Ostwald, H. Lienhart and A. Delgado

Institute of Fluid Mechanics, Friedrich-Alexander-University Erlangen-Nuremberg, Germany

Abstract:

Investigations on transition in pipe flow (PF) were extensively conducted and reported by [8, 9, 3, 5]. Wygnanski *et al.* [8, 9] showed that transition at low-Re triggered by a short-time finite amplitude disturbance starts with distinct flow structures, namely puffs and slugs. Puff structures can be initiated at low Reynolds numbers by inducing short-time, large amplitude localized disturbances in the pipe and at higher Reynolds number, disturbances evolve from puff to slug through multiple splitting. Slug is the more developed state of the puff toward a fully developed turbulent PF. Wygnanski *et al.* [8, 9] and lately Nishi *et al.* [6], Ertunç *et al.* [2], Krauss *et al.* [4], Avila *et al.* [1] showed that the puff starts to split at $Re > Re_{split}$, before it becomes a turbulent slug, either at the same Re or at a higher Re. In the present work, different types single and multiple puffs and slugs are classified and the probability of their occurrence as well as their propagation speed at the end of pipes with different lengths are evaluated.

The various types of structures are automatically identified so that the occurrence probability of those structures can be evaluated from the vast number of realizations observed. Besides the structure identification, the propagation speed of the structures and the life time of the structures are evaluated, respectively. The sample raw pressure and hot-wire signals depict clearly the influence of Reynolds number. The pressure signals for $Re < 1900$ and $L = 566D$ show no puff structure at the end, but the comparison between $Re = 1830$ and $Re = 1890$ suggests that the disturbances start to sustain longer for the higher Re. At a slightly higher Re, about 1900, the puff structures start to appear by the end of 566 D pipe (figure 1). The hot-wire signals show the splitting puff signals and how the number of splitting apparently increases by the increasing Re. With the further increase in Re, the splitting effect pass into the development of multiple puffs, single slugs and multi slugs. The occurrence probability of the structures is evaluated by dividing the number of detected structures at the exit of the pipe with the number of disturbances introduced. Figure 1 shows the hierarchical formation of transitional structures and suggests also for $Re > 2200$, that at a certain Reynolds number, flow can evolve to different types of structures. The probability of puff splitting increases with the increase in pipe length, i.e. travel time of the structure in the pipe.

References

[1] Avila K., Moxey D., de Lozar A., Avila M., Barkley D. and Hof B., (2011): The onset of turbulence in pipe flow, *Science, accepted*

[2] Ertunç Ö., Krauss J., Nishi M., Ostwald C., Lienhart H. and Delgado A., (2010): Statistics of single and splitting puffs in a pipe flow at low Reynolds numbers, *EFMC 8, Bad Reichenhall*

[3] Eckhardt B., Schneider T. M., Hof B. and Westerweel J., (2007): Turbulence Transition in Pipe Flow, *Annu. Rev. Fluid Mech., vol. 39, pp. 447–468*

[4] Krauss J., Ertunç Ö., Ostwald C., Lienhart H. and Delgado A., (2010): Characterization of the structures in transitional pipe flows, *STAB2010, Berlin*

[5] Mullin T., (2011): Experimental Studies of Transition to Turbulence in a Pipe, *Annu. Rev. Fluid Mech., vol. 43*

[6] Nishi M., Ünsal B., Durst F. and Biswas G., (2008): Laminar-to-Turbulent Transition of Pipe Flows through Puffs and Slugs, *J. Fluid Mech., vol. 614, pp. 425–446*

[7] Nishi M., Ertunç Ö. and Delgado A., (2009): Connection between full-lifetime and breakdown of puffs in transitional pipe flows, *Seventh IUTAM Symposium on Laminar-Turbulent Transition, Stockholm, Sweden, Jun. 23-26, Springer, pp. 537–540*

[8] Wygnanski I. J. and Champagne F. H., (1973): On transition in a pipe. Part 1. The origin of puffs and slugs and the flow in a turbulent slug, *J. Fluid Mech., vol. 59, pp. 281–351*

[9] Wygnanski I. J., Sokolov M. and Friedman D., (1975): On transition in a pipe. Part 2. The equilibrium puff, *J. Fluid Mech., vol. 69, pp. 283–304*

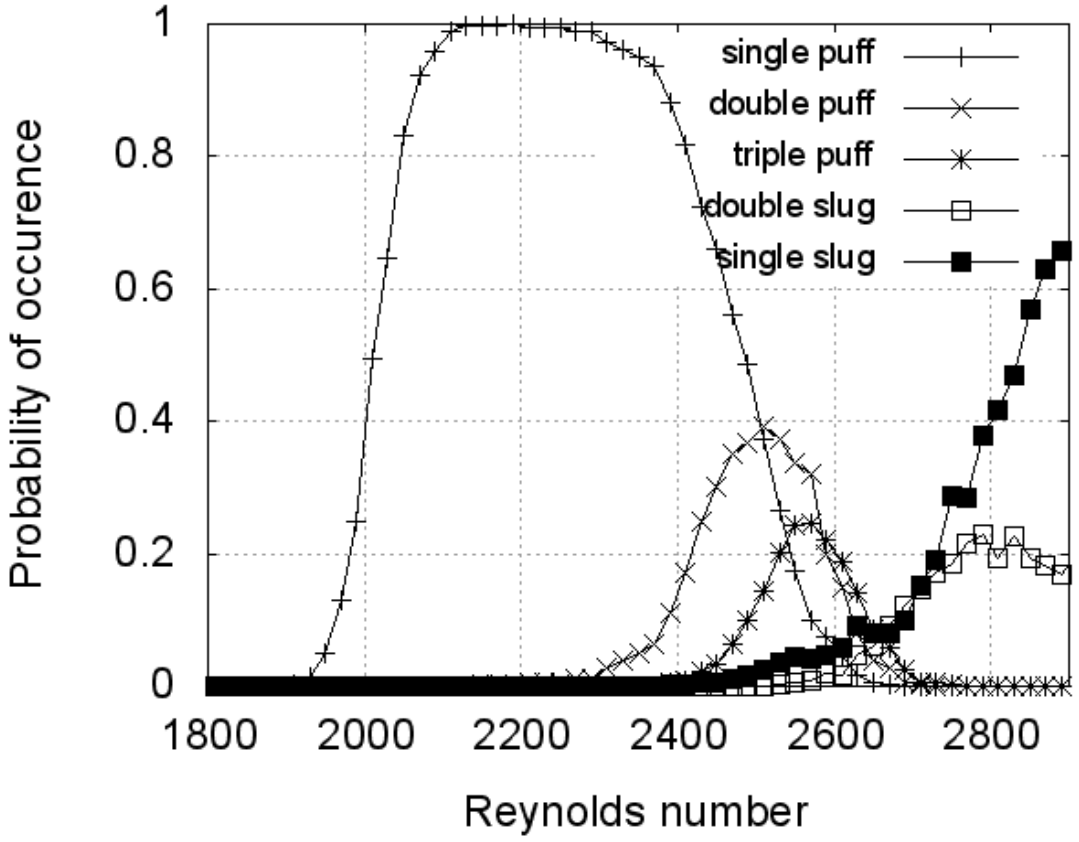

Figure 1: *Probability of occurrence of all types of structures at the exit of* 566 *D pipe*

The Spreading of Turbulence in Pipe Flow

Baofang Song, Marc Avila and Björn Hof[1]

[1] Complex Dynamics and Turbulence group, Max Planck Institute for Dynamics and Self-Organization, Göttingen, Germany

Abstract:
Direct numerical simulation is used to study turbulence in pipe flow in two situations in which the spreading of turbulence is found to be an important issue. First, we aim at eliminating full turbulence by interfering with the energy extraction from the mean shear by streamwise vortices [1, 2, 3]. The mean shear is reduced abruptly by simply flattening the velocity profile. To achieve this, we start with full turbulence in a pipe of 6 diameters length at high Reynolds numbers(Re=10000, 12000 and 15000), then reduce the Reynolds number abruptly to a much lower value(3000). In some cases the initial strong turbulence decays monotonically and the flow relaminarises, but in others it recovers after a sharp decrease in intensity (see Figure 1(a)). The final state depends sensitively on the initial conditions. In those cases where turbulence recovers, localized turbulence patches are found to exist at the valley, as shown in Figure 1(b). Later on, one or more patches spread out and finally contaminate the whole pipe.

Second, in studies of localized turbulent puffs it is argued in Ref. 3 that streamwise vorticity is generated at the trailing edge of the puff due to the inflectional instability of the velocity profile there. Downstream of this edge vorticity moves downstream relative to mean flow [3]. It is speculated that some vortices move far enough and trigger new turbulence pathces which finally grow into a new puff [4]. Here quantative statistics have been obtained to understand this process and to find the criterion which can tell us whether the turbulence patch will spread out or decay. Once obtaining the underlying mechanism, it might be possible to develop control techniques to suppress the spreading of turbulence.

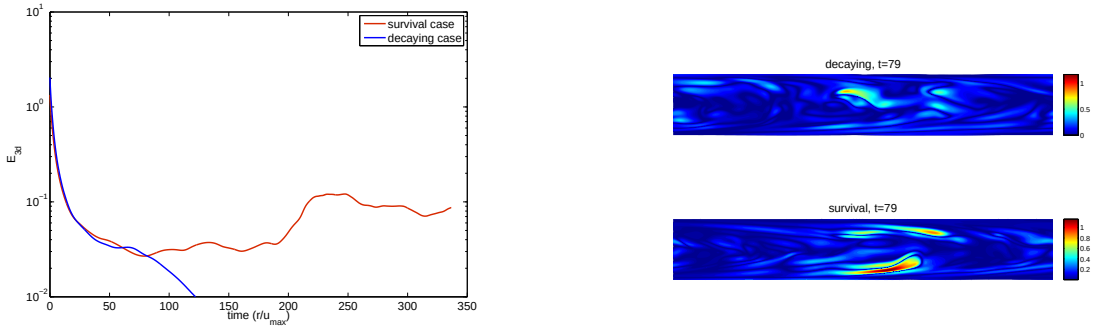

(a) (b)

Figure 1: (a) Time varying E_{3d} for two cases with the Re reduction from 15000 to 3000. (b) Streamwise vorticity on a r-z cross section at the time when the E_{3d} of the survival case reaches the minimum

References

[1] James M. Hamilton, John Kim and Fabian Waleffe, (1995), Regeneration mechanisms of near-wall turbulence structures, *J. Fluid Mech., vol. 287, pp. 317-348*

[2] Javier Jiménez and Alfredo Pinelli, (1999), The autonomous cycle of near-wall turbulence, *J. Fluid Mech., vol. 389, pp. 335-359*

[3] Björn Hof, Alberto de Lozar, Marc Avila, Xiaoyun Tu and Tobias M. Schneider, (2010), Eliminateing Turbulence in Spatially Intermittent Flows, *Science, vol. 327, pp. 1491-1494*

[4] K. Avila, D. Moxey, A. de Lozar, M. Avila, D. Barkley and B. Hof, (2011), The onset of turbulence in pipe flow, *Science, accepted*

Edge States for the Turbulence Transition in the Asymptotic Suction Boundary Layer

Tobias K. Madré [1] and B. Eckhardt [1]

[1] Fachbereich Physik, Philipps-Universität Marburg, Germany

Abstract:
Transition to turbulence in flows where the laminar profile is linearly stable has intrigued physicist for decades. Boundary layers are commonly created in fluid-body interactions and whether a boundary layer is laminar or turbulent heavily influences the flow properties. Prohibiting the transition to turbulence of the boundary layers around the wing of an airplane would for example significantly reduce friction drag and with it fuel consumption. One idea to control turbulence transition in boundary layers is through suction. The simplest case is the asymptotic suction boundary layer (ASBL).

In the ASBL, as in many other shear flows, (transient) turbulent motion is observed despite the linear stability of the laminar profile. The boundary in state space between the basin of attraction of the laminar state and the turbulent region is called "edge of chaos"[1]; an "edge state" is an attracting set inside the edge of chaos. A special numerical technique allows us to approximate trajectories on the edge of chaos to arbitrary accuracy and hence calculate edge states. Lying on the laminar-turbulent boundary, edge states play an important role for understanding the transition to turbulence.

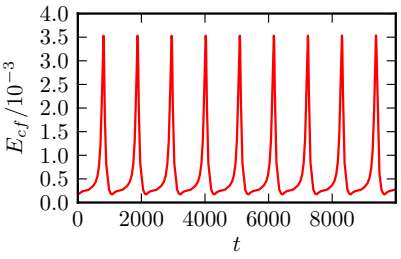

Figure 1: *Periodic bursts in the cross-flow energy of the edge state.*

We calculated the edge state in the asymptotic suction boundary layer; it consists of two alternating streaks and two streamwise-elongated vortices. The structures oscillate and show the characteristics of a traveling wave on short timescales. The time evolution of the cross-flow energy, figure 1, shows periodic bursts and reveals the existence of a second, much longer timescale. At each burst the state is shifted by half a box width in the spanwise direction; the edge state is hence a periodic orbit whose period is twice the bursting period. The edge states structure proved very robust to variations of Reynolds number or box size. We show snapshots of the edge state at Reynolds 400 in figure 2.

We are able to identify the bursting process with a self-sustained regeneration cycle proposed by Hamilton, Kim and Waleffe[2]. Streamwise vortices create streaks by linear advection of the laminar base flow. The streaks are linearly unstable to developing a waviness and finally break-up, the event corresponding to the peak in the turbulent energy. Finally, nonlinear interactions lead to a recreation of the streamwise vortices and the cycle is closed.

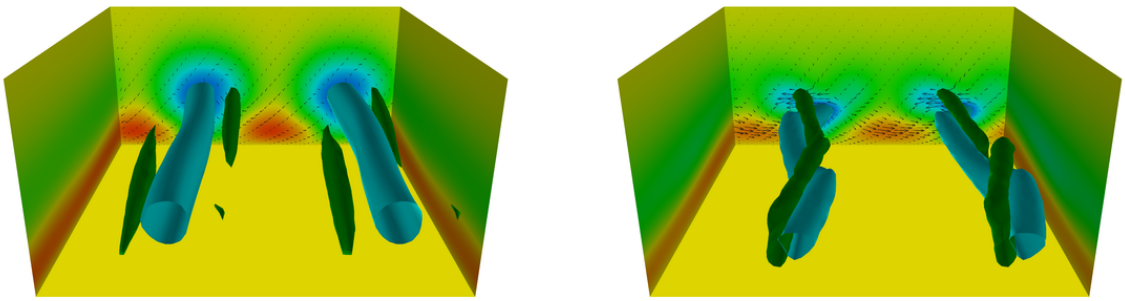

Figure 2: *Vortex-streak-interactions for the edge state. Blue: isocontour of fluctuating downstream velocity component $u = -0.33$, green: isocontour of the λ_2 vortex-detection-criterion. Color-coded on the sides of the box: u. Left picture: t=0, just after a burst; right picture: t=700, just before a burst.*

References

[1] Skufca J. D., Yorke J.A. and Eckhardt B., (2006), Edge of chaos in a parallel shear flow, *Phys. Rev. Lett., vol 96, p. 174101.*

[2] Hamilton J. M., Kim J. and Waleffe F., (1995), Regeneration mechanisms of near-wall turbulence structures, *Journal of Fluid Mechanics, vol. 287, pp. 317-348.*

Session VIII
Biofluid dynamics
Thursday, 11th August, 10:20 – 11:20

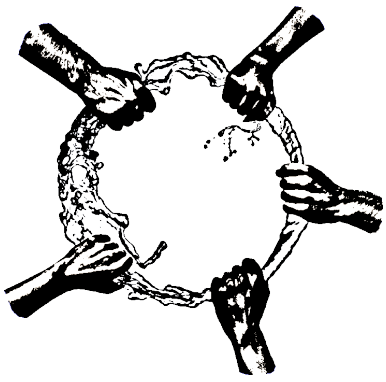

The Hydrodynamics of Swimming Microorganisms

Douglas Brumley [1]

[1] Department of Applied Mathematics and Theoretical Physics, University of Cambridge, UK.

Abstract:

We begin by outlining the results of some recent experiments involving the spherical colonial alga *Volvox carteri*. A *Volvox* colony typically consists of 1-5 $\times 10^4$ biflagellated cells. The cells embedded on the surface of the colony beat their flagella in a coordinated fashion, producing a net fluid motion. Using high-speed imaging and particle image velocimetry (PIV) we have been able to accurately analyse the time-dependent flow fields around such colonies and characterise the metachronal wave propagating on its surface. The speed and wavelength of this metachronal wave can be accurately determined using a two-dimensional Fourier analysis. The time-averaged flow field can be readily calculated, and the results are presented in Figs. 1(b) - 1(d).

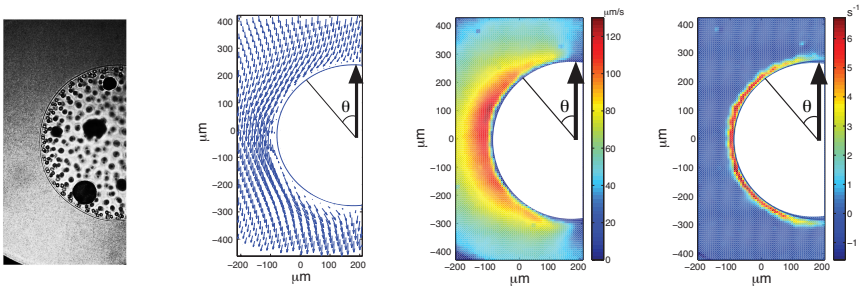

(a) (b) (c) (d)

Figure 1: Figure showing (a) a photograph of a *Volvox* colony which is held by a glass micropipette. Also shown are the time-averaged (b) velocity field, (c) velocity magnitude and (d) vorticity. PIV analysis is conducted using frames n and $n + 10$, corresponding to a time interval of 1/100 sec. The subsequent results are averaged over 1300 frames.

We adopt the squirmer model of Blake [1] to describe the boundary condition at the surface of the colony:

$$u_r\big|_{r=a} = \sum_n A_n(t) P_n(\cos\theta), \qquad u_\theta\big|_{r=a} = \sin\theta \sum_n B_n(t) W_n(\cos\theta), \tag{1}$$

where P_n is the n^{th} Legendre polynomial and W_n is defined as $W_n(\cos\theta) = \frac{2}{n(n+1)} P_n'(\cos\theta)$. We consider a time-independent squirmer with zero radial velocity on the sphere surface ($A_n(t) = 0$ and $B_n(t) = B_n \; \forall \; n$). In these circumstances, the model boundary conditions presented in Eq. (1) are in good agreement with the time-averaged flow found experimentally, facilitating the use of this squirmer model. Using this, we calculate the forces and torques acting on two interacting squirmers in the lubrication limit. This interaction becomes significant when the spacing between organisms is sufficiently small. We follow elements of the work by Ishikawa *et al.* [2], finding small corrections to some of the terms. We also perform the lubrication analysis to higher order, allowing us to calculate the first non-vanishing contributions to the normal force. Importantly, the lubrication theory permits the analysis of suspensions with a high volume fraction of organisms, through pairwise addition of interactions.

We use this theory to investigate the stability of a monolayer of close-packed spherical squirmers, from both analytical and numerical standpoints. In particular, we assess the stability of the system subject to small translational and rotational perturbations. The two parameters which we vary are $\beta = B_2/B_1$, which essentially measures the stresslet strength, and G_{bh}, which quantifies the extent of bottom-heaviness. Without the inclusion of an inter-particle repulsive force, we find that the monolayer is always unstable to small perturbations. The presence of this repulsive force can establish translational stability, though in addition, a sufficiently large value of G_{bh} is required to ensure the squirmers are stable to orientational perturbations. This is in very good agreement with simulations conducted by Ishikawa *et al.* in which a full boundary element method is employed to describe the dynamics of a suspension of squirmers.

References

[1] J. R. Blake, (1971), A spherical envelope approach to ciliary propulsion, *Journal of Fluid Mechanics, vol. 46, pp. 199-208.*

[2] T. Ishikawa, M. P. Simmonds, and T. J. Pedley, (2006), Hydrodynamic interaction of two swimming model micro-organisms, *Journal of Fluid Mechanics, vol. 568, pp. 119-160.*

Dynamics of the vitreous humour and stress on the retina generated during eye rotations

J. Meskauskas [1], R. Repetto [2] and J.H. Siggers [3]

[1] Department of Engineering of Structures, Water and Soil, University of L'Aquila, L'Aquila, Italy
[2] Department of Civil, Environmental and Architectural Engineering, University of Genoa, Genoa, Italy
[3] Department of Bioengineering, Imperial College London, London, UK

Abstract:
The vitreous humour is a transparent viscoelastic fluid that occupies the approximately spherical vitreous chamber. Its properties have been studied by several authors [1, 2, 3]. During eye rotations, flow in the vitreous produces stresses on the retina that may play a role in the development of vitreoretinal diseases such as retinal detachment.

We study the relaxation behaviour of a viscoelastic fluid in a rigid sphere. Assuming that the displacements and velocities of the fluid particles are small, we can neglect nonlinear terms in the equations of motion. By expanding the velocity and pressure as a superposition of spherical harmonic functions and seeking a non-trivial solution we find the eigenvalues and eigenfunctions of the system. We consider different rheological models of the vitreous, and invariably find the existence of complex eigenvalues, whose imaginary parts represent natural frequencies of oscillation of the system, and whose real parts are all negative, indicating that the motion decays over time. For all rheological models considered we find that the natural frequency associated with the least damped modes approximately ranges between 10 and 30 rad/s, which is in the physiological range.

Next, we consider the fluid motion driven by small-amplitude azimuthal torsional oscillations of the domain, which represent saccades of the eyeball. We compute the time-averaged total kinetic energy of the system and show that it assumes large values when the system is forced at resonant frequencies (see figure 1), at which the velocity away from the boundary becomes larger than at the boundary.

In further work we study the effect of a weak departure of the shape of the domain from a sphere, analysing two shapes that are of clinical interest. Firstly, we focus on *myopic* eyes, which in general are not only larger than emmetropic eyes, but also elongated in the antero-posterior direction. This induces a significant increase of the shear stress on the retina in the posterior segment of the eye (see figure 2), which might provide a mechanical explanation for the more requent occurrence of posterior vitreous detachment and retinal detachment in these patients. Secondly, we consider eyes subjected to *scleral buckling*, a surgical procedure whose aim is to induce a deformation in the shape of the sclera in order to facilitate sealing a retinal break. Also in this case the geometry of the domain influences the stress distribution on the retina (see figure 3), which might be significant for the modelling of the reattachment process.

References

[1] Lee B., Litt M., Buchsbaum G.: Rheology of the vitreous body. Part I: Viscoelasticity of human vitreous. *Biorheology* **29**:521-533, 1992.

[2] Nickerson C. S., Park J., Kornfield J. A., Karageozian H.: Rheological properties of the vitreous and the role of hyaluronic acid. *Journal of Biomechanics* **41** (9):1840-6, 2008.

[3] Swindle K., Hamilton P., Ravi N.: In situ formation of hydrogels as vitreous substitutes: Viscoelastic comparison to porcine vitreous. *Journal of Biomedical Materials Research - Part A* **87A** (3):656-665, 2008.

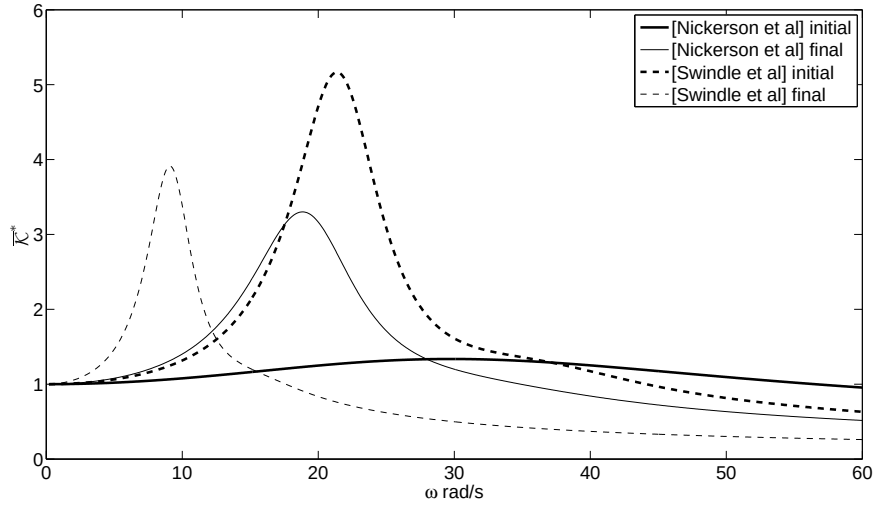

Figure 1: Plots of the normalised kinetic energy $\overline{\mathcal{K}}^*$ against frequency. The energy is scaled with the kinetic energy of a rigid body with the same density as the fluid and rotating with the same angular velocity as the fuid domain.

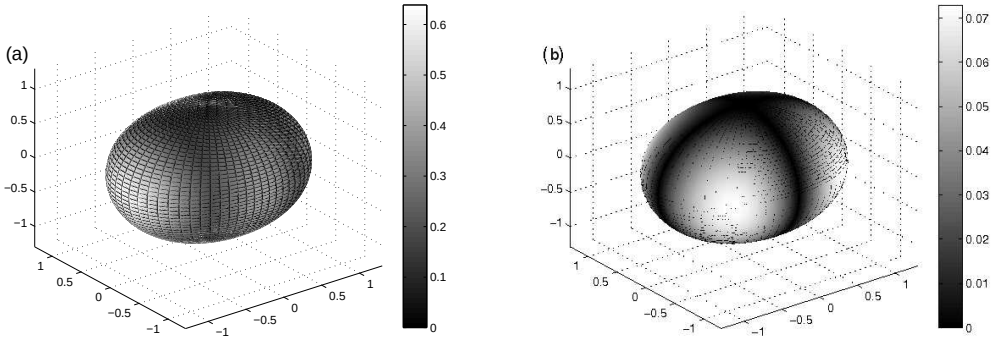

Figure 2: Spatial distribution of the (a) maximum tangential stress, and (b) maximum normal stress over time for the myopic shape, using the rheological values reported in [2].

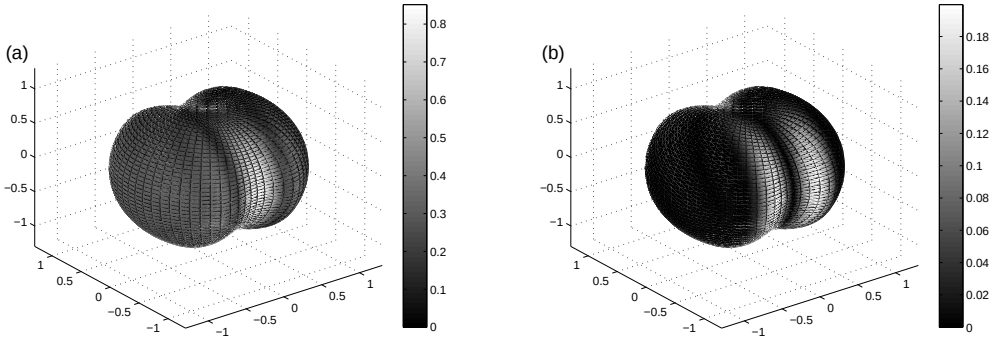

Figure 3: Spatial distribution of the (a) maximum tangential stress, and (b) maximum normal stress over time in the case of scleral buckling, using the rheological values reported in [2].

An analytical model of a side-to-side anastomosis

Adriana Setchi [1], J. Mestel [2] and K. Parker [1] and J. Siggers [1]

[1] Department of Bioengineering, Imperial College London, London, UK
[2] Department of Mathematics, Imperial College London, London, UK

Abstract:
The human circulatory system is fascinating due to its complexity. There exist many cases where mathematical modelling of the flow has given insight into this complexity. In particular, this work aims to construct matched Papkovich-Fadle-eigenfunction expansions for the solution of flow through a shunt in the body. Such a solution can be applied to model side-to-side anastomoses (surgical connections between blood vessels or segments of gut), or fistulas between arteries and veins (e.g. during hemodialysis).
Papkovich-Fadle functions were first used in elastic theory [1]. Many problems have been solved in this manner since then including slow flow over slots [2], cavities [3] or through constrictions [4]. These can be applied to model biological problems such as aneurysms, atherosclerosis or vasoconstrictions.

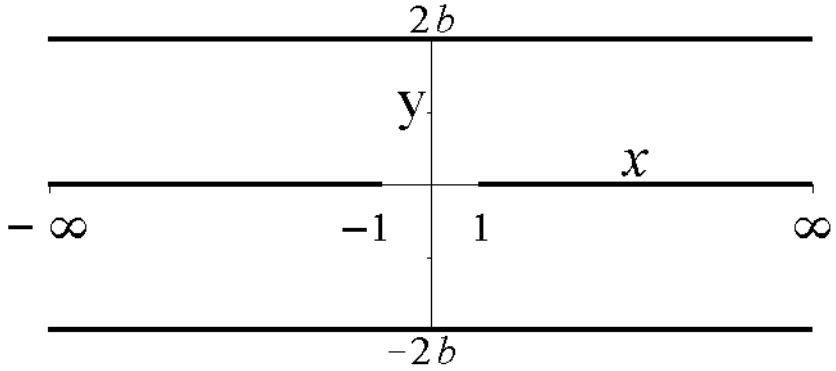

Figure 1: *Geometry of two channels with a shunt between them*

This work considers a low-Reynolds-number flow of a non-Newtonian and incompressible fluid in a two-dimensional geometry of two similar infinite channels with a shunt between them as shown in Figure 1. These assumptions make it possible to simplify the Navier-Stokes equations to the system

$$-\nabla p + \mu \nabla^2 \underline{u} = 0 \qquad \text{and} \qquad \nabla . \underline{u} = 0 \ . \tag{1}$$

By defining a streamfunction $\Psi(x, y)$ such that $u = \frac{\partial \Psi}{\partial y}$ and $v = -\frac{\partial \Psi}{\partial x}$ these simplify further to a single biharmonic equation

$$\nabla^4 \Psi = 0 \ . \tag{2}$$

No-slip boundary conditions $\left\{ \frac{\partial \Psi}{\partial n} = 0, \Psi = \text{const} \right\}$ are imposed on all solid boundaries. In addition, Poiseuille flow is prescribed at $x = \pm\infty$. Note that the equation is linear and steady. It is possible to construct time-dependent solutions by adding steady solutions instantaneously. This can be done using time-dependent boundary conditions at infinity such as clinical pressure or flux measurements.
The biharmonic equation $\nabla^4 \Psi = 0$ is not uniquely solved using separation of variables. Progress can be made by dividing the geometry into subregions. For each of these the boundary conditions determine the Papkovich-Fadle eigenfunction expansions. Three linearly independent steady solutions will be presented at the conference.

References

[1] Smith R.C.T., (1952), The bending of a semi-infinite strip, *Aust. J. Sci. Res., vol. 5, pp. 227-237*

[2] Trogdon S.A. and Joseph D.D., (1982), Matched eigenfunction expansions for slow flow over a slot, *J. Non-Newtonian Fluid Mech., vol. 10, pp. 185-213*

[3] Driesen C.H., Kuerten J.G.M. and Streng M., (1998), Low-Reynolds-number flow over partially covered cavities, *J. Eng. Math., vol. 34, pp. 3-20*

[4] Phillips, T., (1989), Singular matched eigenfunction expansions for stokes flow around a corner, *J. Appl. Math., vol. 43, pp. 13-26*

Experimental study of the asymmetric heart valve prototype

M. Vukicevic[1], S. Fortini[2], G. Querzoli[3], A. Cenedese G.[2] and G. Pedrizzetti[1]

[1] Dipartimento Ingegneria Civile e Architettura, University of Trieste, Italy
[2] Dipartimento Ingegneria Civile, Edile e Ambientale - University 'La Sapienza', Rome, Italy
[3] Dipartimento Ingegneria del Territorio - University of Cagliari, Italy

Abstract:
Recent clinical studies of the left ventricular flow have revealed that the blood motion is significantly modified after the implant of mechanical mitral prosthesis [1, 2]. Indeed, natural mitral valve is characterized by asymmetric leaflets while, on the opposite, common mechanical prostheses are symmetric. An original (home-made) asymmetric mechanical valve made with two unequal leaflets is presented here (see Figure 1). The experimental examination has been performed in the apparatus already used for the previous investigations [3, 4]. The corresponding flow field is analysed experimentally by Feature tracking, the image analysis technique described in [3], and compared with that of symmetric valves. The results show that the symmetry-breaking gives rise to a fluid dynamics behaviour closer to that of natural valves. The concept of asymmetry thus has a potential usefulness to improve the flow field after implanting a mechanical prosthesis. The study has limitations due to the lower manufacture quality of the prototype with respect to industrial valves that may cause uncontrollable differences in the comparison. Therefore, many further elements must be carefully verified for a thorough comparison with existing symmetric valves. Nevertheless, these findings suggest that breaking of the symmetric may help in development of devices with behaviour closer to that of asymmetric natural valves [5].

Figure 1: *Asymmetrical valve prototype*

References

[1] Faludi, R., Szulik, M., D'hooge, J., Herijgers, P., Rademakers, F., Pedrizzetti, G. and Voigt. J.-U., (2010) Left ventricular flow patterns in healthy subjects and patients with prosthetic mitral valves: An in vivo study using echocardiographic particle image velocimetry. *J. Thorac. Cardiovasc. Surg.,* 139, 1501-1510.

[2] Pedrizzetti, G., Domenichini, F. and Tonti, G., (2010), On the left ventricular vortex reversal after mitral valve replacement. *Ann. Biomed. Eng.*, 38, 769-773.

[3] Cenedese, A., Del Prete, Z., Miozzi, M. and Querzoli, G., (2005), A laboratory investigation of the flow in the left ventricle of a human heart with prosthetic, tilting-disk valves. *Experiments in Fluids*, 39, 322–335.

[4] Querzoli, G., Fortini, S. and Cenedese, A., (2010), Effect of the prosthetic mitral valve on vortex dynamics and turbulence of the left ventricular flow. Phys. Fluids, 22, 041901.

[5] Hong, G.R., Pedrizzetti, G., Tonti, G., Li, P., Wei, Z., Kyung Kim, J., Baweja, A., Liu, S., Chung, N., Houle, H., Narula, J. and Vannan, M.A. (2008) Characterization and Quantification of Vortex Flow in the Human Left Ventricle by Contrast Echocardiography Using Vector Particle Image Velocimetry. *JACC Cardiov Imaging*, 1, 705-717.

Session IX
Numerical methods for hydrodynamic stability
Thursday, 11th August, 11:30 – 12:30

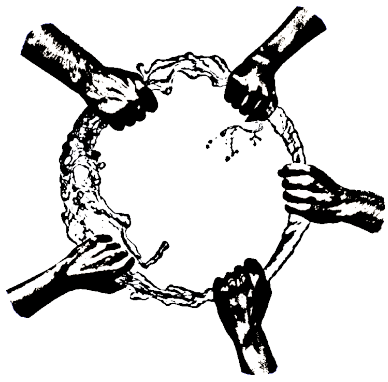

Low order time-stepping methods for global instability analysis

F. Gómez[1], R. Gómez[1] and V. Theofilis[2]

[1] INTA Instituto Nacional de Técnica Aeroespacial, Madrid, Spain
[2] School of Aeronautics, Universidad Politécnica de Madrid, Madrid, Spain

Abstract:
Investigation of instability mechanisms is essential for the understanding of the transition process from laminar to turbulent flow. Linear instability theory provides insight in these instability mechanisms in a large number of fluid dynamics problems. This linear stability theory is concerned with the evolution of a small amplitude disturbances superimposed upon a basic state or "base flow". Any flow quantity is then decomposed in general into a three-dimensional steady base flow and superposed three-dimensional amplitude functions of the unsteady small perturbations. According to the TriGlobal Ansatz [1]

$$\mathbf{q}(x,y,z,t) = \bar{\mathbf{q}}(x,y,z) + \epsilon\hat{\mathbf{q}}(x,y,z)\mathrm{e}^{\sigma t} + c.c. \tag{1}$$

where $\epsilon \ll 1$, $\sigma = \sigma_r + \sigma_i$, with σ_r representing the amplification/damping rate and σ_i the frequency of the disturbance sought, while barred and hatted quantities denote basic and disturbance flow quantities, respectively.

In principle, the assumptions underlying this TriGlobal [1] linear instability lead to a problem easier to solve numerically than the direct numerical simulation (DNS), but the large size of the discretized matrices makes the numerical solution challenging due to prohibitely expensive computing requirements. Time-stepping approaches can provide one solution for this class of problems using a Jacobian-free methodology [2], in which the matrix never need to be formed. This enables the study of global linear stability problems on small-main-memory machines at the expense of long time integrations. Though efficient, a potential pitfall of the time-stepping approach is that results are sensitive to the quality of spatial integration of the equations. The objective of this paper is to provide insight to this issue by employing different time-stepping schemes, based on commonly available spatial integration techniques, such as (high-order) spectral collocation and (second order) FV techniques. At present, the time-stepping approach of Chiba [3] has been implemented in conjunction with two direct numerical simulation algorithms, one based on the typically-used in this context high-order method, serving as reference, and another based on low-order methods representative of those in common use in industry.

As standard validation case, a regularized lid-driven cavity has been studied using a spectral DNS algorithm and a low order FVM solver. Since the eigenvalue spectrum is known in this problem, a parameter sweep has been carried out in order to identify the optimum parameters for its recovery. In agreement to Goldhirsch et. al. [4], it has been found that one of the required conditions in order to obtain a correct i-th eigenvalue is:

$$|Re(\lambda_i - \lambda_m)|\,\tau \gg 1 \tag{2}$$

where τ is the time integration length and λ_m is the the m-th eigenvalue, being m the dimension of the Krylov subspace. Figure (1) shows a comparison between the least stable mode obtained both with the BiGlobal (BG) [5] and the present time-stepping (TS-SM, TS-FVM) methodologies with two different DNS. The validation of this case have been useful to demonstrate the strong influence of the parameters involved in the time-stepping approach, such as time-integration length, initial-perturbation size and mesh resolution. Work is underway and more full comparisons will be presented at the time of the Conference.

References

[1] Theofilis, V.,(2011), Global linear instability, *Annual Review of Fluid Mechanics, vol. 43, pp. 319-352*

[2] Knoll, D. and Keyes, D.,(2004), Jacobian-free Newton Krylov methods: a survey of approaches and applications, *Journal of Computational Physics, vol. 193, pp. 357-397*

[3] Chiba, S.,(1998), Global stability analysis of incompressible viscous flow, *J. Jpn. Soc. Comput. Fluid Dyn. vol. 7, pp. 20-48*

[4] I. Goldhirsch, Steven A. Orszag, B.K. Maulik,(1987), An Efficient Method for Computing Leading Eigenvalues and Eigenvectors of Large Asymmetric Matrices, *Journal of Scientific Computing, vol. 2, pp. 33-58*

[5] Theofilis, V., Duck, P. W., and Owen, J.,(2004), Viscous linear stability analysis of rectangular duct and cavity ows, *Journal of Fluid Mechanics, vol. 505, pp. 249-286*

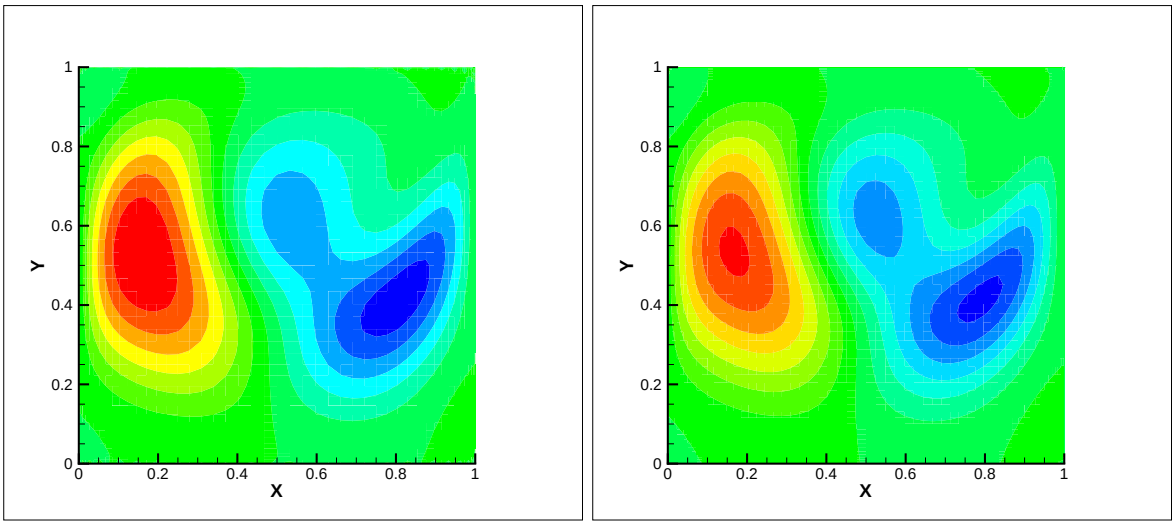

(a) v First Eigenvalue BG

(b) v First Eigenvalue TS-SM

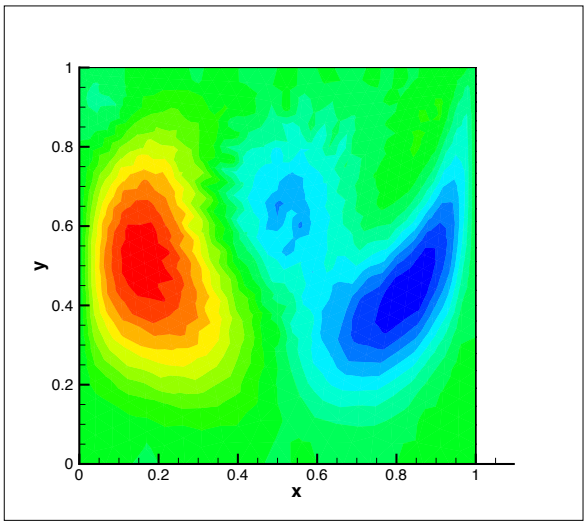

(c) v First Eigenvalue TS-FVM

Figure 1: Preliminary results and validation with BiGlobal Methodology

Theoretical aspects of High-Order Finite Difference Methods for Global Flow Instability

Soledad Le Clainche Martínez [1], M. Hermanns[1] and V. Theofilis [1]

[1] School of Aerospace Engineering, Universidad Politécnica de Madrid/School of Aeronautics, Madrid, Spain

Abstract:
The main goal of this work is to apply a new stable high order (order q) finite-difference method (FD-q), based on non-uniform grid points [3], to instability analysis of complex flows. Motivation is offered by the high cost of spectral methods typically used for this class of problems [4], which can be substantially reduced by exploiting the sparsity offered by the FD-q scheme, without sacrificing accuracy.

The properties of this methods are as good as spectral collocation methods properties. Figure 1 shows Runge phenomenon oscillations in a uniform, CGL and FD-q discretization respectively. The huge oscillations produced on the boundaries with a uniform discretization disappear using a CGL discretization. In this case, such oscillations have equal amplitudes. Using a FD-q discretization the Runge phenomenon oscillations are constant an even smaller that the ones produced with CGL. Therefore, polynomial interpolation error is smaller when using FD-q instead of CGL.

The new method has been validated on the classic Orr-Sommerfeld equation, comparing its results at different orders against spectral collocation method based on the Chebyshev Gauss-Lobbatto (CGL) points, and results obtained by alternative FD numerical methods, such as Dispersion-Relation-Preserving finite difference (DRP) [1], Compact finite difference (also known as Padé schemes) [2] and Summation by parts operators [5]. Figure 2 shows the relative error of the different techniques in recovering the Plane Poiseuille Flow (PPF) eigenspectrum; it may be seen that at all orders of discretization the FD-q method presents better resolution properties, reaching convergence before any alternative FD method.

This message is reinforced by results of pseudospectrum of PPF, where the quality of the CGL discretization is recovered using a FD-q method order 16. See figure 3.

These favorable resolution properties of the FD-q method are subsequently applied to recover the BiGlobal eigenspectrum of square regularized lid-driven cavity at $Re = 1000, \beta = 15$. Table 1 shows convergence study results of three FD-q and a CGL discretization, which establish the FD-q spatial discretization as a viable alternative to the latter method.

Results of application to other complex flows will be available at the time of the Conference.

Table 1: *BiGlobal instability analysis of the regularized lid-driven cavity flow at $A = 1$, $Re = 1000$ and $\beta = 15$. Convergence of the most unstable mode for different spatial schemes.*

N	FD-8	FD-16	FD-24	CGL
32	0.1167494	0.1085822	0.1088816	0.1083455
40	0.1121854	0.1081735	0.1082842	0.1083697
48	0.1095856	0.1085076	0.1083438	0.1083468
56	0.1086749	0.1084422	0.1083214	0.1083409
64	0.1084124	0.1083639	0.1083276	0.1083386
72	0.1083568	0.1083268	0.1083310	0.1083383

References

[1] Tam C. and Webb J., (1992), Dispersion-Relation-Preserving Finite Diference Schemes for Computational Acoustics, *J. Comput. Phys., vol. 107, pp. 262-281*

[2] Lele S. K., (1992), Compact Finite Difference Schemes with Spectral-like Resolution, *J. Comput. Phys., vol. 103, pp. 16-42*

[3] Hermanns M. and Hernández J. A., (2008), Stable high-order finite-difference methods based on non-uniform grid points distributions, *Int. J. for Num. Meth. in Fluids, vol. 56, pp. 233-255*

[4] Theofilis V., (2011), Global linear instability, *Ann. Rev. Fluid Mech., vol. 43, pp. 319-352*

[5] Bo Strand, (1992), Summation by Parts for Finite Difference Approximations for d/dx, *J. Comput. Phys., vol. 110, pp. 47-67*

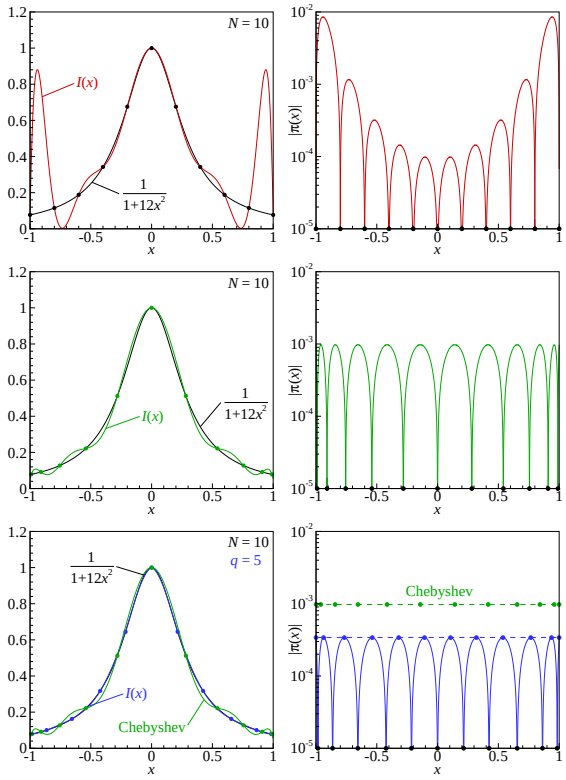

Figure 1: *From up to down: Runge phenomenon using a uniform, CGL and FD-q discretization*

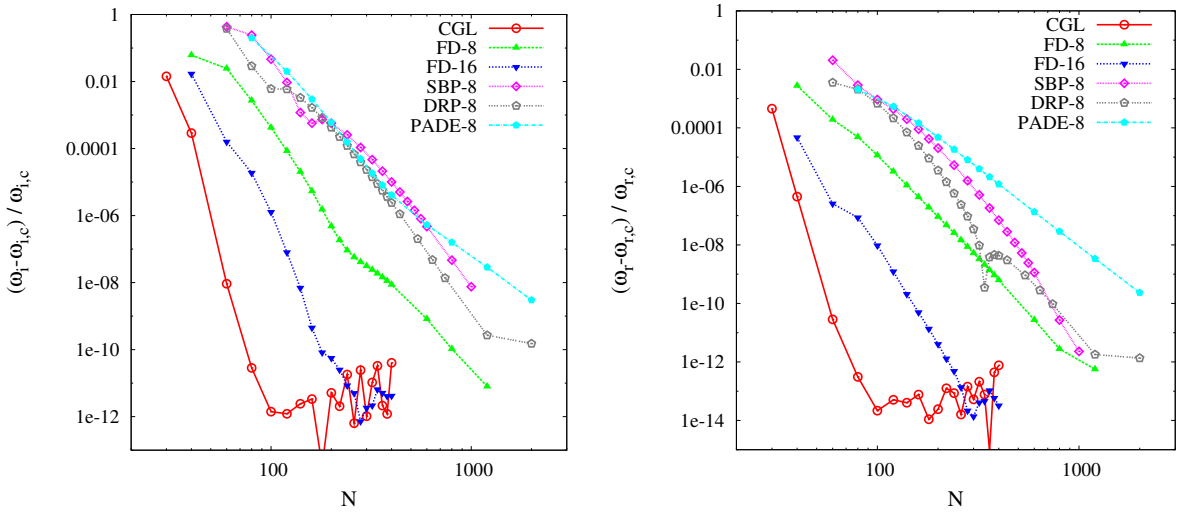

Figure 2: *Relative error comparison for different numerical methods in a Plane Poiseuille flow*

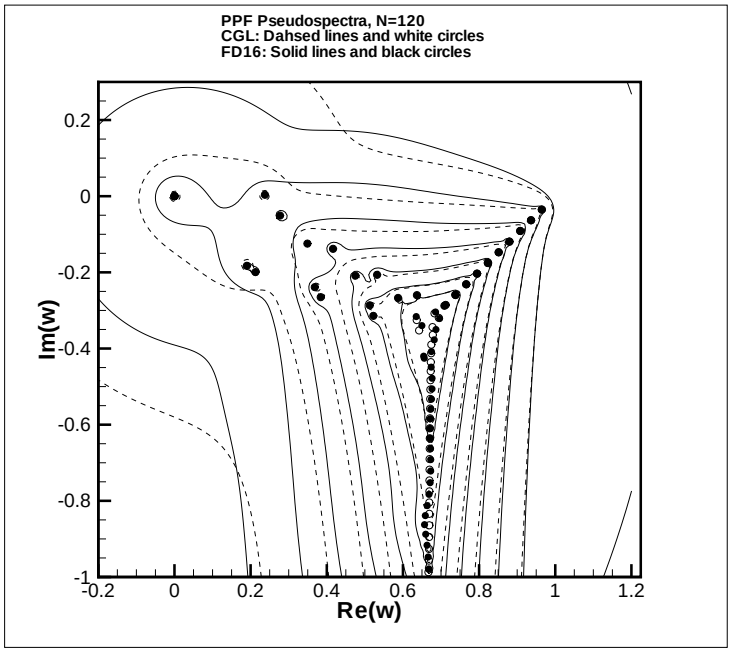

Figure 3: *Spectrum and Pseudospectrum in a Plane Poiseuille flow using CGL (dashed lines and white circles) and FD-16 (solid lines and black circles)*

Three-dimensional parabolized stability equations applied to the nonparallel Batchelor vortex

P. Paredes [1], V. Theofilis [1] and D. Rodriguez [2]

[1] School of Aeronautics, Universidad Politécnica de Madrid, Madrid, Spain
[2] Engineering and Applied Sciences, California Institute of Technology, Passadena, USA

Abstract:
The present contribution discusses the development of a PSE-3D instability analysis algorithm, in which a matrix forming and storing approach is followed. Up to the present time, the building blocks of the algorithm have been implemented and extensively validated and some very promising results have been obtained. Alternative high-order numerical schemes for spatial discretization [1] are used instead of spectral schemes. Attention is paid to the issue of efficiency, which is critical for the success of the overall algorithm. To this end, use is made of a parallelizable sparse matrix linear algebra package which, as expected, is shown to perform substantially more efficiently in combination with finite-difference discretizations. Validation work has focused on each of the building blocks of the algorithm, including temporal and spatial BiGlobal EVP solutions (the latter necessary for the initialization of the PSE-3D) and classic PSE analysis (originally developed by [2]) in cylindrical coordinates on the nonparallel Batchelor vortex for comparisons between PSE and PSE-3D; excellent agreement is shown. The complete algorithm will be discussed at the time of the Conference.

Linearized stability analysis is based upon the decomposition of all flow variables into a steady mean component upon which small-amplitud three-dimensional disturbances are permitted to develop (i.e. $\bar{\mathbf{q}} = \mathbf{Q} + \mathbf{q}$, with $\mathbf{q} \ll \mathbf{Q}$). By allowing a mild dependence of the base flow on the streamwise spatial coordinate z, an eigenmode Ansatz is introduced, according to which

$$\mathbf{q}(x,y,z,t) = \hat{\mathbf{q}}(x,y,z) exp[i\theta(z,t)], \quad \theta(z,t) = \int_z \beta(z')dz' - \omega t \tag{1}$$

Applied to the linearized Navier-Stokes equaitons this leads to the following system of equations that define the three dimensional Parabolized Stability Equations (PSE-3D).

$$\{\mathcal{L}_0 + U_x\}\hat{u} + U_y\hat{v} + \hat{p}_x + U_z\hat{w} + \left\{\left(W - \frac{2i\beta}{Re}\right)\hat{u}_z\right\} = 0 \tag{2}$$

$$\{\mathcal{L}_0 + V_y\}\hat{v} + V_x\hat{u} + \hat{p}_y + V_z\hat{w} + \left\{\left(W - \frac{2i\beta}{Re}\right)\hat{v}_z\right\} = 0 \tag{3}$$

$$\{\mathcal{L}_0 + W_z\}\hat{w} + W_x\hat{u} + W_y\hat{v} + i\beta\hat{p} + \left\{\left(W - \frac{2i\beta}{Re}\right)\hat{w}_z + \hat{p}_z\right\} = 0 \tag{4}$$

$$\hat{u}_x + \hat{v}_y + i\beta\hat{w} + \hat{w}_z = 0 \tag{5}$$

where $\mathcal{L}_0 = i\beta W + U\mathcal{D}_x + V\mathcal{D}_y - \frac{1}{Re}(\mathcal{D}_{xx} + \mathcal{D}_{yy} - \beta^2) - i\omega$. Implicit in this derivation is that the disturbance takes the form of a rapidly varying phase function and a slowly varying shape function (i.e. $\partial_z = \mathcal{O}(Re^{-1})$), for which terms $\mathcal{O}(Re^{-2})$ are neglected.

The studied flow is the realistic Batchelor vortex [3] that is symplified to

$$U_r = 0, \quad U_\theta = \frac{\kappa}{r}\left(1 - exp\left(\frac{-r^2}{\delta(z)^2}\right)\right), \quad U_z = \alpha(z) exp\left(\frac{-r^2}{\delta(z)^2}\right) \tag{6}$$

where

$$\kappa = constant, \quad \alpha(z) = -\kappa^2 \frac{Re_0\, log(z/Re_0)}{8z}, \quad \delta(z) = 2\sqrt{z/Re_0}. \tag{7}$$

Figure 1 shows the comparison between conventional PSE analysis in cylindrical coordinates and PSE-3D analysis results for the nonparallel Batchelor vortex at $Re = 1200$, $\alpha = 0.9$, $\delta = 1.0$ and $\omega = -2.0$. For the same case, Figure 2 show three-dimensional perturbation obtained by spatial BiGlobal analysis and PSE-3D analysis.

References

[1] Hermanns, M., Hernández, J.A. (2008), Stable high-order finite-difference methods based on non-uniform grid point distributions, *International Journal for Numerical Methods in Fluids, vol. 56, pp. 233-255*

[2] Herbert, T. (1994), Parabolized stability equaitons, *Annual Review of Fluid Mechanics, vol. 29, pp. 245-283*

[3] Batchelor, G. (1964), Axial flow in trailing line vortices, *Journal of Fluid Mechanics, vol. 4, pp. 645-658*

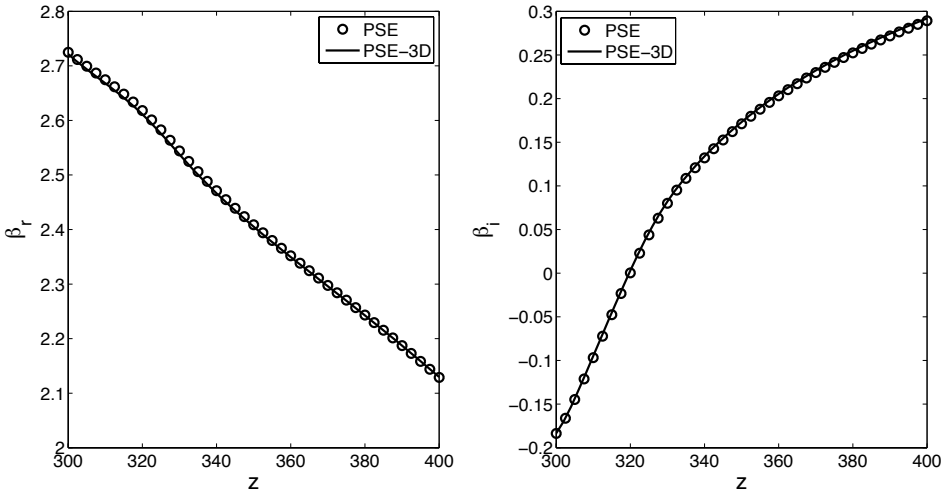

Figure 1: Comparison between PSE in cylindrical coordinates and PSE-3D evolution of the streamwise wavenumber β of the realistic Batchelor vortex flow at $Re = 1200$, $\alpha = 0.9$, $\delta = 1.0$ and $\omega = -2.0$ for the most unstable mode

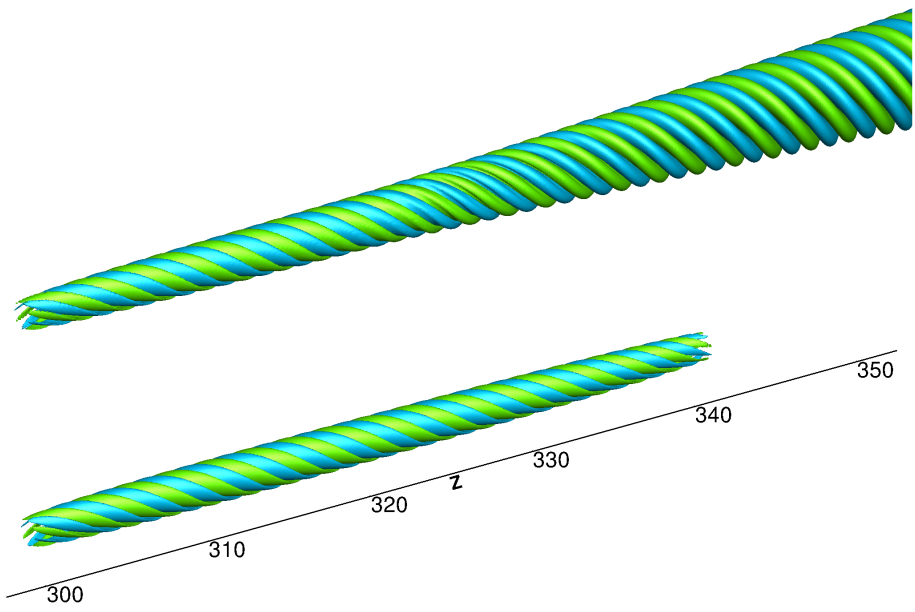

Figure 2: Iso-surfaces of the streamwise velocity three dimensional amplitude function of the realistic Batchelor vortex flow at $Re = 1200$, $\alpha = 0.9$, $\delta = 1.0$ and $\omega = -2.0$ for the most unstable mode with (top) spatial BiGlobal analysis and (bottom) PSE-3D analysis. Blue represents $u_z = -1$ and green $u_z = 1$.

Computer Extended Series Solution for Dean Flow

F. Tettamanti, A.J. Mestel [1]

[1] Department of Mathematics, Imperial College London, London, SW7 2AZ, UK

Abstract:

Dean was the first to formally study fully developed flows through toroidal pipes of finite curvature [3]. Whilst different authors have used various methods to model these flows, their nature has yet to be fully appreciated [1]. In particular, the asymptotic behaviour of the flow at large Dean number (K) and the bifurcation structure of the solution family remains largely unknown. In light of the development of new analytic continuation techniques and enhanced computational power, we revisit this problem. Our aim is not only to address a classical problem in fluid dynamics but also to vindicate the use of computer extended series in this field.

The governing equations for this flow are the Dean equations:

$$\begin{aligned} \nabla^4\psi &= \frac{1}{r}\left(\frac{\partial\psi}{\partial\theta}\frac{\partial}{\partial r}-\frac{\partial\psi}{\partial r}\frac{\partial}{\partial\theta}\right)\nabla^2\psi-\frac{Kw}{r}\left(r\cos(\theta)\frac{\partial w}{\partial r}-\sin(\theta)\frac{\partial w}{\partial\theta}\right) \\ \nabla^2 w &= \frac{1}{r}\left(\frac{\partial\psi}{\partial r}\frac{\partial w}{\partial\theta}-\frac{\partial\psi}{\partial\theta}\frac{\partial w}{\partial r}\right)-4 \end{aligned} \tag{1}$$

Herein, we consider a series solution in K of the stream function and down-pipe flow (Dean's Series), building on the work of Van Dyke [5]:

$$w(r,\theta)=\sum_{n=0}^{\infty} w_n(r,\theta)K^n \qquad \psi(r,\theta)=\sum_{n=0}^{\infty}\psi_n(r,\theta)K^n$$

We expand Dean's series up to the K^{198} term, by computer extension. Using Domb-Sykes analysis, we find the radius of convergence to be limited by a square-root singularity of K in the complex plane (see Figure (1)). The series is analytically continued by means of an Euler transform. We conclude that the transformed series is valid for all K and that it agrees with numerical results [6] (see Figure (2)). Previously reported differences are a result of the slow convergence of the series.

We study the bifurcation of the solutions by using the generalised Padé approximants (GPA) method introduced by Drazin and Tourigny [4]. The solution is mapped in the complex plane of K and, where possible, we compare it with numerical results found by path continuation.

We present an analogous solution for toroidal pipes of finite curvature with elliptic cross-section.

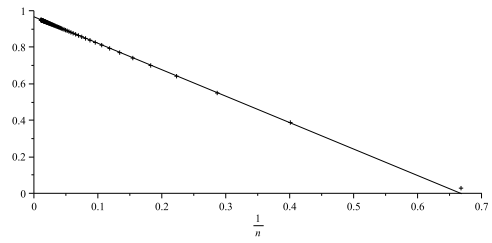

Figure 1: Domb-Sykes plot: ratio of the coefficients of the flux ratio $Q(K)$ (a_n) plotted against $\frac{1}{n}$

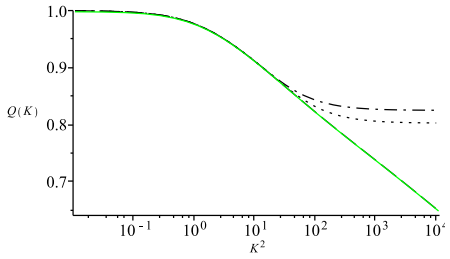

Figure 2: $Q(K)$ against K^2: - - 80 coefficients Euler transformed (ET); ··· 96 coefficients (ET) ; - Numerical Solutions (NS) [6]; Generalised Padé Approximant (GPA): - - $d = 12$

References

[1] S.A. Berger, L. Talbot, and L.S. Yao. Flow in curved pipes. *Annual Review of Fluid Mechanics*, 15:461–512, 1983.

[2] P. Daskopoulos and A.M. Lenhoff. Flow in curved ducts: bifurcation structure for stationary ducts. *Journal of Fluid Mechanics*, 203:125–148, 1989.

[3] W.R. Dean. The stream-line motion of fluid in a curved pipe. *Philosophical Magazine*, 5:673–695, 1928.

[4] P.G. Drazin and Y. Tourigny. Numerical study of bifurcations by analytic continuation of a funcgtion defined by a power series. *SIAM Journal of Applied Mathematics*, 56:1–18, 1996.

[5] M. Van Dyke. Extended stokes series: laminar flow through a loosely coiled pipe. *Journal of Fluid Mechanics*, 86:129–145, 1978.

[6] J.H. Siggers and S.L. Waters. Steady flow in pipes with finite curvature. *Physics of Fluids*, 17(7), 2005.

Session X

Hydrodynamic stability

Thursday, 11th August, 13:30 – 14:30

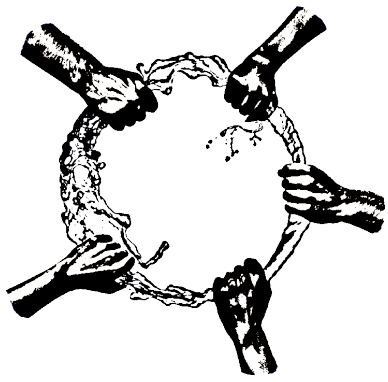

Modulated Thermocapillary Patterning of Nanoscale Polymer Film Melts

M. Dietzel [1] and S. M. Troian [2]

[1] Institute of Nano- & Microfluidics, Center of Smart Interfaces, TU Darmstadt, Darmstadt, Germany
[2] Applied Physics, California Institute of Technology, Pasadena, U.S.A.

Abstract:

Polymer films of initial thickness O(100 nm) molten on a planar substrate and subject to a large transverse thermal gradient were experimentally shown by several groups to undergo an instability to form arrays of elongated pillars separated by a few microns. The films are confined from the top next to a thin air layer by a second cooled planar substrate to impose the thermal gradient and the pillars grow until they bridge the plate separation distance. There has been some debate about the source of this instability since the governing characteristic numbers are far outside the regime where the short-wavelength (SW) Bénard-Marangoni (BM) instability typically observed for thicker films is active. We demonstrate analytically and numerically that the pillar formation can be nevertheless well attributed to stresses due to a temperature-dependent surface tension (thermocapillarity) acting tangent to the gas-polymer film and that the film deformation is a consequence of an unexplored nano-scaled limit of the well-known deformational or long-wavelength (LW) BM instability [1]. Before the pillars make contact with the upper substrate, the film flow is well described with the Navier-Stokes equations in the slender gap approximation leading to a non-linear evolution equation of the local film height in time. A linear stability analysis provides the characteristic wavelength of film deformation which is found to be in good agreement with the experimentally observed pillar pitch and is mainly a function of the initial film height, plate separation distance and the temperature difference between the plates. It is further verified that the wavelength is practically independent of the temperature-dependent melt viscosity even for very large transverse thermal gradients. The negligible influence of gravity implies the absence of characteristic numbers of onset, i.e. nanometer thick films are always unstable to thermocapillary stresses for non-vanishing temperature differences.
The large inherent film interface deformation are particularly promising for the parallel and non-contact fabrication of passive optical devices such as waveguides and ring resonators since structures can be created out of the melt and thus exhibit specularly smooth interfaces after solidification. We show with a number of numerical simulations of the non-linear film evolution equation that the modulation of the thermocapillary stresses by actively controlling the interfacial temperature distribution of the molten film is a viable route to produce technically useful patterns according to the imposed lateral temperature field in one process step. The method offers a competitive alternative to more conventional micro-fabrication techniques such as photolithography with a resolution limit directly linked to the characteristic wavelength of the corresponding LW-BM instability.

References

[1] Vanhook S.J., Schatz M.F., Swift J.B., McCormick W.D. and Swinney H.L., (1997), *J. Fluid Mech., **345**, 45*

Global stability analysis of flow through an aneurysm

Shyam Sunder Gopalakrishnan, Benoît Pier and Arie Biesheuvel

Laboratoire de mécanique des fluides et d'acoustique (CNRS - Université de Lyon).
École centrale de Lyon, 36 avenue Guy-de-Collongue, 69134 Écully, France.

Abstract:
The global linear stability analysis of flow through a model fusiform aneurysm is carried out numerically. A gaussian profile was used to model the wall channels to account for the bulge, that gradually straightens out to a uniform circular pipe in the upstream and downstream direction. Three model configurations were considered in the study, characterised by the bulge length and the maximum diameter of the bulge. These parameters for the first model (*Model A*) were $3.0D$ and $1.5D$, the second model (*Model B*) were $3.0D$ and $2.0D$ consistent with the one used in [1] and *Model 3* in [2] and for the third model (*Model C*) were $3.0D$ and $3.0D$, where D is the inlet pipe diameter. A steady parabolic velocity profile was imposed at the inlet. The global stability analyses were carried out on base flows that were axisymmetric on which non-axisymmetric perturbations were allowed to grow. For *Model B*, the flow was found to be weakly unstable to global eigenmodes of azimuthal modenumbers 4 and 5 at a Reynolds number (based on the maximum centerline velocity and pipe diameter) $Re \approx 9700$. *Model A* which had a smaller maximum bulge diameter was found to be unstable at even higher Reynolds numbers whereas for *Model C* which had a larger maximum bulge diameter became unstable at a lower Reynolds number. The least stable eigenmodes are concentrated at the downstream end of the bulge and were characterised by their slow oscillatory nature. Analyses were also carried out on *Model B* with varying inlet swirl while still preserving the axisymmetric base flow configuration. The presence of inlet swirl was found to have a stabilizing effect on the stability properties. The results obtained are found to be consistent with those presented in [1].

Preliminary Results:
The computations shown in figure 1 were carried out on *Model B*. Figure 1a shows the leading global modes characterized by their axial, radial and azimuthal velocity components (top to bottom) for azimuthal modenumber $m = 4$ at $Re = 9700$. The spatial distribution of the global modes shows that they are localized at the downstream end of the bulge. Figure 1b shows a typical eigenvalue spectrum obtained from the linear stability analysis at $Re = 9700$ for various values of m. The temporal growth rate of the eigenmodes σ is plotted in the y-axis and their frequency ω in the x-axis. The least stable eigenmodes are observed for $m = 4, 5$ with a non-zero frequency.

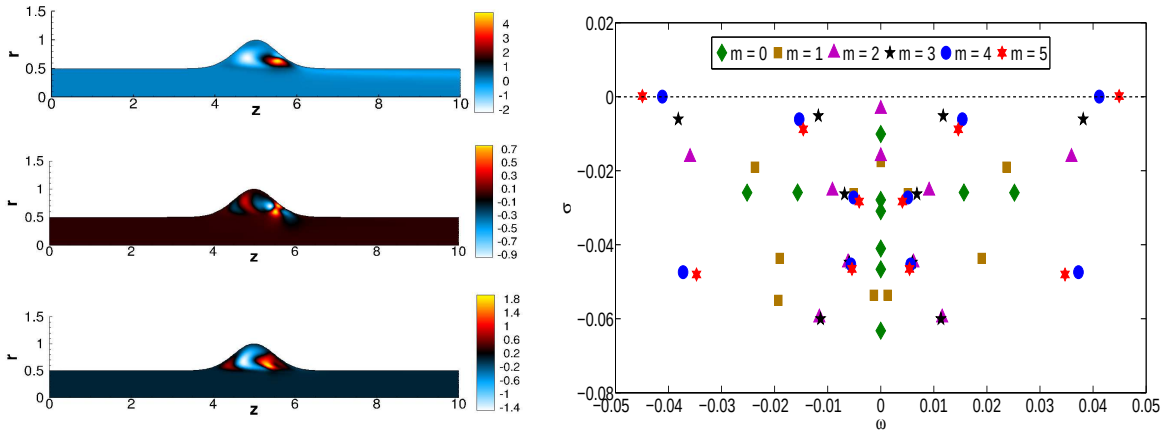

(a) (b)

Figure 1: (a) Global modes visualized by their axial, radial and azimuthal (top to bottom) velocity components. Parameter settings: *Model B*, $m = 4, Re = 9700$. (b) Typical eigenvalue spectrum in the (ω, σ) plane for different azimuthal modenumbers m. Parameter settings: *Model B*, $Re = 9700$.

We intend to present the results obtained from our stability analyses for different models along with the effect of varying inlet swirl on *Model B* during the conference.

References

[1] G. J. Sheard and H. M. Blackburn, Steady inflow through a model aneurysm: global and transient stability. *17th Australasian Fluid Mechanics Conference, Auckland, New Zealand*, 5–9 December (2010).

[2] A.-V. Salsac, S. R. Sparks, J.-M. Chomaz and J. C. Lasheras, Evolution of the wall shear stresses during the progressive enlargement of symmetric abdominal aortic aneurysms. *J. Fluid Mech.* **560**, 19–51 (2006).

Onset of Sustained Turbulence in Couette Flow

Liang Shi [1], Marc Avila [1] and Björn Hof [1]

[1] Complex Dynamics and Turbulence Group, Max Planck Institute for Dynamics and Self-Organization, Göttingen, Germany

Abstract:
The transition to sustained turbulence is studied numerically in Couette flow. At moderate Reynolds numbers, the flow is characterised by large-scale larminar-turbulent bands and exhibits complex spatio-temporal dynamics ([3],[4]). Individual bands are observed to either decay or spread and eventually split. We here first inverstigate the probability distribution of the lifetime and splitting time of localized turbulent bands. Both are shown to be exponentially distributed, with a characteristic mean time scaling superexponentially with Re (see Figure 1). The intersection of these two superexponential curves marks the Reynolds number beyond which turbulent bands split faster than they decay and it is determined to be $Re_c = 325 \pm 2$ based on half gap. Here for $Re > Re_c$, overall the turbulent fraction starts to increase. These findings are in very good agreement with the reported results in other shear flows like in pipe flow (see [1], [2], [5] and [6]). In extensive numerical simulations we further determine the size distribution close to this intersection point. Our measurements show that the size distributions become scale invariant, supporting that the onset of sustained turbulence is a phase transition. We presently measure the critical exponents for turbulence fractions and correlations close to the transition and test if they fall into known universality classes.

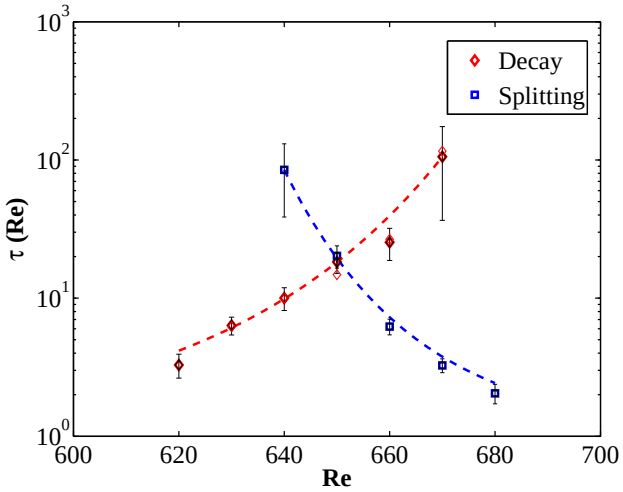

Figure 1: *Characteristic mean time as a function of Re*

References

[1] Avila, K., Moxey, D., De Lozar, A., Avila, M., Barkley, D., Hof, B., (2011): Onset of Sustained Turbulence in Pipe Flow. *Under review with Science.*

[2] Avila, M., Willis, A., Hof, B., (2010): On the Transient Nature of Localized Pipe Flow Turbulence. *J. Fluid Mech.* **646**:127-136.

[3] Barkley, D., Tuckerman, L., (2005): Computational Study of Turbulent Laminar Patterns in Couette Flow. *Phys. Rev. Lett.* **94**.

[4] Duguet, Y., Schlatter, P., Henningson, D., (2010): Formation of Turbulent Patterns Near the Onset of Transition in Plane Couette Flow. *J. Fluid Mech.* **650**.

[5] Hof, B., Westerweel, W., Schneider, T., Eckhardt, B., (2006): Finite Lifetime of Turbulence in Shear Flows. *Nature* **443**.

[6] David Moxey, Dwight Barkley, (2010): Distinct Large-Scale Turbulent-Laminar States in Transitional Pipe Flow. *Proc. Natl. Acad. Sci. USA* **107**.

Influence of disk aspect ratio on wake behaviour

T.Bobiński [2], S.Goujon-Durand [1] and J.E.Wesfreid [1]

[1] PMMH - ESPCI, CNRS UMR 7636, 10, rue Vauquelin, 75231 Paris Cedex 05, France
[2] Warsaw University of Technology, Institute of Aeronautics and Applied Mechanics, ul. Nowowiejska 24, 00-665 Warsaw, Poland

Abstract:
Flow past a disk was investigated experimentally in a low velocity water channel in the range of intermediate Reynolds number. Systematic experiments with flow visualisation and PIV measurements are presented in order to measure the velocity field in the wake of a disk . Disks with different aspect ratio (AR=d/h) varing from 1 to 24 were investigated in the range of the Reynolds numbers from 50 to 500, where stationary and oscillatory instability appear. It is presented the influence of aspect ratio on value of on-set instability, evolution of perturbation and obtained vorticity bifurcation branches on the instability. Three flow regimes can be distinguished for each of disk. The first one is steady axisymmetric flow with toroidal recirculation zone. It bifurcates to a steady flow with a planar symmetry containing two longitudinal counter-rotating vortices. With next bifurcation flow becomes unsteady and hairpin shedding is observable. Characteristic flow structures described above are presented in fig. 1. Using PIV measurements it was determined the value of the onset instability for different aspect ratio(fig. 2).

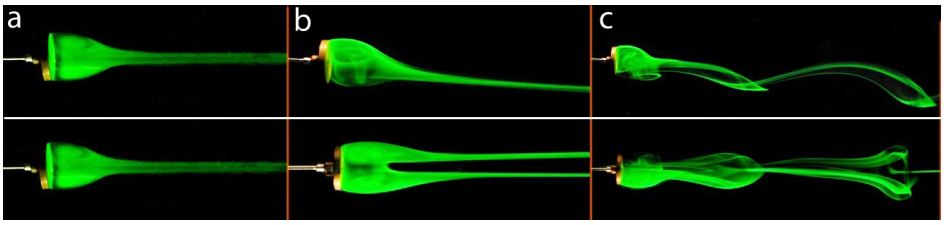

Figure 1: *Visualisation patterns for different flow regimes. Images on top and bottom are side view and top view respectively: a. steady axisymmetric flow, b. steady flow with planar symmetry, c. unsteady flow with hairpin shedding*

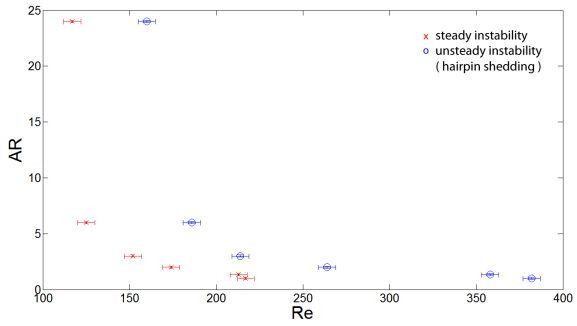

Figure 2: *Onset values for disks with different aspect ratio*

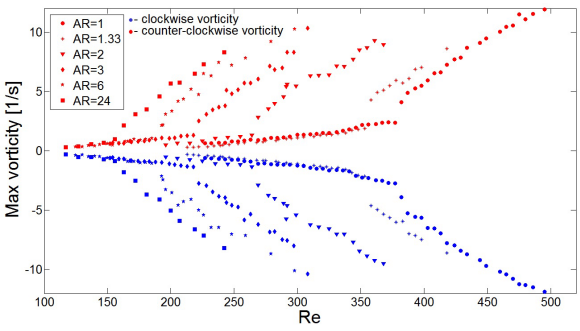

Figure 3: *Longitudinal vorticity component bifurcation branches*

References

[1] Auguste F., Fabre D., Magnaudet J., (2010): Bifurcations in the wake of a thick circular disk, *Theoretical and Computational Fluid Dynamics, vol.24, pp.305-313*

[2] Meliga P., Chomaz J.M. and Sipp D., (2009): Global mode interaction and pattern selection in the wake of disks: a weakly nonlinear expansion *J. Fluid Mech., vol.633, pp. 159-189*

[3] Fabre D., Auguste F. and Magnaudet J., (2008), Bifurcation and symmetry breaking in wake of axisymmetric bodies, *Phys. Fluids, vol.20(5), pp. 228-244*

[4] Gumowski K., Miedzik J., Goujon-Durand S., Jenffer P., Wesfreid J.E., (2008): Transition to a time-dependent state of fluid flow in the wake of a sphere, *Phys. Rev. E, vol.77, pp.055308*

Session XI

Tayler-Couette flow and turbulent transport

Thursday, 11th August, 14:40 – 15:40

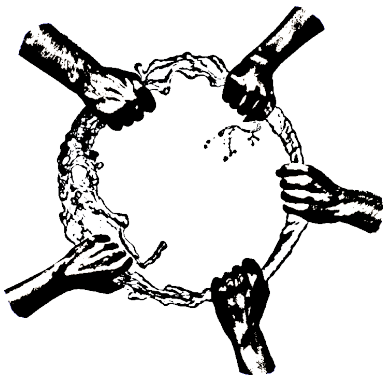

Torque Calculations for Taylor-Couette Flow

Hannes Brauckmann [1] and Bruno Eckhardt [2]

[1,2] Fachbereich Physik, Philipps-Universität Marburg, Germany

Two recent experiments [1, 2] in Taylor-Couette (TC) for $Re_S \sim 10^5$ to 10^6 have provided torque measurements that go much beyond the pioneering study of Wendt [3]. Among the unexpected features is their finding of a torque maximum for moderately counterrotating cylinders. In an effort to explore the origin of this phenomenon we present direct numerical simulations (DNS) of TC flow for Re_S up to $3 \cdot 10^4$.

Our DNS are based on a Fourier-Chebyshev scheme for an axially periodic domain [4]. The simulations were performed for shear Reynolds numbers $2 \cdot 10^3 < Re_S < 3 \cdot 10^4$, with

$$Re_S = \frac{2}{1+\eta} \left| \eta Re_o - Re_i \right| , \qquad Re_o = \frac{r_o \omega_o (r_o - r_i)}{\nu} , \qquad Re_i = \frac{r_i \omega_i (r_o - r_i)}{\nu} , \tag{1}$$

where ν is the kinematic viscosity, r_o (r_i) the radius of the outer (inner) cylinder, ω_o (ω_i) the outer (inner) angular velocity and $\eta = r_i/r_o = 0.71$. Various rotation ratios $a = -\omega_o/\omega_i$ were realized for the different shear rates. Here the focus is on the accurate computation of the torque G. Convergence of the code was verified using three criteria: resolution of all spectral directions with relative amplitudes $\sim 10^{-4}$, agreement of torque measurements at the inner and outer cylinder to within 10^{-3}, agreement of dissipation values estimated from torque and volume dissipation ε to within 10^{-2}. The latter requirement turned out to be the most demanding.

As derived in [5], the torque is given by $G = \nu^{-2} J^\omega$ with the angular velocity current

$$J^\omega = r^3 \left(\langle u_r \omega \rangle_{A(r),t} - \nu \partial_r \langle \omega \rangle_{A(r),t} \right) , \tag{2}$$

where u_r and u_φ denote velocity components, $\omega = u_\varphi / r$ the angular velocity and $\langle \cdots \rangle_{A(r),t}$ stands for the average over a cylindrical surface of radius r and over time. The transport quantity J^ω can be computed at all radial locations and is independent of r. For the realized flow states we study the spatial and temporal characteristics of J^ω at the inner and outer cylinder as well as at midgap. Within these calculations we find that the fluctuations at the inner and outer cylinder are much smaller than in the middle. The pdf's are compared to experimental observations of Lewis and Swinney [6]. We also find, near $Re_S = 30\,000$ and thus much below the values in [1, 2], the formation of a torque maximum near $a = 0.4$ for fixed Re_S, see Figure 1.

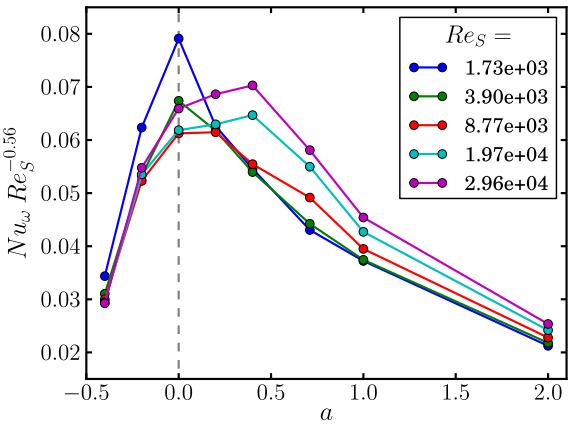

Figure 1: *Normalized torque $Nu_\omega = G/G_{lam}$ as a function of the rotation ratio $a = -\omega_o/\omega_i$. The different data, connected by straight lines to guide the eye, correspond to different Re_S. One notes that the maximum in a moves from $a = 0$ for $Re_S < 8\,772$ to $a \sim 0.4$ for $Re_S > 19\,737$.*

References

[1] van Gils D. P. M., Huisman S. G., Bruggert G.-W., Sun C. and Lohse D., (2011), Torque Scaling in Turbulent Taylor-Couette Flow with Co- and Counterrotating Cylinders, *Phys. Rev. Lett., vol. 106, p. 024502*

[2] Paoletti M. S. and Lathrop D. P., (2011), Angular Momentum Transport in Turbulent Flow between Independently Rotating Cylinders, *Phys. Rev. Lett., vol. 106, p. 024501*

[3] Wendt F., (1933), Turbulente Strömungen zwischen zwei rotierenden konaxialen Zylindern, *Ingenieur-Archiv, vol. 4, pp. 577-595*

[4] Meseguer A., Avila M., Mellibovsky F. and Marques F., (2007), Solenoidal spectral formulations for the computation of secondary flows in cylindrical and annular geometries, *Eur. Phys. J. Special Topics, vol. 146, pp. 249-259*

[5] Eckhardt B., Grossmann S. and Lohse D., (2007), Torque scaling in turbulent Taylor-Couette flow between independently rotating cylinders, *J. Fluid Mech., vol. 581, pp. 221-250*

[6] Lewis G. S. and Swinney H. L., (1999), Velocity structure functions, scaling, and transitions in high-Reynolds-number Couette-Taylor flow, *Phys. Rev. E, vol. 59, pp. 5457-5467*

Dimensionality influence on the passive scalar transport observed through experiments on the turbulunce shearless mixing

S.Di Savino[1], M.Iovieno[1], L.Ducasse[1] and D.Tordella[1]

[1] Aerospace Engineering Department, Politecnico of Torino, Torino, Italy

Abstract:
The transport of a passive substance by a turbulent flow is important in many natural and engineering contexts, e.g. turbulent mixing, combustion, pollution dispersal. The evolution of the scalar concentration is not only a footprint of the organized velocity structures, but the scalar statistics are in part decoupled from those in the velocity field, showing an intrinsic intermittency, with large fluctuations on small scales which dominate high moments [1, 2].

We present new results concerning the passive scalar turbulent transport in two and three dimensions in a shear-less mixing layer. We consider the system where one energetic turbulent isotropic field is left to convectively diffuse into a low energy one [3, 4]. In this system the region where the two turbulent flows interact is associated to a high intermittent thin layer that propagates into the low energy region. We have seen that the diffusion process in 2D is faster then in 3D. In 2D the time growth of the interaction width is super-diffusive, while in 3D is slightly sub-diffusive, as in the wind tunnel experiments by Veeravalli and Warhaft (JFM 1990). In both cases the passive scalar temporal spreading follows the spreading of corresponding kinetic energy field. The presence of the turbulent energy gradient is felt on the distribution of statistical quantities, as the skewness, kurtosis and spectra, across the layer. In two dimension, the passive scalar spectrum computed inside the mixing region presents an exponent in the inertial range which is half of the usually met exponent of the velocity fluctuation spectrum, typically close to - 3. In three dimension, we instead observed a mild difference between these two spectral exponents.

The results are obtained from direct numerical simulations of the diffusion of the passive scalar across the interface which separates the two isotropic decaying turbulent fields with different kinetic energy. The size of the computational domain is $4\pi \times (2\pi)^2$ (discretized with 1200×600^2 grid points) in the 3D simulations and $(2\pi)^2$ (discretized with 1024^2 grid points) in the 2D simulations [5, 6]. For details on the numerical technique, see [3, 4].

References

[1] Shraiman B.I., Siggia, E.D.,(2000), Scalar turbulence, *Nature. 405 (6787), 639–646*

[2] Warhaft, Z.,(2000), Passive scalar in turbulent flows, *Ann. Rev. Fluid Mech.32, 203–240*

[3] Tordella D., Iovieno M.,(2006), Numerical experiments on the intermediate asymptotis of the shear-free turbulent transport and diffusion, *Fluid Mech. 449, 429–441*

[4] Tordella D., Iovieno M., Bailey P.R.,(2008), Sufficient condition for Gaussian departure in turbulence, *Phys. Rev. E. 77, 016309/1-11*

[5] Tordella D., Iovieno M., Ducasse L,(July 2010), Diffusion of a passive scalar across a turbulent energy step, *DSFD-10,*

[6] Tordella D. Iovieno, M.,Ducasse L.(September 2010), Passive scalar diffusion through a turbulent energy gradient, *EFMC-10*

Torque scaling in turbulent Taylor-Couette flow with co- and counter-rotating cylinders

Sander G. Huisman, Dennis P.M. van Gils, G.-W. Bruggert, Chao Sun, and Detlef Lohse

Department of Applied Physics, University of Twente, Enschede, The Netherlands

Abstract:
A new turbulent Taylor-Couette system ('Twente Turbulent Taylor-Couette' (T^3C)) consisting of two independently rotating cylinders has been constructed [1]. The gap between the cylinders has a height of 0.927 m, an inner radius of 0.200 m, and a gap width of 0.080 m. The maximum angular rotation frequencies of the inner and outer cylinder are 20 Hz and 10 Hz respectively, resulting in Reynolds numbers of the inner and outer cylinder of $Re_i = 2 \times 10^6$ and $Re_o = \pm 1.4 \times 10^6$, respectively. We measure and analyze the global transport properties with this system. For all Re_i, Re_o, the dimensionless torque G scales as a function of the Taylor number Ta (which is proportional to the square of the difference between the angular velocities of the inner and outer cylinder) with an universal effective scaling law $G \propto Ta^{0.88}$, corresponding to $Nu_\omega \propto Ta^{0.38}$ for the Nusselt number characterizing the vorticity transport between the inner and outer cylinder. The transport is most efficient for the counter-rotating case along the diagonal in phase space with $\omega_o \approx -0.4\omega_i$.

Global transport properties of turbulent flows are of prime importance for many applications of fluid dynamics, but also for a fundamental understanding, as they reflect the interplay between boundary layer and bulk. The two canonical systems to analyse the transport properties in closed turbulent systems are Rayleigh-Bénard (RB) convection and Taylor-Couette (TC) flow, and they are conceptionally closely related [5, 2, 3]. In RB flow, heat (in dimensionless form the Nusselt number) is transported from the hot bottom plate to the cold top plate [6, 7], whereas in TC flow angular velocity is transported from the inner to the outer cylinder (for $\omega_i > \omega_o$). In analogy to RB flow, Eckhardt *et al.* [3] identified, from the underlying Navier-Stokes equations,

$$J^\omega = r^3(\langle u_r \omega \rangle_{A,t} - \nu \partial_r \langle \omega \rangle_{A,t}) \tag{1}$$

as relevant conserved transport quantity, representing the flux of angular velocity from the inner to the outer cylinder. Here $u_r(u_\phi)$ is the radial (azimuthal) velocity, $\omega = u_\phi/r$ the angular velocity, and $\langle \dots \rangle_{A,t}$ characterizes averaging over time and an area with constant r from the axis. J^ω is made dimensionless with its value $J^\omega_{lam} = 2\nu r_i^2 r_o^2(\omega_i - \omega_o)/(r_o^2 - r_i^2)$ for the laminar case, giving a "Nusselt number" as dimensionless transport quantity, $Nu_\omega = J^\omega/J^\omega_{lam} = G/G_{lam}$ where $r_{i,o}$ and $\omega_{i,o}$ denote the radius and the angular velocity of the inner and outer cylinder, respectively, ν is the kinematic viscosity of the fluid. Nu_ω is closely connected to the torque τ that is necessary to keep the inner cylinder rotating at constant angular velocity, or in dimensionless form to

$$G = \frac{\tau}{2\pi L \rho_{fluid} \nu^2} = Nu_\omega \frac{J^\omega_{lam}}{\nu^2} = Nu_\omega G_{lam} \tag{2}$$

where L is the height of the cylinder and ρ_{fluid} the density of the fluid.

The hitherto explored phase diagram of TC flow with independently rotating cylinders is shown in fig. 1a. In this paper we will focus on the required torque for fully developed turbulent flow (Re_i, $Re_o > 10^5$) with fixed $\eta = 0.716$ with independently rotating inner and outer cylinder, which hitherto has not been explored. The examined parameter space in this paper is shown in the space of (Re_i, Re_o) in fig. 1b. The analysis of Eckhardt *et al.* [3] and the analogy of the TC system to the RB system suggest to better plot Nu_ω as function of the Taylor number

$$Ta = \frac{1}{4}\sigma d^2 (r_i + r_o)^2 (\omega_i - \omega_o)^2 \nu^{-2} \tag{3}$$

where $\sigma = (((1+\eta)/2)/\sqrt{\eta})^4$, i.e., along the diagonals $\omega_o = -a\omega_i$. This is done in figure 2. An *universal*, i.e. a-independent, effective scaling $Nu_\omega \propto Ta^\gamma$ with $\gamma \approx 0.38$ is clearly revealed. This corresponds to a scaling of $G \propto Re_i^{1.76}$ for the dimensionless torque along the straight lines in the parameter space fig. 1, to $c_f \propto Re_i^{-0.24}$ for the drag coefficient, and to $G \propto Ta^{0.88}$. The compensated plots $Nu_\omega/Ta^{0.38}$ in fig. 2b demonstrate the quality of the effective scaling and in addition show the a-dependence of the prefactor of the scaling law. That a-dependence of the prefactor $Nu_\omega/Ta^{0.38}$ is plotted in fig. 2c. It shows a pronounced maximum around $a = 0.4$, i.e., for the moderately counter-rotating case, signalling the most efficient angular velocity transport from the inner to the outer cylinder at that value. A similar maximum was found in [4].

We will finally report on recent results on local measurements of the internal flow.

References

[1] D. P. M. van Gils, G. Bruggert, D. P. Lathrop, C. Sun, and D. Lohse (2010), Twente Turbulent Taylor-Couette (T^3C): strongly turbulent two-phase flow between independently rotating cylinders, *Rev. Sci. Instrum.*

[2] B. Dubrulle and F. Hersant (2002), Momentum transport and torque scaling in Taylor-Couette flow from an analogy with turbulent convection, *Eur. Phys. J. B*

[3] B. Eckhardt, S. Grossmann and D. Lohse (2007), Torque scaling in turbulent Taylor-Couette flow between independently rotating cylinders, *J. Fluid Mech.*

[4] M.S. Paoletti and D.P. Lathrop (2010), Angular Momentum Transport in Turbulent Flow between Independently Rotating Cylinders, *Phys. Rev. Lett.*

[5] P. Bradshaw (1969), The analogy between streamline curvature and buoyancy in turbulent shear flow, *J. Fluid Mech.*

[6] G. Ahlers and S. Grossmann and D. Lohse (2009), Heat transfer and large scale dynamics in turbulent Rayleigh-Bénard convection, *Rev. Mod. Phys.*

[7] D. Lohse and K. Q. Xia (2010), Small-scale properties of turbulent Rayleigh-Bénard convection, *Ann. Rev. Fluid Mech.*

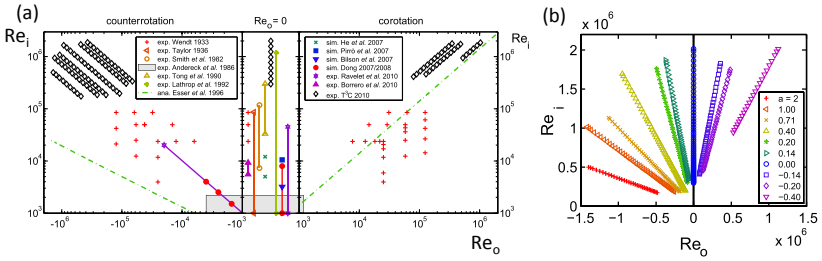

Figure 1: (a) Explored phase space (Re_o, Re_i) of TC flow with independently rotating inner and outer cylinder. Right of the horizontal axis the cylinders are co-rotating, left of it counter-rotating, and a log-log representation has been chosen. Our own data points of this publication are the black diamonds. (b) Our own data points in the phase diagram on a linear scale.

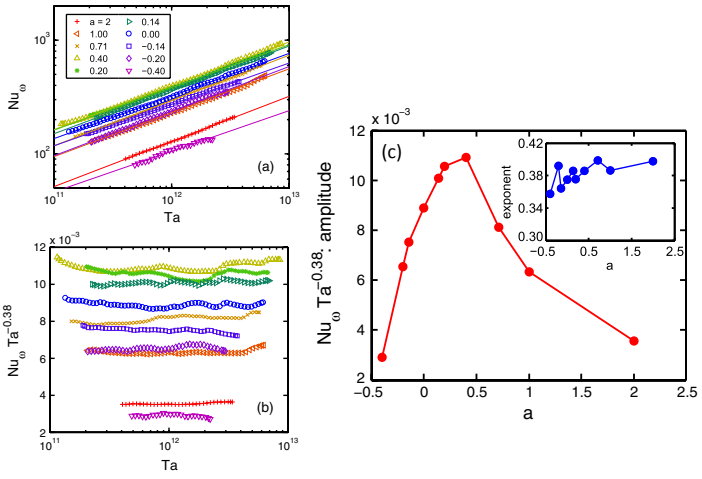

Figure 2: (a) Nu_ω vs. Ta for various a, see fig. 1b for the location of the data in parameter space. An universal effective scaling $Nu_\omega \propto Ta^{0.38}$ is revealed. The compensated plots $Nu_\omega/Ta^{0.38}$ in (b) show the quality of the effective scaling and the a-dependent prefactor of the scaling law. (c) Prefactor of the effective scaling law $Nu_\omega \propto Ta^{0.38}$ as function of $a = -\omega_o/\omega_i$. The inset shows the effective exponents γ which results from an individual fit of the scaling law $Nu_\omega \propto Ta^\gamma$.

Hydrodynamic instabilities in the eccentric Taylor–Couette–Poiseuille flow

Colin Leclercq, Benoît Pier and Julian Scott

Laboratoire de mécanique des fluides et d'acoustique, (CNRS–Université de Lyon)
École centrale de Lyon, 36 avenue Guy de Collongue, 69134 Écully, France

Abstract:
The extremely rich dynamical behaviour of the flow generated by a system as simple as two concentric cylinders in differential rotation have lead to extensive research over the last century. Indeed Taylor–Couette (TC) centrifugal instability is at the origin of hydrodynamic stability theory. With the increase of computational power, it is now possible to analyse the stability of even more complex three-dimensional flows, that are more relevant to industrial configurations.
The flow of interest in this work is a deviation from traditional TC with inner cylinder rotation, including additional pressure-driven axial flow and eccentricity of the two cylinders. The effects of these two variations of TC on stability thresholds were both studied separately [4, 3] but the combined effects of the two ingredients yet remain to be investigated. Four non-dimensional parameters govern this problem: azimuthal Reynolds number, non-dimensional axial pressure gradient, eccentricity and radii ratio. The resulting eccentric Taylor–Couette–Poiseuille flow is representative of the flow of drilling mud in an oil wellbore during drilling operations: mud is pumped down through a flexible drillstring then flows back to the surface through the annular domain. Although this mud displays some non-Newtonian behaviour, instability phenomena are here investigated with a Newtonian model. While faster rotation of the inner cylinder tends to destabilize this open flow, axial convection sweeps perturbations downstream and these two competing effects are expected to drive the convective/absolute nature of the instabilities. The linear stability of the base flow will be investigated in this framework. Then what new states can be expected after onset of instability and influence of non-linearity? Another topic of interest is the impact of the fluid on drillstring vibrations: under the influence of the hydrodynamic forces, what will be the trajectory of the drillstring (periodic, quasi-periodic, chaotic, ...)?
A 3D incompressible pseudo-spectral DNS solver was developed for numerical analyses. It uses modified bipolar coordinates [2] to map the annular domain to the rectangle $\Omega = \{(\xi, \phi) \in [-1, 1] \times [0, 2\pi[\}$. Chebyshev polynomials on Gauss-Lobatto collocation points are used in the pseudo-radial coordinate ξ while Fourier decompositions are used in the pseudo-azimuthal ϕ and axial coordinates. The algorithm is based on a linear multistep projection method with pressure prediction step [1], and is 2^{nd} order accurate in time. Non-linear and some diffusion terms are treated explicitly (Adams–Bashforth) while higher-order stiff diffusion terms are included implicitly. Some validation results will be presented along with a set of base flows displaying different patterns expected to lead to different stability properties.

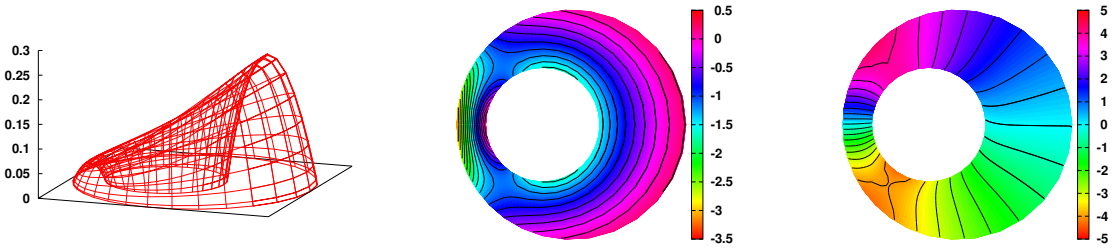

(a) (b) (c)

Figure 1: *Base flow ((a) axial velocity, (b) axial vorticity, (c) pressure) for moderate eccentricity.*

References

[1] Raspo I., Hugues S., Serre E., Bontoux P. and Randriamampianina A., (2002), A spectral projection method for the simulation of complex three-dimensional rotating flows, *Computers & Fluids, vol. 31, pp. 745-767*

[2] Wood W. W., (1957): The Asymptotic Expansions at Large Reynolds Numbers for Steady Motion Between Non-Coaxial Rotating Cylinders, *J. Fluid Mech., vol. 3, pp. 159-175*

[3] Martinand D., Serre, E. and Lueptow, R. M., (2009): Absolute and convective instability of cylindrical Couette flow with axial and radial flows, *Phys. Fluids, vol. 21*

[4] Diprima,R. C. and Stuart,J. T., (1972): Non-local effects in the stability of flow between eccentric rotating cylinders, *J. Fluid Mech., vol. 54:3, pp. 393-415*

Session XII
Geophysical flows
Friday, 12th August, 10:20 – 11:20

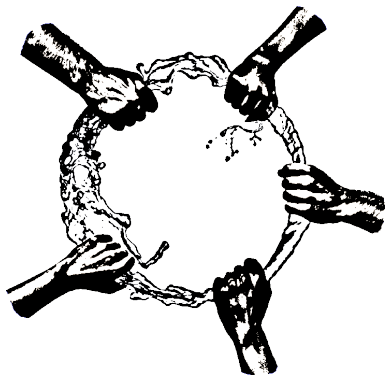

Life Cycles of Periodic Salt Fingers

M. Joana Andrade [1]

[1] Department of Mathematics, Imperial College London, London, United Kingdom

Abstract:
Double-diffusive convection is the name given to convective motions resulting from density variations in a fluid caused by the presence of two agents that have different rates of diffusion. If the slower diffusing agent has an unstable stratification, convection can occur even if the overall stratification of the fluid is stable,with narrow convection cells known as salt fingers growing from the interface between two homogenous horizontal layers.
Described in 1956 as an oceanographic curiosity, salt-fingers are now recognized as an important mechanism for vertical transport in fluids and may play a key role in areas so diverse as stellar formation, ecology, vulcanology and materials engineering. Of particular importance are thermohaline (heat-salt) salt fingers, which are believed to play a crucial role in the maintenance and dynamics of the thermohaline circulation in the oceans [4].
Observations, experiments and some theoretical studies suggest that salt finger layers are either composed of periodic rolls or of many similar sized fingers in a checkerboard tessellation, with each up-finger surrounded by 4 down-fingers; and that a weak horizontal shear field may induce a 2-D finger pattern where the mixing is not too dissimilar from the 3-D ([1] and [2]). This, together with the fact that the equations describing the structure and evolution of a periodic salt finger field admit very symmetric solutions to a 2D salt finger, lead us to approach the problem by modelling 1/2 of a single 2D up-finger. We used a finite difference method developed by Moore, Peckover and Weiss [3] to solve a set of non-dimensional equations derived from the Navier-Stokes equation with the Boussinesq approximation applied and the diffusion equations for T, the faster diffusing agent, and S, the slower diffusing agent.
Most of the theoretical work and numerical simulations of the salt finger regime stem from the study of thermohaline or salt-sugar systems, and as such, it is generally accepted that the natural evolution of the fingering process will lead from a time dependent growth period to a steady (or at least quasi-steady) equilibrium state. While we have confirmed that this certainly is the case for thermohaline systems, with our observed values of velocity being of the order of 10^{-3} cm/s and time scales of $O(10^4)$, our findings, based on the data collected in over 100 simulations, don't necessarily support the case for a steady state, pointing instead to a life cycle where clearly defined stages alternate. It is possible to identify four distinct stages during the life cycle: a first stage of overstable oscillation, a second of rapid growth (salt-fountain) [5], driven by the diffusion of T, a third of slow growth and retraction (convecting-layers) [6], conditioned by the advection of S, and a fourth and culminating stage of viscous decay.
By default salt finger systems will evolve as stable systems where only the fast diffusing stabilizing agent T is present (salt fountains). If, and when, the influence of the slow diffusing agent S is sufficient to overturn the influence of the T field, the system will evolve as a system with the general characteristic of an unstable system where only the destabilizing agent is present (convecting-layers), reverting to its default stable state as the influence of S wanes.
The typical life cycle is thus composed of alternation of salt-fountains and convecting-layers that will last until the destabilizing agent is no longer capable of overcoming the influence of the stabilizing one and viscous decay follows the last salt-fountain stage.

References

[1] Kamakura K. and Ozoe H., (2001), Numerical analysis of salt-finger phenomena near the interface between two liquid layers in a cubic enclosure, *Numer. Heat Transfer, vol.40, pp. 861-872*

[2] Linden P., (1974), Salt fingers in a steady shear flow, *Geophysical and Astrophysical Fluid Dynamics, vol.6, pp.1-27*

[3] Moore D., Peckover R. and Weiss N., (1974), Difference methods for time-dependent two-dimensional convection, *Computer Physics Communications, vol.6, pp. 198-220*

[4] Schmitt R., (1983), The characteristics of salt fingers in a variety of fluid systems, including stellar interiors,liquid metals, oceans, and magmas, *Physics of Fluids, vol.26, pp. 2373-2377*

[5] Stern M., (1960), ,The 'salt fountain' and thermohaline convection, *Tellus, vol.12, pp. 172-175*

[6] Stern M. and Turner J., (1969), Salt fingers and convecting layers, *Deep-Sea Res., vol.16, pp. 497-511*

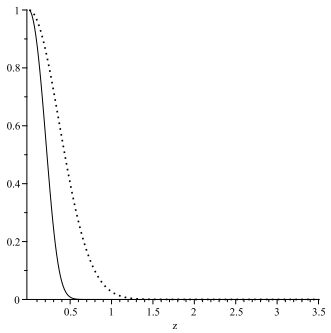

Figure 1: *Salt-fountain: normalized non-dimensional salt(—) and heat(...) fluxes (over the top half of 1/2 an up-finger)*

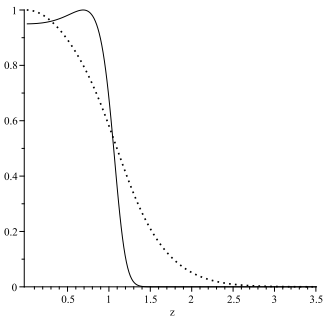

Figure 2: *Convecting-layers: normalized non-dimensional salt(—) and heat(...) fluxes (over the top half of 1/2 an up-finger)*

The effects of capillary forces on two-phase gravity currents in porous media.

Madeleine Golding [1]
Work done in collaboration with Jerome Neufeld [1], Marc Hesse [2] and Herbert Huppert [1]

[1] Institute of Theoretical Geophysics, Department of Applied Mathematics and Theoretical Physics, University of Cambridge, UK
[2] Jackson School of Geosciences, University of Texas at Austin, USA

Abstract:
The effect of capillary forces on the propagation of a two-phase gravity current is investigated analytically and numerically, motivated by problems in groundwater hydrology and the geological storage of carbon dioxide (CO_2) (1). In such settings, a fluid invades a porous medium saturated with an immiscible second fluid of differing density and viscosity. The action of capillary forces in the porous medium results in spatial variations of the saturation of the two fluids. Once the aspect ratio of the gravity current is large, fluid flow is mainly horizontal and therefore both fluids are approximately in hydrostatic equilibrium. The local saturation is determined by the vertical balance between capillary and gravitational forces. Gradients in the hydrostatic pressure along the current drive fluid flow in proportion to the saturation-dependent relative permeabilities, and determine the shape and dynamics of such two-phase currents. Our study indicates that axisymmetric two-phase gravity currents fed by a constant flux propagate like $t^{1/2}$, similar to their single-phase counterparts (2). The effect of capillary forces is encapsulated in the constant of proportionality in the radial expression, and also in the height profile of the current. We show how our two-phase model can be used to understand the propagation and residual trapping of geologically sequestered carbon dioxide.

References

[1] M.J. Golding, J.A. Neufeld, M.A. Hesse and H.E. Huppert, (2011), Two-phase gravity currents in porous media, *J. Fluid Mech., doi:10.1017/jfm.2011.110*

[2] S. Lyle, H.E. Huppert, M. Hallworth, M. Bickle and A. Chadwick, (2005), Axisymmetric gravity currents in a porous medium, *J. Fluid Mech. , vol. 543, pp. 293-302.*

Rain in a test-tube?

Tobias Lapp [1,2], Martin Rohloff [1,2], Bjoern Hof [1,2], Michael Wilkinson [3] and Juergen Vollmer [1,2]

[1] Max-Planck-Institut for Dynamics and Self-Organization, Goettingen, Germany
[2] Physics Department, Goettingen University, Germany
[3] Open University, Milton Keynes, United Kingdom

Abstract:
Demixing of multiphase fluids is important for many industrial and natural processes like alloys, magmas and clouds. For the latter the mechanisms of droplet creation, growth and interaction, and their effects on the droplet size distribution are currently under vivid discussion. Arguably there is a bottleneck in the growth of diffusively grown droplets before they grow efficiently by collisions. It is still pourly understood how rain formation can be explained for observed time scales as small as 20 minutes [1, 2].

We present an experiment in which repeated precipitation cycles are observed. A binary mixture of water and isobutoxyethanol is subject to a slow temperature ramp. To follow the temperature dependent equilibrium compositions, the two composite phases expell droplets. They are nucleated and grow by diffusive transport of supersaturation. The temperature ramp is designed in a way that the total droplet volume growth rate is kept constant [3]. Once the droplets reach a size of about 10μm, they start to sediment and collide with other droplets. This allows them to grow with an increasing speed. When most of the droplets are sedimented, the sample is cleared and new droplets are nucleated. A new precipitation cycle starts.

The sample cell is mounted in a water bath with controlled temperature (see figure 1). A mercury vapor lamp together with a few lenses and an aperture slit produces a light sheet illuminating one plane of the sample. One of the to phases is labeled by a fluorescent dye (Nile Red). A high resolution camera takes magnified images of the droplets.

A tailor-made particle tracking algorithm based on image processing with the MATLAB Image Processing Toolbox identifies and tracks droplets in the range of 4 to 40μm radius. We measure the time resolved droplet size distribution (figure 2), particle velocities and flow velocities.

We measure the dependence of the dynamics on the heating rate and the material properties (density difference, viscosity, diffusion coefficient, surface tension,...) which depend on temperature. We compare the experimental observations with theoretical modelling for droplet growth and analyze the interplay nucleation, diffusion, sedimentation and collisions.

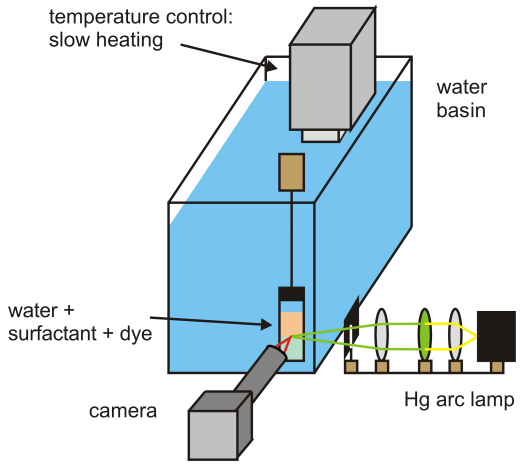

Figure 1: *Experimental Setup. The sample cell is placed in a temperature controlled water bath. A Hg vapor lamp illuminates the sample. Images are taken with a high resolution camera.*

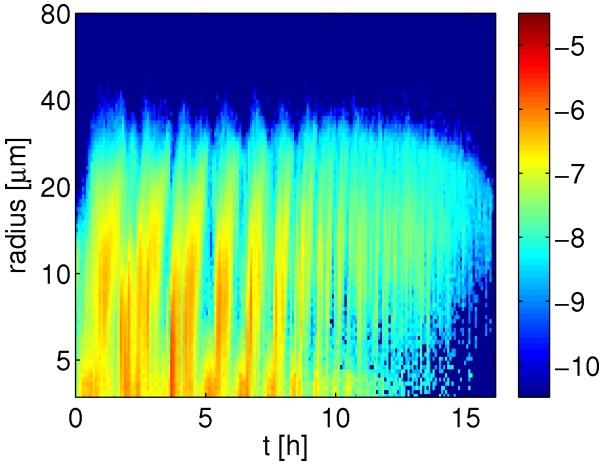

Figure 2: *Droplet size distribution. The temperature is ramped for 16 hours. More than twenty oscillations in the size distribution can be observed. The colorbar is the decadic logarithm of the droplet number density.*

References

[1] Shaw, R. A. (2003), Particle-Turbulence Interactions in Atmospheric Clouds, *Annual Review of Fluid Mechanics, vol. 35, pp. 183-227*

[2] Bodenschatz, E., Malinowski, S. P., Shaw, R. A. and Stratmann, F. (2010) Can We Understand Clouds Without Turbulence?, *Science, vol. 327, pp. 970-971*

[3] Auernhammer, G. K., Vollmer, D. and Vollmer, J. (2005) Oscillatory instabilities in phase separation of binary mixtures: Fixing the thermodynamic driving *Journal of Chemical Physics, vol. 123, pp. 134511-8*

Temperature and salinity microstructure of a double-diffusive staircase

Tobias Sommer [1,2], J. Carpenter [2], M. Schmid [1] and A.Wüest [1,2]

[1] Surface Waters, Eawag, Kastanienbaum, Switzerland
[2] Institute of Biogeochemistry and Pollutant Dynamics, Environmental Sciences, ETH, Zürich, Switzerland

Abstract:
We present the most detailed observations to date of a double-diffusive thermohaline staircase of diffusive-type in a natural environment. Specifically, we extend previous microstructure observations by combining simultaneous, and highly-resolved, temperature and salinity microstructure profiles. This allows, for the first time, field observations in the sub-mm scale of the double-diffusive boundary layer and sheds light on some of the proposed theories of the staircase structure.
The measurements were carried out during two expeditions in 2010 and 2011 on Lake Kivu (East-Africa; surface area of 2300 km^2 and volume of 550 km^3). We collected 225 profiles with a free falling Rockland Scientific microstructure profiler, which add up to a total profiling distance of 55 km, containing about ten thousand double-diffusive steps and layers. The temperature and salinity interface of each step was completely and simultaneously resolved by two temperature and two conductivity probes. The observed staircases were quantified by the thicknesses of interfaces and mixed layers and the steps in temperature and salinity across interfaces.
The flux of heat and salt through a double-diffusive interface is usually assumed to be dominated by molecular diffusion. However, our measurements showed inversions in more than half the salinity interfaces. This indicates that turbulence from the mixed layers or horizontal intrusions penetrate the interface and that molecular flux through the interface might be an underestimate. For undisturbed interfaces the ratio of temperature interface thickness to salinity interface thickness r is generally larger than one and reaches values up to ten. Large values of r are found for low R_ρ (ratio of stabilizing effect of dissolved substances to the destabilizing effect of temperature). They are mainly due to surprisingly sharp salinity interfaces with thicknesses as small as only a few millimetres. For large R_ρ, r approaches a value of two. We put our observations under natural conditions into theoretical context by comparing them to direct numerical simulations and predictions from linear stability theory.

Session XIII
Waves and stability
Friday, 12th August, 11:30 – 12:30

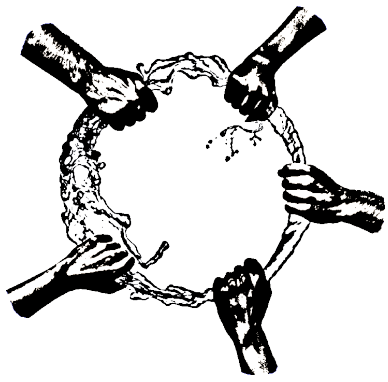

Finite Rossby deformation radius V-states and their stability

H. Płotka [1] and D. G. Dritschel [1]

[1] School of Mathematics and Statistics, University of St Andrews, St Andrews, UK

Abstract:
Vortices, or eddies, are an omnipresent feature of the Earth's oceans and atmosphere, and of the atmospheres of the planets. They occur at many different spatial and temporal scales, and can be extremely complex. Certain idealisations need to be made to better understand their fundamental properties. The quasi-geostrophic (QG) approximation used in this study filters out the flow's short-lived, high frequency unbalanced motions (relating to inertia-gravity waves), and retains just the balanced, dominant motions, relating to vortices. It does so by setting both the Froude $\mathcal{F} = U/c$ and Rossby $\mathcal{R} = U/(Lf)$ numbers to be small (where U is the typical velocity, L is the typical horizontal length scale, f is the Coriolis frequency and c is the gravity wave speed).

Important for the understanding of vortical motions are the properties they exhibit in equilibrium and the conditions necessary for their stability. We consider steadily rotating simply-connected vortex equilibria, or V-states, in a rotating frame of reference, which have a finite Rossby deformation radius $L_D = c/f$. L_D is a key length scale for rapidly rotating, strongly stratified geophysical flows, and finite values of L_D typify the Earth's oceans, and the atmospheres of the giant gas planets.

Kirchhoff elliptical vortices are well-known barotropic elliptical equilibria, i.e. ones with $L_D = \infty$. Ref. [1] analytically determined that a condition necessary for stability is that their aspect ratio λ (i.e. the ratio of the length of their minor to major axes) exceeds 1/3. This has been confirmed numerically (see, e.g. [2, 3]), and extensive studies examining the evolution of these vortices have been done (see, e.g. [4, 5] and others). Equilibria having a finite L_D have not been so widely studied. Ref. [6] considered the two-fold symmetric equilibria for a range of parameters. We extend their work, first by generating equilibria similar to theirs, only over a more dense range of aspect ratios and $\gamma = 1/L_D$, and then by addressing the linear stability and nonlinear evolution of the equilibria, which, to the authors' knowledge, has not been done before.

We generate families of equilibria of constant area $A = \pi$, spanned by γ (with $0.25 \leq \gamma \leq 10$) and λ. Starting with a circular vortex, we obtain dumbbell-shaped equilibria, a few examples of which are shown in figure 1. These branch off the classical elliptical equilibria. We perform a full linear stability analysis on these equilibria, following ref. [7], the results of which are shown in figure 2. We find two modes of instability: a large-L_D asymmetric (wave 3) mode for $\gamma \lesssim 3$, and a small-L_D symmetric (wave 4) mode for $\gamma \gtrsim 3$. The nonlinear evolution of perturbed unstable equilibria exhibits major structural changes of the vortex shape. We compute the nonlinear evolution of these equilibria around marginal stability using the contour surgery algorithm [8, 9]. We find that the small-L_D mode sheds no filaments during an instability, unlike the large-L_D one. We also find three different types of instabilities: (1) vacillations for some λ values when $\gamma = 5$ to 6, (2) filamentation for $\gamma \lesssim 1$, and (3) an asymmetric split of the vortex for $1 \lesssim \gamma \lesssim 4$ and a symmetric split for $\gamma \gtrsim 4$. A summary of all simulations is presented in figure 3.

Future work involves examining the stability and evolution of finite L_D doubly-connected V-states of unequal size and vorticity, which, to the authors knowledge has so far been done only in the barotropic limit. The authors also aim to move away from the QG limit to the shallow-water approximation, which would gain us further insight into more realistic geophysical flows, in which unbalanced inertia-gravity waves are present.

References

[1] Love A. E. H., (1893), On the Stability of certain vortex motions, *Proc. London Math. Soc., vol. 25, pp. 18-42.*

[2] Burbea J. and Landau M., (1982), The Kelvin waves in vortex dynamics and their stability, *J. Comp. Phys., vol. 45, pp. 127-156.*

[3] Dritschel D. G., (1986), The nonlinear evolution of rotating configurations of uniform vorticity, *J. Fluid Mech., vol. 172, pp. 157-182.*

[4] Mitchell T. B. and Rossi L. F., (2008), The evolution of Kirchhoff elliptic vortices, *Phys. Fluids, vol. 20, pp. 054103.*

[5] Polvani L. M. and Flierl G. R., (1986), Generalized Kirchhoff vortices, *Phys. Fluids, vol. 29, pp. 2376.*

[6] Polvani L. M. and Zabusky N. J. and Flierl G. R., (1989), Two-layer geostrophic vortex dynamics. Part 1. Upper-layer V-states and merger, *J. Fluid Mech., vol. 205, pp. 215-242.*

[7] Dritschel D. G., (1995), A general theory for two-dimensional vortex interactions, *J. Fluid Mech., vol. 293, pp. 269-303.*

[8] Dritschel D. G., (1988), Contour surgery: a topological reconnection scheme for extended integrations using contour dynamics, *J. Comp. Phys., vol. 77, pp. 240-266.*

[9] Dritschel D. G., (1989), Contour dynamics and contour surgery: numerical algorithms for extended, high-resolution modelling of vortex dynamics in two-dimensional, inviscid, incompressible flows, *Comput. Phys. Rep., vol. 10, pp. 77-146.*

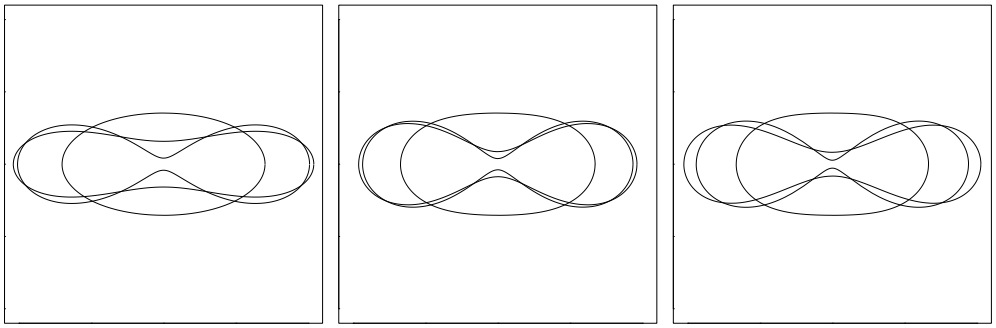

Figure 1: *Equilibrium contour shapes for* $\gamma = 0.5$ *(left), 3.0 (middle), 8.0 (right). Here, we see* $\lambda = 0.5$*,* λ_c *(the first state for which the vortex is unstable under nonlinear evolution), and the final equilibrium attained* λ_f*. Note that* $|x|, |y| \leq 2.2$*.*

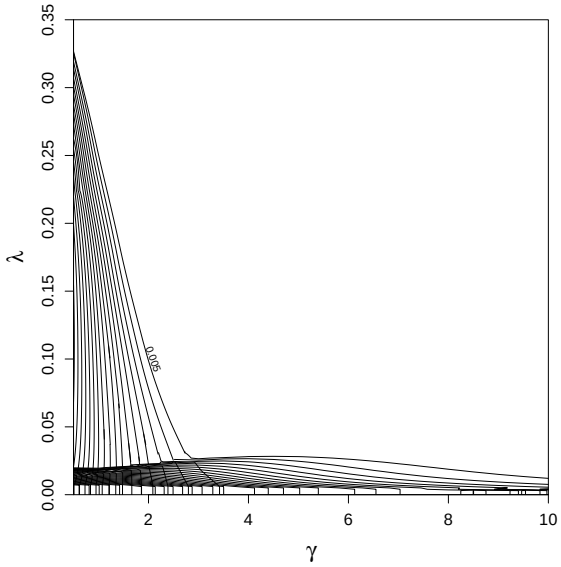

Figure 2: *Contour plots of modes 1 and 2 of the growth rates* σ_r*. 30 contour levels are shown; the contour interval is 0.005.*

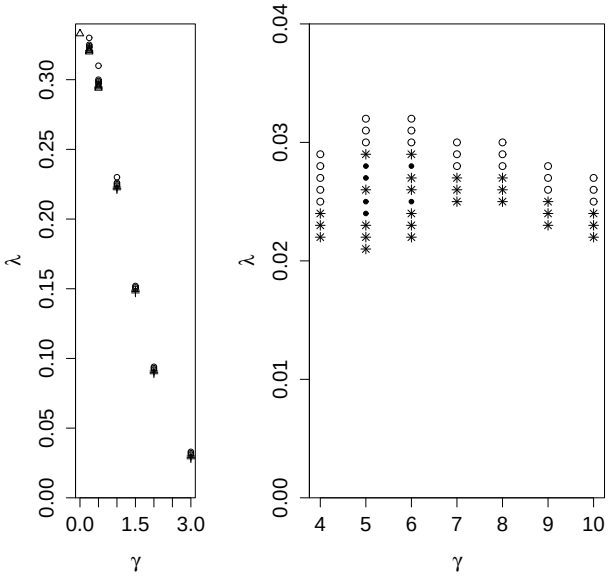

Figure 3: *Overview of simulations ran. Here, we have the following:* ∘ *steady state;* • *type 1 instability, vacillation;* △ *type 2 instability, filamentation;* + *type 3i instability, asymmetric split;* ∗ *type 3ii instability, symmetric split.*

Stabilizing effect of cyclonic rotation on waves sustained by a strongly-stratified columnar vortex

Junho Park [1] and Paul Billant [1]

[1] LadHyX, CNRS, Ecole Polytechnique, 91128 Palaiseau Cedex, France

Abstract:
In strongly stratified fluids, the waves sustained by a vertical columnar vortex are different from those in homogeneous fluids. According to Billant & Le Dizès[1] and Le Dizès & Billant[2], the waves exist only for nonzero azimuthal wavenumber m and their frequency w_r lies in the interval $[0,m\Omega]$ in the case of the Rankine vortex, where Ω is the angular velocity of the vortex core. These waves are unstable due to an outward radiation from the vortex. Here, we investigate the effect of a planetary rotation on these waves. We show that a positive Coriolis parameter f is stabilizing. The maximum growth rate w_i decreases exponentially as f increases and becomes negligibly small $(O(10^{-5}))$ when $f \approx 0.5m\Omega$. The frequency of the first branch which originates from the two dimensional limit still lies in the interval $[0,m\Omega]$ independently of f. As displayed in figure 1, the waves can be either (a) decaying exponentially outside the vortex core or (b) unstable and propagating outwards, depending on the Rossby number $Ro = 2\Omega/f$. These results for small Ro agree with those obtained in the quasi-geostrophic limit[3]. Strikingly, we show however the existence of other branches whose frequency lies in the interval $[-f,m\Omega - \sqrt{f(f+2\Omega)}]$. The mechanism of these waves is explained by a WKBJ analysis for large axial wavenumbers.

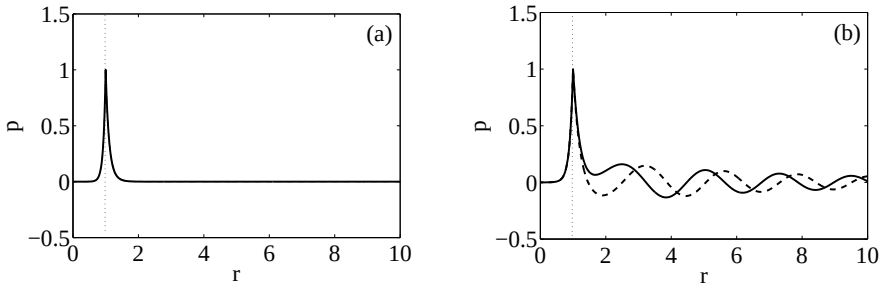

Figure 1: *Pressure p(r) of the waves for the dimensionless axial wavenumber $\kappa = 5$, the azimuthal wavenumber $m = 1$ and for $Ro = 2$ (a) and $Ro = 20$ (b). The solid and dashed lines represent the real and imaginary parts, respectively. The dotted line indicates the boundary of the vortex core.*

References

[1] P. Billant and S. Le Dizès, (2009), Waves on a columnar vortex in a strongly stratified fluid, *Phys. Fluids, 21, 106602*

[2] S. Le Dizès and P. Billant, (2009), Radiative instability in stratified vortices, *Phys. Fluids, 21, 096602*

[3] T. Miyazaki and H. Hanazaki, (1994), Baroclinic instability of Kirchhoff's elliptic vortex, *J. Fluid Mech., 261, 253-271*

Experimental time reversal of water wave

A.Przadka [1], A.Maurel [2], V.Pagneux[3] and P.Petitjeans[1]

[1] Laboratoire de Physique et Mecanique des Milieux Heterogenes, ESPCI, Paris, France
[2] Laboratoire d'Acoustique de l'Universite du Maine, Paris, France
[3] Institut Langevin, ESPCI, Paris, France

Abstract:
The phenomenon of the time-reversal surface water waves in the capillary-gravity regime, closed in the chaotic cavity, was investigated experimentally. The injection of a short pulse imposed by the wave generator leads (after several reflections from the boundaries of the tank/obstacles) to the appearance of the complex pattern. The elevation of the surface is measured during the direct wave propagation in a few points. By re-injection of the time-reversed signals in the corresponding measurement positions, the temporal and spatial refocalisation can be observed in the initial source point, despite the non-negligible wave attenuation (fig.1). The half of the wavelength spatial refocalisation limit has been achieved.

During the direct and reverse propagation the wave elevation was measured with good accuracy in time and in space using an optical method (Fourier Transform Profilometry), based on the analysis of the deformation of projected fringes [Cobelli et al. [1], Maurel et al. [2]].

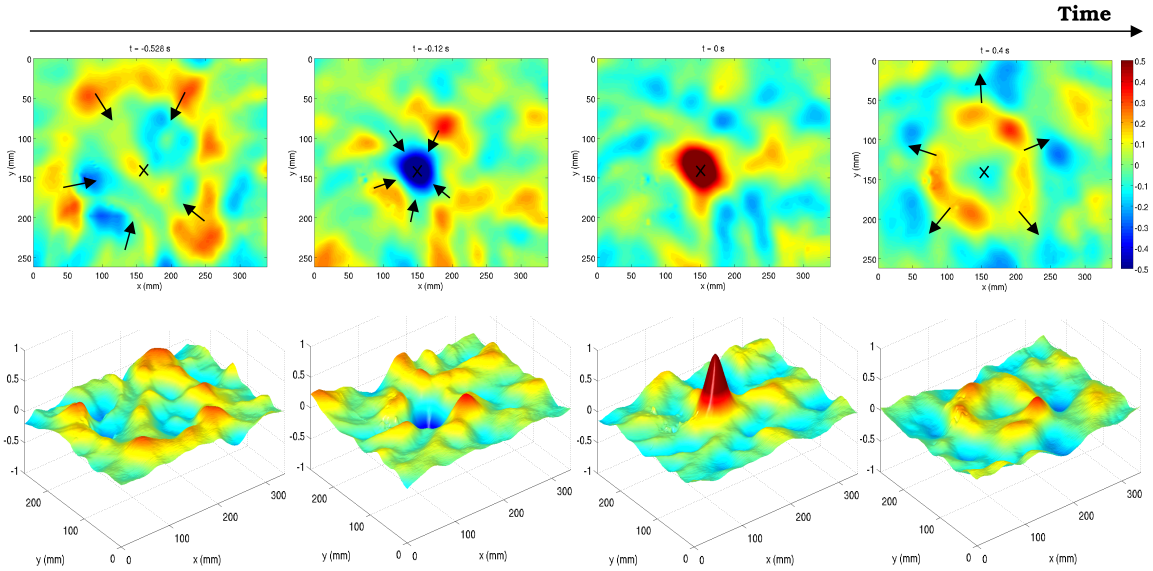

Figure 1: *2D and corresponding 3D resulting spatial refocalisation, typical measured fields of the water surface elevation during the reverse propagation (the fields are measured with an acquisition rate of 125 Hz). The colorbar is scaled to 0.5 of the maximum amplitude.*

References

[1] Cobelli P., Maurel A., Pagneux V. and Petitjeans P., (2009): Global measurement of water waves by Fourier transform profilometry, *Experimental Fluids, vol.46, pp.1037-1047*

[2] Maurel A., Cobelli P., Pagneux V. and Petitjeans P., (2009): Experimental and theoretical inspection of the phase-to-height relation in Fourier transform profilometry, *Applied Optics, vol.48(2), pp.380-392*

[3] Draeger C. and Fink M., (1997): One-channel time reversal of elastic waves in a chaotic 2D-silicon cavity, *Physical Review Letters, vol.79(3), pp.407-410*

Shock structure in He-Ar mixture and its comparison with experimental results

D. Madjarević [1]

[1] Department of Mechanics, University of Novi Sad/Faculty of Technical Sciences, Novi Sad, Serbia

Abstract:
Multi-temperature model of gaseous mixtures is proposed within the framework of extended thermodynamics with the aim to capture essentially non-equilibrium processes [3, 1]. In mathematical sense it is represented by the hyperbolic system of partial differential equations with stiff source terms which reflect the dissipative character of the model. The aim of this study is to compare theoretical predictions of the model with measurements of shock wave structure in Helium-Argon mixtures.

It will be assumed that mixture is consisted of two components, both of them being ideal gases with negligible viscosity and heat conductivity. Dissipation in the system is caused by diffusion of components and the difference of their temperatures. The model will be transformed into a system of ordinary differential equations by assuming the solution in the form of a travelling wave. Numerical solution of the problem will be a heteroclinic orbit connecting two equilibrium states. Main feature of the solution is the inequality of component temperatures within the shock profile between equilibrium states [2].

The data obtained by numerical computation will then be compared with the measurements of shock structure in Helium-Argon mixture [4, 5]. It will be shown that even such a simple multi-temperature model is in a good accordance with experimental data. The discrepancies between theoretical and experimental results are observed in temperature profiles (Figure 1). They are of the same nature is in more sophisticated numerical calculations based upon Boltzmann equations for non-reacting mixtures [6].

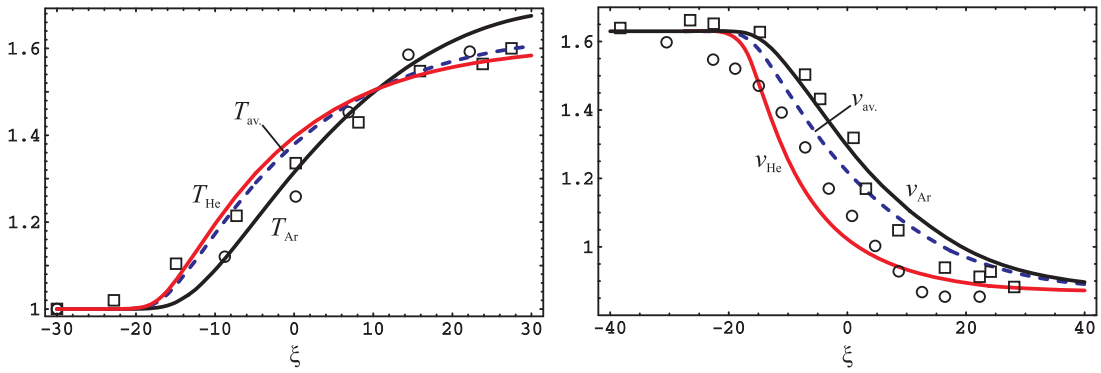

Figure 1: *Temperature and velocity profiles of Helium (red) and Argon (black). Circles (He) and squares (Ar) represent experimental data. Dashed blue line represents numerically evaluated average temperature of the mixture*

References

[1] Ruggeri T., Simić S., (2007), On the hyperbolic system of mixture of Eulerian fluids: A comparison between single and multi-temperature models, *Mathematical Methods in the Applied Sciences, vol. 30, pp. 827-849*

[2] Simić S., Ruggeri T., (2007): Shock structure in a hyperbolic model of binary mixture of non-reacting gases, *Proceedings of 1st International Congress of Serbian Society of Mechanics, D. Šumarac, D. Kuzmanović, Kopaonik, pp. 237-246*

[3] Müller I. and Ruggeri T. (1998): *Rational Extended Thermodynamics*, Springer-Verlag, New York.

[4] Center R. E., (1967), Measurement of Shock-Wave Structure in Helium-Argon Mixtures, *The Physics of Fluids, vol. 10 (8), pp. 1777-1784*

[5] Harnett L. N., Muntz E. P., (1972), Experimental Investigation of Normal Shock Wave Velocity Distribution Functions in Mixtures of Argon and Helium, *The Physics of Fluids, vol. 15 (4), pp. 565-572*

[6] Abe K., Oguchi H., (1974), Shock wave structures in binary gas mixtures with regard to temperature overshoot, *Physics of Fluids, vol. 17 (6), pp. 1333–1334*

Participants

Ahmadi, Somayeh	soahmadi88@yahoo.com
Andrade, Joana	mja@ic.ac.uk
Blackbourn, Luke	uke@mcs.st-and.ac.uk
Bobinski, Tomasz	tomsoft@gmail.com
Brauckmann, Hannes	hannes.brauckmann@physik.uni-marburg.de
Brumley, Douglas	douglas.brumley@gmail.com
Burridge, Henry	h.burridge09@imperial.ac.uk
Carrasco, Francisco Gomez	fgomezcarrasco@gmail.com
Connick, Owen	owen.connick05@imperial.ac.uk
Dammann, Christian Dammann	christian.dammann@phys.uni-goettingen.de
De Santi, Francesca	francesca.desanti@polito.it
Dekterev, Dmitriy	dekterev_da@mail.ru
Di Savino, Silvio	silvio.disavino@polito.it
Dietzel, Mathias	dietzel@csi.tu-darmstadt.de
Dimitriadis, Panayiotis	dimitriadispanos@yahoo.gr
Doychev, Todor	todor.doychev@kit.edu
Ezhova, Ekaterina	ezhova@hydro.appl.sci-nnov.ru
Fani, Andrea	andrea.fani@for.unipi.it
Ghanem, Akram	akram.ghanem@univ-nantes.fr
Golding, Madeleine	mjg88@cam.ac.uk
Gopalakrishnan, Shyam Sunder	shyam7sunder@gmail.com
Grozescu, Annabella	annabella.grozescu@gmail.com
Gruncell, Brian	brkg105@soton.ac.uk
Happenhofer, Natalie	natalie.happenhofer@univie.ac.at
Herraez, Ivan	ivan.herraez.hernandez@uni-oldenburg.de
Hill, Jonathan	jh1306@ic.ac.uk
Huisman, Sander	s.g.huisman@gmail.com
Knorps, Maria	maria.knorps@gmail.com
Kononenko, Iryna	kononenko.iryna@gmail.com
Krauss, Jens	jens.krauss@lstm.uni-erlangen.de
Kumar, Dinesh	dkverma.iitk@gmail.com
Lakhanpal, Chetan	PMCL@leeds.ac.uk
Lapp, Tobias	tobias.lapp@ds.mpg.de
Le Clainche, Soledad	soledad.leclainche@upm.es
Leclercq, Colin	colin.leclercq@ec-lyon.fr
Li, Ling	l.li@tu-ilmenau.de
Lopez Carranza Santiago, Nicolas	santiago.lopez@ensem.inpl-nancy.fr
Luebke, Martin	martin.luebke@uni-kassel.de
Madjarevic, Damir	damirm@uns.ac.rs
Madré, Tobias	tobias.madre@physik.uni-marburg.de
Marinc, Daniel	d.marinc@aia.rwth-aachen.de
Mariotti, Alessandro	alessandro.mariotti@for.unipi.it
Meskauskas, Julia	julia.meskauskas@gmail.com
Mistry, Dhiren	dm529@cam.ac.uk
Moussa, Tala	tala.moussa@univ-nantes.fr
Ovsyannikov, Andrey	andrey.ovsyannikov@ec-lyon.fr
Paredes González, Pedro	pedro.paredes@upm.es
Park, Junho	junho.park@ladhyx.polytechnique.fr
Pfeifer,Jens	Jens.Pfeifer@physik.uni-marburg.de
Płotka, Hanna	hanna@mcs.st-andrews.ac.uk
Postacchini, Matteo	m.postacchini@univpm.it
Pryce, David	d.pryce10@imperial.ac.uk
Przadka, Adam	adam.przadka@espci.fr
Rodriguez Imazio, Paola Carolina	paolaimazio@df.uba.ar
Rolland, Joran	joran.rolland@ladhyx.polytechnique.fr

Rozema, Wybe	wybe.rozema@nlr.nl
Samanta, Devranjan	devranjansamanta@gmail.com
Sargent, Cristina	cristina.sargent04@imperial.ac.uk
Scarsoglio, Stefania	stefania.scarsoglio@polito.it
Schiffer, Stefanie	stefanie.schiffer@dlr.de
Schmeling, Daniel	daniel.schmeling@dlr.de
Setchi, Adriana	asetchi@imperial.ac.uk
Shi, Liang	liang.shi@ds.mpg.de
Skripkin, Sergey	Skryp91@mail.ru
Sommer, Tobias	tobias.sommer@eawag.ch
Song, Baofang	baofang.song@ds.mpg.de
Szewc, Kamil	kamil.szewc@gmail.com
Tettamanti, Florencia	fat03@ic.ac.uk
Torma, Peter	tormapeti@gmail.com
Traugott, Hadar	htroygot@gmail.com
Vaidya, Haresh Anant	haresh.vaidya@lstm.uni-erlangen.de
van Opstal, Timo	t.m.v.opstal@tue.nl
Vinokurov, Alexey	alexey_vin@mail.ru
Vukicevic, Marija	mvukicev@gmail.com
Wagner, Sebastian	Sebastian.Wagner@DLR.de
Wardach-Święcicka, Izabela	izkaw@imp.gda.pl
Wu, Wei	wei.wu@dlr.de
Wysocki, Oliver	oliver.wysocki@dlr.de
Yoffe, Sam	sam.yoffe@ed.ac.uk
Zammert, Stefan	Stefan.Zammert@physik.uni-marburg.de
Zavadsky, Andrey	anderyza@post.tau.ac.il
Zlonkevich, Fedor	fedorm462@mail.ru